APPLIED COMPUTER SCIENCE

The Journal is a peer-reviewed, international, multidisciplinary journal covering a broad spectrum of topics of computer application in production engineering, technology, management and economy.

The main purpose of Applied Computer Science is to publish the results of cutting-edge research advancing the concepts, theories and implementation of novel solutions in computer technology. Papers presenting original research results related to applications of computer technology in production engineering, management, economy and technology are welcomed.

We welcome original papers written in English. The Journal also publishes technical briefs, discussions of previously published papers, book reviews, and editorials. Especially we welcome papers which deals with the problem of computer applications in such areas as:

- manufacturing,
- engineering,
- technology,
- designing,
- organization,
- management,
- economics,
- innovations,
- competitiveness,
- quality and costs.

The Journal is published quarterly and is indexed in: BazTech, Cabell's Directory, CNKI Scholar (China National Knowledge Infrastucture), ERIH PLUS, Index Copernicus, J-Gate, Google Scholar, TEMA Technik und Management.

Letters to the Editor-in-Chief or Editorial Secretary are highly encouraged.

LIST OF REVIEWERS
(2017)

Önder Ayer
Trakya University, Turkey

María del Carmen Alarcón del Amo
Universitat Autònoma de Barcelona, Spain

Josef Basl
University of West Bohemia, Czech Republic

Anna Dziubińska
Lublin University of Technology, Poland

Milan Edl
University of West Bohemia, Czech Republic

José Luis Gascó
University of Alicante, Spain

Milan Gregor
University of Zilina, Slovakia

Henning Heuer
Technische Universität Dresden, Germany

Nina Horidko
Russian Academy of Sciences, Russia

Tomasz Jachowicz
Lublin University of Technology, Poland

Zhadyra Konurbayeva
D. Serikbayev East Kazakhstan State Technical University, Republic of Kazakhstan

Tomasz Kopecki
Rzeszow Univeristy of Technology, Poland

Ivan Kuric
University of Zilina, Slovakia

Paweł Lonkwic
The State School of Higher Education in Chełm, Poland

Alejandro Medina
University of Salamanca, Spain

Juan Antonio Mondéjar Jiménez
Universidad de Castilla-La Mancha, Spain

Igor Muraszko
Pavel Sukhoi State Technical University of Gomel, Belarus

Wiesław Piekarski
University of Life Sciences in Lublin, Poland

Teet Örd
University of Tartu, Estonia

Jolanta Słoniec
Lublin University of Technology, Poland

Jerzy Stamirowski
Kielce University of Technology, Poland

Peter Trebuňa
Technical University of Košice, Slovakia

Anna Kosek
Netherlands Organisation for Applied Scientific Research (TNO), Netherlands

CONTENTS

Applied Computer Science, vol. 13, no. 4, pp. 7–19
doi: 10.23743/acs-2017-25

Submitted: 2017-07-16
Revised: 2017-10-19
Accepted: 2017-12-01

current process control, tool wear monitoring system, process optimization

Damian KOLNY[*], Dorota WIĘCEK[*], Paweł ZIOBRO[**], Martin KRAJČOVIČ[***]

APPLICATION OF A COMPUTER TOOL MONITORING SYSTEM IN CNC MACHINING CENTRES

Abstract

The article presents practical knowledge about production process optimisation as a result of implementing a specialized system monitoring the work of machining tools. It features complex results of the conducted research with use of dedicated equipment and software, whose unconventional application may appear to be an effective IT tool for taking operational and strategic decisions in the machining area. This results from the possibility of analysing the obtained data in both current and long-term perspective, and taking decisions on this basis, which significantly conditions the rationality of using this type of solutions.

1. INTRODUCTION

The automotive industry has already achieved a lot, but still car manufacturers continue striving for increasing processes efficiency to retain the profitability level and achieve competitive advantage. Among numerous mechanical manufacturing techniques, machining is the most commonly used (60–70%) and consumes more than half of the energy necessary for production processes (Wittbrodt, 2014). It seems to have a bright future – it is estimated that precise,

[*] University of Bielsko-Biala, Faculty of Mechanical Engineering and Computer Science, 43-309 Bielsko-Biała, Willowa 2, +48 33 82 79 253, dkolny@ath.bielsko.pl, dwiecek@ath.bielsko.pl

[**] ZPT Industry | Automation | Research & Development | Innovations, pawel.ziobro@zp-team.pl

[***] University of Zilina, Industrial Engineering Department, 010 26 Žilina, Univerzitná 1, Slovak Republic, + 421 41 513 2718, martin.krajcovic@fstroj.uniza.sk

high-speed machining will develop in the years to come, especially in the automotive sector and in aviation. Financial aspects related to production cost cutting and continuously rising customer requirements result in creating even more complicated product shapes by designers and constructors (Więcek, 2013). This often causes a decreased element mass, and, consequently, problems during manufacturing (this relates also to tools). The subject of tools can also be considered here from the logistic point of view in form of tools management. Many authors in their works on machining economy assume tool cost on the level of 2–8% of general manufacturing costs (Wittbrodt, 2014). However, machining tools market analysis and practical research of manufacturing processes show that the actual cost of tools can reach far above 10 per cent. Despite inaccurate data, it is possible to state that the cost is rather high, so rational tool management is one of the solutions for production cost reduction.

Although many research centres are engaged in building machining process monitoring systems, and this issue has been extensively described in many publications (Jurko, 2007; Kuljanic & Sortino, 2005; Kuryjański, 2011; Storch, 2001), the production practice in many companies shows that that the issue of tool condition and the machining process monitoring and forecasting has not been solved and is still present. Factors like production processes complexity, automation and robotization of the manufacturing processes, common usage of flexible production systems, growing requirements related to elements' accuracy contribute to the need of implementing and using the technologies which allow for effective machining process monitoring (Nouri, Fussell, Ziniti & Linder, 2015).

However, modern machining tools require complex and very detailed control for three reasons. The first one are progressive changes in tools' construction, like direct coolant (oil mist) supply to the machined area, based on the MQL system (Minimal Quality Lubrication), which, to some extent, leads to 'weakening' of the tool construction. The second reason is a consequence of the first one – new constructional solutions result in increased tool prices (new projects, technologies, materials, etc.). The last factor concerns the phase of tool testing, conducted in order to research tool quality before they are launched to the market – production practice is the best test, particularly in the automotive industry, where machining is the dominant technique.

The aim of the article is to present the conducted analyses and research with the use of an advanced system monitoring the work of tools used in the machining process. This type of solution allowed, above all, for a precise visualization of the machining process by means of a specialist Digital Way–WP Visu_C software, which, subsequently, created a basis for taking decisions related to the need and way of optimization. The research range covered aspects like detecting chippings and fractures and monitoring machining tool wear, parameterization and optimization of the machining process, researching the influence of material structure on its machinability, as well as regenerated tools' analysis. The presented part of research is a result of unconventional application of the mentioned system,

whose target effect is widely understood production cost reduction due to manufacturing process optimization and reasonable tool management. The presented issue is a current representation of one of many challenges faced by the automotive industry, in which searching for innovative solutions to problems is an ongoing process.

2. TOOL STRENGHT AND TOOL WEAR MONITORING

During machining, a tool, and in fact its cutting edge, plays a crucial role, as it undergoes mechanical, and thermal processes, as a result of which its working capability is worsened due to changing its properties and appearance of damages in its material. The progressing tool wear brings about even worse tool work performance, until it is not sufficient. Such wear may cause complete tool damage, and can even damage the material of the machined element.

Tool wear can also be considered from the tool endurance point of view. This is so called catastrophic tool failure, which can lead to a production break. This is a very dangerous phenomenon, which, with limited supervision, may cause a complete tool failure, damages to the machined product, and even machine tool damage. Catastrophic tool failure may take following forms – fig.1.

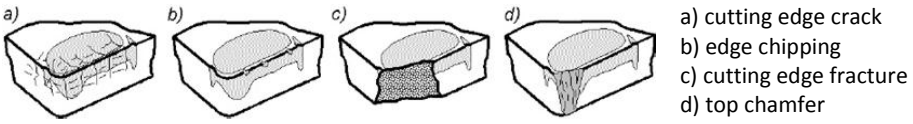

Fig. 1. Forms of blade endurance wear (Jemielniak, 2002)

Cutting edge cracks usually takes place during intermittent machining, in the conditions when the cutting edge undergoes numerous thermal and mechanical hits. The thermal fatigue causes cracks which are perpendicular to the edge, whereas mechanical wear produces parallel ones. During further machining, the cracks are growing, get connected, often causing cutting edge fracture. Cutting edge chipping is caused by local excess of its endurance. As a result of this process, the edge's geometry - actually of the chipped fragment – is violently changed in a very adverse way. In the place of chipping the load and susceptibility to further chipping increase, which, the course of action, may lead to early complete wear, and even a fracture. In case of breakages, the causes can be similar to chipping, but breakages are significantly larger, which means that in the moment of breaking off the tool instantly loses its cutting properties. Breakages and chipping most frequently take place if a tool is excessively used, and their occurrence during initial work phases can be related to wrongly selected parameters and cutting conditions, or insufficient quality of the tool itself (Jemielniak, 2002; Kuryjański, 2011).

If a tool does suffer any of the above described defects, its durability is limited by the time of dulling the cutting edge, which is equal to losing its cutting properties necessary to realize a given machining operation. The opposite process is sharpening, in order to bring back the lost cutting properties. The two issues set the period of cutting edge durability, which means the time of its work between two subsequent blunting cases, with unchanged machining conditions. The sharpening process cannot be repeated infinitely. There comes a moment when bringing back cutting properties is impossible. The sum of tool durability periods, from the beginning to the end of its exploitation, determines tool life.

There are many factors influencing the need to implement machining monitoring systems in production industry (Nouri et al., 2015). Currently, producers on the market of monitoring systems of machining tools condition provide very differentiated offer with different efficiency. The monitoring techniques applied in these systems can generally be divided into 2 groups: direct and indirect methods (Wittbrodt, 2014).

Direct methods, based on geometric measures of cutting edge wear, are used occasionally due to difficulties related to their application, like lack of access to the cutting area during machining, low effectivity and accuracy of measurements, high time consumption. This type of methods involve, among others, optical, electro-resistant, induction, radiometric or pneumatic techniques.

Indirect methods find much wider application in industry. They consist in monitoring tool variables on the basis of signal, where, thanks to special analysis, a given (forecast) level of tool wear can be determined. These methods generate signal measure when a tool is working, which allows for conducting current control. They are based on measuring the effects, not the wear itself, where cutting edge wear level is assessed by means of measuring physical dimensions, among which cutting force (Kious, Ouahabi, Boudraa, Serra & Cheknane, 2010) and derivative measurements (torque, engine power), acoustic emissions (Barreiro, Fernández-Abia, González-Laguna & Pereira, 2017) and vibration measurements are predominant (Addona & Teti, 2013; Nouri et al., 2015). In comparison to direct methods, they are characterized by technically simpler estimation of wear features. However, the obtained results are usually burdened with uncertainty and a need of two-stage operation: the first step is to measure a given physical value, and the next one is to develop proper dependences which make it possible to assess tool condition. For each machining process, proper sensors are selected and installed for monitoring purposes, depending on the physical measures interesting for a user. Thanks to the signals received by the sensors, own transmission systems generate the measured signals and inform the user, who can take appropriate action if the results are worrying (Wittbrodt, 2014).

3. AN EXAMPLE OF TOOL WEAR MONITORING SYSTEM

This part of the article concern the issue of an exemplary implementation of an advanced tool wear monitoring system and its practical usage. Despite long-term research conducted in this area, it is very problematic to find many practical solutions and realized implementations, mainly due to financial reasons.

The accuracy of the applied system comes from the fact of gathering and processing own data. The appliance has a unique patented measuring system and its own calculation algorithm. The measuring part is connected in series with a spindle motor, whereas the processing part communicates with numerical controller (NC) and programmable logic controller (PLC). By means of a dedicated software, it visualizes machining curves, the level of tool wear, alarm curves, and makes it possible to change control parameters. The system's operation scheme is presented in fig. 3. There is a possibility of connecting to a computer system, which will store machining data for the sake of long-term analysis. In order to monitor a given process, it is necessary to define the following base functions (fig. 2):

- control beginning and end on the level of the machining program,
- a learning curve - introducing an optimal model into the system,
- control beginning and end in the dedicated application
- upper tolerance range - the admissible upper level of machining set as a percentage in relation to the learning curve (optimal course),
- lower tolerance range - the admissible lower level of machining set as a percentage in relation to the learning curve (optimal course).

Defining the learning curve is performed by realizing a machining process on a new tool. Tolerance ranges, selected on the basis of empirical experience, provide a strict framework, within which a proper course of the process is assumed. In case of exceeding the given parameters by any machining process, the systems stops it, preventing from producing faulty products and machine breakdowns.

The system registers and illustrates the power parameter during tool's operation in form of 3 functions: absolute power, corrected power, derivative power. Absolute power is a value measured from the beginning till the end of spindle's work, within which there is a certain fragment responding to tool's operation in a given cycle, in order to learn the structure of the given process and determine the beginning and the end of control for the tool itself. Corrected power is a value reflecting operation of the tool, without considering the spindle's work and is used to detect tool chipping. Derivative power is a value which registers fast changes of torque applied to the tool (formula 1) and is used for advanced analysis of tool work, informing a user about even a microscopic tool losses suffered during the machining process.

$$P' = \frac{\Delta P}{\Delta t} \tag{1}$$

where: P' – power derivative,
ΔP – power value change between successive readings,
Δt – passage of time between successive readings.

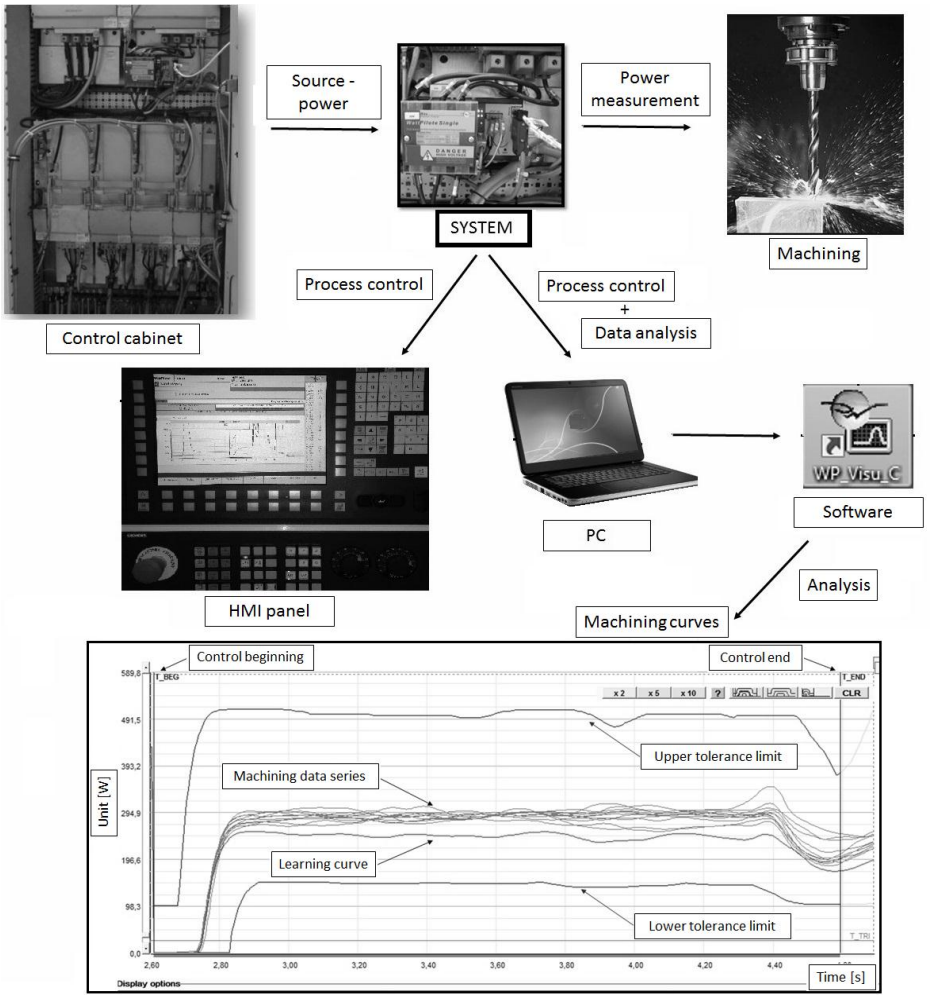

Fig. 2. System's operation scheme with visualization of the machining process

The most important system's parameters are the following:
- maximum number of controlled machining cases: 120,
- minimal control time: 0.07 s, maximal: 50 min,
- sampling speed: 40 kHz,
- simultaneous control of power, power derivative and energy,
- measurement accuracy: 0.01%.

The main aim of using this type of systems is early detection of tool defects, spindle protection against collision with a workpiece and protection against producing faulty products, which influences the reduction of costs related to tool management and manufacturing in general.

4. PRACTICAL APPLICATIONS

Basing on production practice, chosen applications were presented for the system, whose practical implementation options depend on user's needs and invention.

Tools' operation monitoring

The first step involves observing the machining process before any action or decision is taken about changes to process structure. The system installed in a tool machine allows for 2 monitoring modes: current control (stopping the process by exceeding the set parameters) and 'passive' observation for process analysis.

The following research fragment was conducted on the basis of experimental drilling process with an installed monitoring system. The task of this system was to gather data in order to observe a full course of the machining process throughout the whole tool life. General process structure and the first series of the gathered data are presented in figure 3, with the assumed tool life of 600 pieces. After the drill performed about 80 machining cycles, the first chippings were observed (fig. 4), the so called death symptoms.

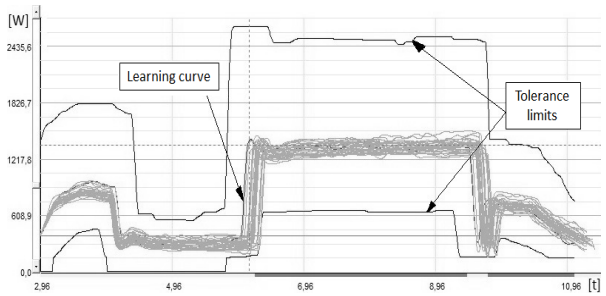

Fig. 3. The first series of data, stable process, close to the ideal course

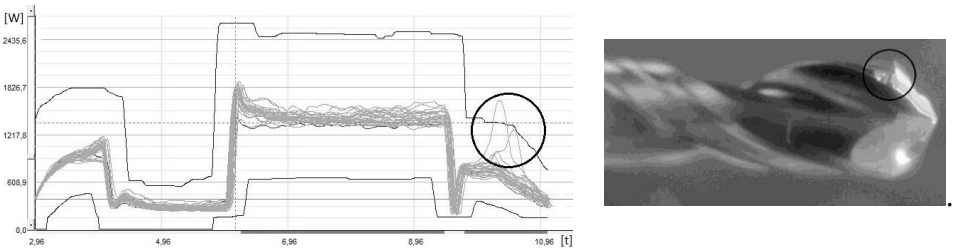

Fig. 4. Next series of data – first tool chipping is visible

In such a case in normal conditions the process should be stopped. In a further part of the experiment progressive partial chipping of the tool was observed, up to 484. machining – when tool fracture occurred (fig. 5).

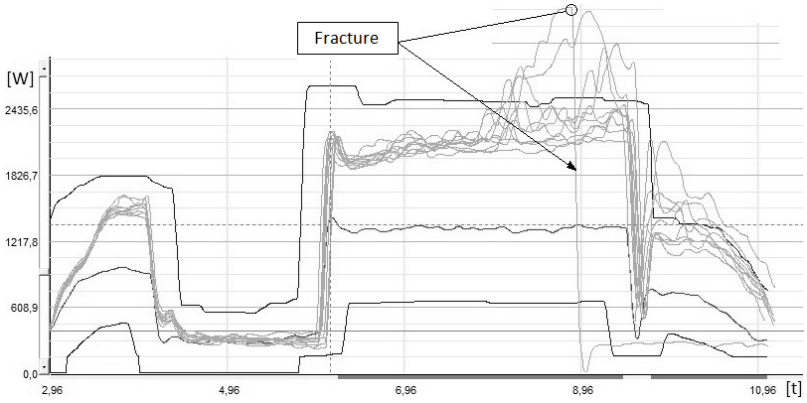

Fig. 5. Premature tool fracture

As a result, the tool was damaged in such a degree that its regeneration was not possible. Conducting this type of research aims at analysing the process itself and carrying out attempts, if the set tolerance ranges are effective and can stop the process in a right moment, protecting the tool, the workpiece and the machine against damages.

The presented example illustrates graphs of the corrected function, used mainly to detect significant chipping, fractures and tool faults. Figure 6 features another program's function – derivative function – which is used to even more advanced analysis of tool work. By means of this function, the system is able to alarm a user about even a slight tool fault occurring during the machining process.

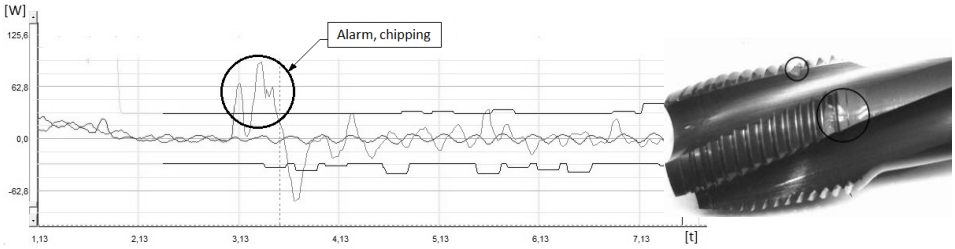

Fig. 6. Derivative function graph with a curve illustrating tool chipping and a sample image of a chipped screw tap detected during machining

In practice, defining appropriate work tolerance limits for a given tool in a process is difficult and requires conducting thorough process and applying many advanced parameters and additional functions.

Achieving tool life

The following analysis is a continuation of research works related to the previously presented drilling process and concerns an attempt to systematise the achieved tool life (a drill for deep drilling). A long-term data analysis focused on this one tool in a given production process showed very unstable work. As a result, with assumed tool life on the level of 600 pieces declared by the producer, a significant part did not perform even a half of the assumed number. Figure 7 presents an example of a tool which was chipped after machining 300 pieces.

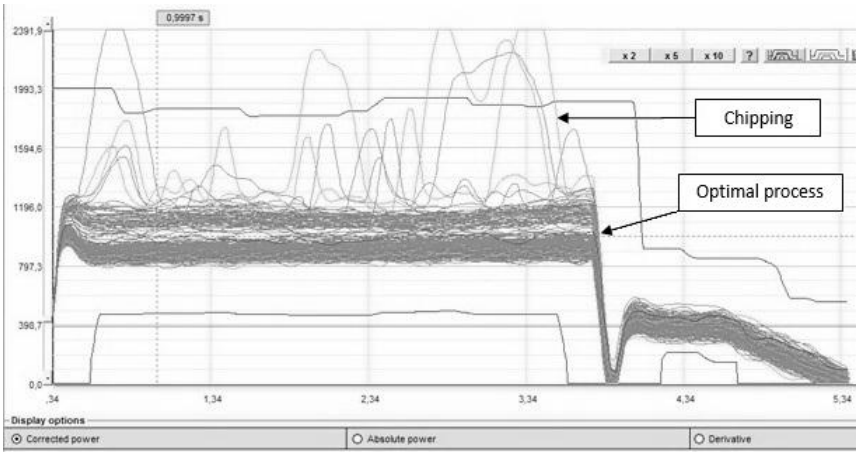

Fig. 7. Visualization of about 300 machining curves (deep drilling) – with signs of process instability

Within the conducted project, in order to achieve the assumed tool life level, activities related to tool geometry verification and modification were undertaken, basing on the gathered and visualized data from the course of tool work in the period of several months.

Another graph (fig. 8) relating to the same machining process, performed on the database of 1000 machining cycles using one tool, is a result of a developed concept of new tool geometry, which in the phase of further usage (testing) showed that, the applied changes respond to customer requirements and they achieve, and even exceed the tool life declared by the producer.

In influence of regeneration on tool work

The next analysis is related to economical aspects – regenerating tools. It is much more profitable (less costly) to finish using a given tool for machining early enough, not to lead to excessive wear, chipping or breakage (fig. 9) and be able to regenerate it and use it the process.

The cost of tool regeneration (that is bringing back its original geometry) is often a few times lower than the cost of a new tool. However, it happens that tools after regeneration are not suitable for further work much earlier than initially assumed (fig. 9). The research conducted in this area also showed the results of inappropriately performed regenerations.

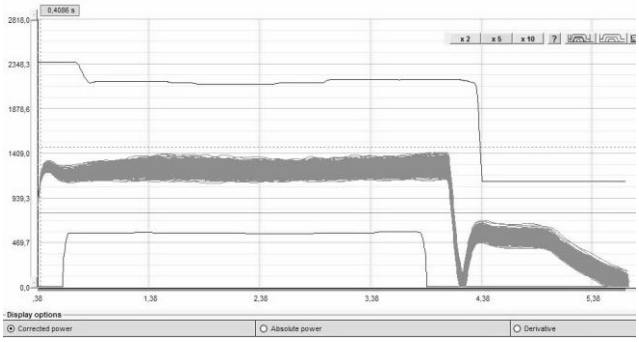

Fig. 8. Visualization of 1000 machining curves – optimal process

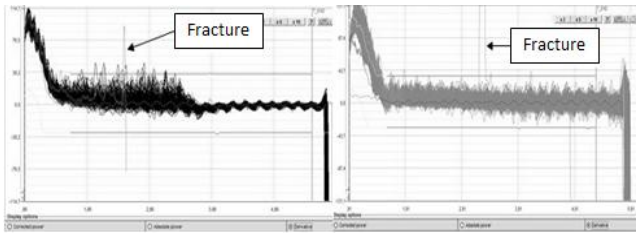

Fig. 9. Regenerated screw tap – syndromes of improper sharpening, too many curves exceeding the assumed tolerance limits (own study)

On the basis of this example the tolerance limits were narrowed, as in the end the tool was broken anyway. Solving this type of problem is not easy. The difficulty lies in finishing the work of a new or regenerated tool early enough, so that it can undergo regeneration as long as possible and that the regeneration makes sense – the greater the tool wear, the weaker effect its regeneration will bring.

The influence of material structure on its machinability

It often happens in production practice that due to optimization of final product characteristics, there is a need to introduce technological changes and changes to the machined material composition. Figure 10 presents machining of 2 components produced from alloy of different hardness. On the basis of the data gathered by the system it was stated that 'type2' detail made from the harder alloy exhibits better machining properties, with lower load of the machine-tool system. This lets us suppose that in the long-term tool life will be prolonged, however, this process requires further observation and analysis.

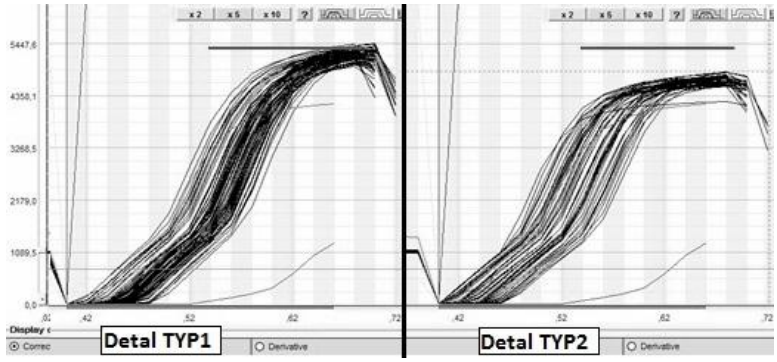

Fig. 10. Machinability tests of details manufactured from materials of different composition

Reducing cycle time and control frequency

Most machining centres are equipped with a mechanism used to control tool presence of lack of tool (also fractures) by means of contact. This solution aims at informing an operator about machine 'condition' after the performed work. Each tool control performed in this way takes about 1.5–2 seconds. With a tool work monitoring system, it is possible to completely resign from this type of control, as the system will do the same in real time, informing a user about actual tool condition, even in case of minor chipping. As a result, machining cycle time for one element on a unit using 10 machining tools can be reduced by 20 seconds.

A fully implemented and properly parametrised system, after a series of studies and analyses, can, in the long run, reduce the frequency of statistical process control, which is particularly time consuming in the automotive sector due to rigorous quality requirements. This will contribute to full automation of the control process, its quality and widely understood cost reduction.

5. SUMMARY

The level of machining processes optimization using advanced tool wear monitoring systems will be strictly dependent on the experience of staff operating a given system. Using this kind of software in practice may lead to increased requirements faced by tools manufacturers on the basis of growing awareness of technologists and engineers in the area of advanced inter-process monitoring techniques. Conducting long-term analyses is a starting point to identify abnormalities in own process due to tool faults (with excluded share of material faults), and a signal to start conducting common research and development projects with tool suppliers. Another aspect is an emerging possibility of using a connection between a tool monitoring system and a specialized and innovative software as elements of Industry 4.0. Connecting the tool monitoring system, its software on the operator's panel, and additionally plugged PC panel with a well-developed application for data analysis made it possible to diagnose early symptoms of an approaching anomaly related to electrospindle's operation. This way the conducted research reached a practical aspect and contributed to initiating works on a new application aimed at diagnosing and early warning, according to the idea of 'talking machines'. These analyses will also facilitate the decisions related to tool purchasing and parameterization. The described solutions allow also to conduct research on tool quality offered by different producers, thanks to which we can achieve a balanced management level in the area of own tool management costs. Continuous development in the automotive industry, all information and innovative solutions which allow to increase effectiveness of the conducted production activity create a chain of added value, which significantly increases widely understood enterprise competition on the dynamically changing global market.

REFERENCES

Addona, D. M. D., & Teti, R. (2013). Image data processing via neural networks for tool wear prediction. *Procedia CIRP*, *12*, 252–257. doi: 10.1016/j.procir.2013.09.044

Barreiro, J., Fernández-Abia, A. I., González-Laguna, A., & Pereira, O. (2017). TCM system in contour milling of very thick-very large steel plates based on vibration and AE signals. *Journal of Materials Processing Technology*, 246, 144–157. doi:10.1016/j.jmatprotec.2017.03.016

Jemielniak, K. (2002). *Automatyczna diagnostyka stanu narzędzia i procesu skrawania*. Warszawa: Oficyna Wydawnicza Politechniki Warszawskiej.

Jurko, J. (2007). Monitoring and Diagnosis of Drill Wear and the Thermodynamic Phenomenas of Material Removal by drilling of Stainless Steels. In: E.E. Gdoutos (Ed.) *Experimental Analysis of Nano and Engineering Materials and Structures* (vol. 37, 77–78). Dordrecht: Springer. doi: 10.1007/978-1-4020-6239-1_37

Kious, M., Ouahabi, A., Boudraa, M., Serra, R., & Cheknane, A. (2010). Detection process approach of tool wear in high speed milling. *Measurement*, *43*, 1439–1446. doi:10.1016/ j.measurement.2010.08.014

Kuljanic, E., & Sortino, M. (2005). TWEM a method based on cutting forces monitoring tool wear in face milling, *Mach. Tools Manuf. J.*, *45*, 29–34. doi:10.1016/j.ijmachtools.2004.06.016

Kuryjański, R. (2011). *Obróbka skrawaniem i obrabiarki*. Warszawa: Expol.

Nouri, M., Fussell, B. K., Ziniti, B. L., & Linder, E. (2015). Real-time tool wear monitoring in milling using a cutting condition independent method. *International Journal of Machine Tools and Manufacture*, *89*, 1–13. doi:10.1016/j.ijmachtools.2014.10.011

Storch, B. (2001). *Podstawy obróbki skrawaniem*. Koszalin: Wydaw. Politechniki Koszalińskiej.

Więcek, D. (2013). Implementation of Artificial Intelligence in Estimating Prime Costs of Producing Machine Elements. *Advances in Manufacturing Science and Technology*, *37*, 43–53. doi: 10.2478/amst-2013-0004

Wittbrodt, P. (2014). Nadzorowanie i prognozowanie stanu narzędzi skrawających w procesie skrawania. *Innowacje w Zarządzaniu i Inżynierii Produkcji* (cz. 1, 833–834). Zakopane: Oficyna Wydawnicza Polskiego Towarzystwa Zarządzania Produkcją.

Applied Computer Science, vol. 13, no. 4, pp. 20–34
doi: 10.23743/acs-2017-26

Submitted: 2017-10-08
Revised: 2017-10-19
Accepted: 2017-12-01

resource-constrained multi-stage project scheduling, discounted cash flows, milestones, priority algorithms

Marcin KLIMEK[*]

PRIORITY ALGORITHMS FOR THE PROBLEM OF FINANCIAL OPTIMISATION OF A MULTI-STAGE PROJECT

Abstract

The article presents the problem of the financial optimisation of a multi-stage project from the contractor's perspective, where customer's payments are analysed as a cash inflow (contractor's revenues) after completing contractual stages and contractor's expenses incurred for the activities executed. In order to solve the problem, priority algorithms are proposed: single-pass and multi-pass ones, using different priority rules and techniques for generating solutions dedicated to the investigated optimisation model. The article presents a comparison of the effectiveness of individual algorithms in the case of adequately prepared test problems.

1. INTRODUCTION

One of the most frequently discussed optimisation issues is the problem of project scheduling with limited availability resources, known as RCPSP (Resource-Constrained Project Scheduling Problem). Various types of resources, methods of executing activities, optimisation criteria, etc. are analysed for RCPSP. An overview of the research can be found in review publications (Hartmann & Briskorn, 2012; Józefowska & Węglarz, 2006). In practice one of the more important aspects of planning a project is the financial optimisation of the project, where in the course of scheduling work activities considerations are given to all cash flows associated with the project, which, in most research studies, are discounted, i.e. the value of their actual NPV (Net Present Value) is calculated

[*] State School of Higher Education, Department of Computer Science, Sidorska 95-97, Biala Podlaska, m.klimek@dydaktyka.pswbp.pl

at an assumed discount rate. Models of maximising discounted cash flows, referred to as RCPSP-DC (RCPSP with Discounted Cash flows), PPS (Payment Project Scheduling) (Mika, Waligóra & Węglarz, 2005; Ulusoy, Sivrikaya-Serifoglu & Sahin, 2001) are considered.

Payment project scheduling is analysed here from the contractor's point of view with maximisation of the discounted cash flows for a project in which the customer establishes, in conjunction with the contractor, the contractual work stages (milestones): deadlines for their completion and the amounts of payments. In the settlements between the customer and the contractor, a penalty system is applied, whereby penalties are imposed for missing the contractual deadline for the realisation of a project stage, to motivate the contractor to complete the project as fast as possible. Failure to meet contractual deadlines for the realisation of project stages leads to charging penalties reducing customers's stage payments to the contractor. In spite of the risk of penalties for untimely execution, the proposed settlement model is beneficial to the contractor since it enables them to obtain earlier payments from the customer for performing the activity, which they can spend on current business, such as completing new activities, purchasing necessary materials, salary payments etc.

The proposed original model of project financial optimisation with defined milestones can be useful in practice. Its application may lead to increasing the control over the process and its timely realisation. The proposed RCPSP model, apart from the author's works, has not been considered in other research studies. In this model staged cash flows are analysed for project scheduling with multiple ways of executing activities, referred to as MMRCPSP (Multi-Mode RCPSP) (He, Wang, Jia & Xu, 2009).

This paper analyses the problem of scheduling a project with limited availability of renewable resources and with one way of executing the activity (single-mode RCPSP), adhering to the criterion of maximising the sum of discounted cash flows: with customer's payments for the completed stages of the project, with contractual penalties for not meeting the deadlines and with contractor's expenses incurred for activity realisation. The aim of the paper is to analyse the effectiveness of the developed priority algorithms for the problem under consideration, in which different priority rules and dedicated techniques for generating a solution are applied, using a forward or backward scheduling strategy with stage shift procedures, or schedule justification. Computational experiments are conducted for the test instances from the PSPLIB (Project Scheduling Problem LIBrary) (Kolisch & Sprecher, 1997), with additionally defined contractual project stages and defined cash flows for financial settlements of works.

2. FORMULATION OF THE PROBLEM

The classic problem of scheduling a project with nonpreemptive activities (tasks) and with one way of executing them is analysed (single-mode RCPSP). The proposed optimisation criterion is the maximisation of the sum of discounted cash flows from the contractor's point of view with the expenditure related to activity realisation and with revenues obtained for executing the contractual stages of the project:

$$F = \sum_{i=1}^{N_A} \frac{CFA_i}{(1+\alpha)^{ST_i}} + \sum_{m=1}^{N_M} \frac{CFM_m}{(1+\alpha)^{MT_m}}, \tag{1}$$

with the following constraints:

$$ST_i + d_i \le ST_j, \qquad \forall (i,j) \in E, \tag{2}$$

$$\sum_{i \in J(t)} r_{ik} \le a_k, \qquad \forall t : t = 1, ST_{N_A+1}, \forall k : k = 1,..K, \tag{3}$$

and for defined contractual stage settlements:

$$MT_m = \max_{i \in MA_m}(FT_i), \qquad \forall m : m = 1,\ldots,N_M \tag{4}$$

$$CFM_m = MP_m - MC_m \cdot \max(MT_m - MD_m, 0), \qquad \forall m : m = 1,\ldots,N_M, \tag{5}$$

where: F – objective function, sum of discounted cash flows from the perspective of the project contractor,
i – activity index, $i = 1, ..., N_A$ (N_A – number of activities),
m – index of the project stage, $m = 1, ..., N_M$ (N_M – number of stages),
CFA_i – the contractor's expenses related to the execution of activity i,
α – discount rate,
ST_i – starting time of the activity i,
CFM_m – customer's payment for the execution of the m-th project stage (revenues from the contractor's perspective) set for the current schedule,
MT_m – completion date of the m-th project stage in the planned schedule,
d_i – duration of the activity i,
E – a set of arcs showing the sequential dependencies between activities of finish-start zero-lag precedence type in the project representation shown as a directed graph $G(V, E)$, wherein V is a set of edges corresponding to activities,
$J(t)$ – a set of activities which are executed during the period $[t–1, t]$,

r_{ik} – demand of the activity i for resources of the type $k = 1 \ldots K$ (K – number of resource types),
a_k – availability of renewable resources of the type k (throughout the duration of the project), the number of the resources used at each moment t cannot exceed a_k,
MA_m – a set of activities to be executed at the m-th project stage,
FT_i – completion date of the activity i ($FT_i = ST_i + d_i$),
MP_m – customer's payment to the contractor for completing m-th project stage,
MD_m – contractual deadline of the m-th project stage,
MC_m – contractual unit penalty for exceeding the deadline of the m-th stage of project MD_m.

The objective of scheduling is to maximise the sum of discounted cash flows (see: formula 1) with precedence constraints (see: formula 2) and resource constraints (see formula 3) and considerations for financial settlements: the contractor's expenses for the activities performed and the customer's stage payments.

In order to determine stage settlements, the following are determined (e.g. by negotiation between the customer and the contractor, whose aim is to find a solution that satisfies both parties), the MA_m group of activities to be performed at a given stage of the project, deadlines for their realisation MD_m, the amount of customer's payments MP_m and contractual unit penalties MC_m for delays in activity completion by the contractor. The system of stage settlements can be useful in practice, because of the benefits of its implementation, both for the customer and the contractor, it may lead to reducing the problem of untimely project completion.

To illustrate the analysed optimisation model, let us consider an example project consisting of 8 activities being realised with the use one resource type with availability equal to 10. This project is shown in fig. 1. using AON (Activity-On-Node) representation. Three contractual project stages (milestones) have been defined:

- stage 1, where $MA_1 = \{0, 1, 2\}$ activities are executed, with contractual completion date $MD_1 = 4$, for which the customer's payment is equal to $MP_1 = 50$, which may be reduced by the cost of possible work delays, calculated on the basis of unit cost $MC_1 = 4$,
- stage 2, at which $MA_2 = \{3, 4, 5\}$ activities are executed, with contractual completion deadline $MD_2 = 8$, for whose completion the customer pays the amount $MP_2 = 50$, which may be reduced by the cost of possible work delays, calculated on the basis of unit cost $MC_2 = 4$,
- stage 3, completing the project, upon which activities $MA_3 = \{6, 7, 8, 9\}$ are performed, within the contractual deadline $MD_3 = 12$, for which the customer makes the payment of $MP_3 = 80$, reduced by the cost of possible delays in project completion, calculated on the basis of unit cost $MC_3 = 10$.

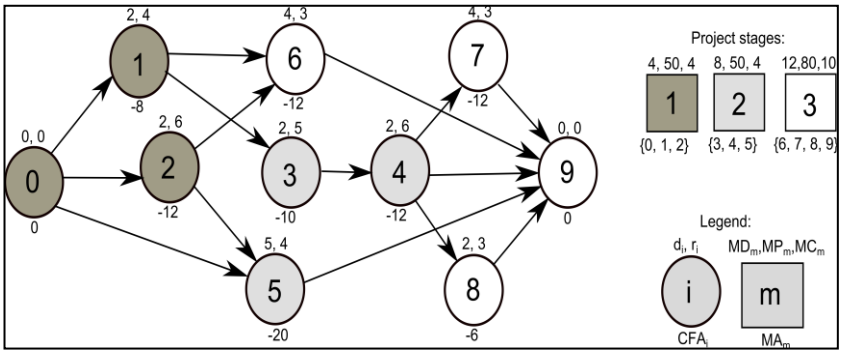

Fig. 1. An example project with staged settlements in AON representation

A discount rate $\alpha = 0.01$ is adopted in the calculation of discounted cash flows.

In relation to the defined contractual cash flows connected with the project, its contractor develops a schedule in which, from their perspective, the sum of discounted cash flows F is maximised (see: formula 1). The growth of F leads to delaying expenses (negative cash flows) borne at the beginning of the activity (lower discounted value) and early acquisition of the customer's payments (positive cash flows) made upon the completion of project stages (higher discounted value). The following part of the article proposes techniques of generating schedules dedicated to the analysed financial problem of multi-stage project optimisation.

3. SCHEDULE GENERATION TECHNIQUES

The solution to the RCPSP (in direct representation) is usually a vector of activity starting time values, on the basis of which an objective function is determined, e.g. the duration of the project or the sum of the discounted cash flows of the project. When searching for a solution, a "convenient" indirect representation is applied, where schedules are encoded, most often as an activity list, a permutation of activities numbers with considerations for precedence relations. For a given activity list, a sequence that meets precedence and resource constraints is determined using decoding procedures SGS (Schedule Generation Scheme) i.e. serial SGS, parallel SGS etc. (Kolisch, 1996a). When building a solution with SGS, it is possible to use forward scheduling or backward scheduling. The analysis of algorithm efficiency and solution generation techniques for RCPSP can be found in review studies (Hartmann & Kolisch, 2000; Kolisch & Hartmann, 2006).

For RCPSP-DC, as well as for the analysed problem of the financial optimisation of a multi-stage project, forward or backward scheduling found through SGS procedures can be improved. Different techniques of generating solutions are used, i.e. bidirectional SGS, right shift or left shift algorithms,

whose overview can be found in work (Vanhoucke, 2006). These techniques are used for developing schedules in which activities (stages) with assigned positive cash flows are started as soon as possible, while the activities (stages) related to the negative cash flows are planned for realisation as late as possible.

With regard to the analysed problem, from the contractor's perspective, it is advisable to collect the customer's payments for completed contractual work stages as soon as possible and incurring expenses related to commenced activities as late as possible (an increase of F always brings about postponing activities, which does not alter the time of completing project stages). Completing of project stages earlier than contractual deadlines stipulate may generate benefits owing to the higher NPV value of the customer's payments made earlier.

Due to the lack of procedures that would generate a solution suitable for the analysed model, the author develops and tests various techniques of creating schedules in their research: dedicated SGS procedures, algorithms activity shifting: right shift (forward scheduling) or left shift (backward scheduling) (Klimek & Łebkowski, 2015b), justification of schedules. In this work, two effective techniques are applied in the developed priority algorithms:

- justification which takes into consideration deadlines for completing contractual project stages,
- backward scheduling in the course of optimising (moving) completion times of contractual work stages (Klimek & Łebkowski, 2015a).

Justification techniques (Valls, Ballestin & Quintanilla, 2005) are used for improving the schedule, found using SGS, and are used for RCPSP, among others for the problem of minimising project duration or the problem with defined activity completion deadlines (RCPSP with Due Dates). One distinguishes RJ (Right Justification) and LJ (Left Justification). Justification of a given activity to the right (left) consists in determining the latest (earliest) possible starting time for this activity, with considerations for precedence and resource constraints. In this study active-ities of maximum finish time (minimum starting time) are successively subjected to right (left) justification in a changing schedule (justification by extremes).

When generating solutions for RCPSP, techniques such as double justification by extremes, successively RJ+LJ or LJ+RJ are used. For the analysed problem it is necessary to modify RJ - when the activities are justified, the current work stage completion time should be considered. For a forward generated schedule, it is advisable to use triple RJ+LJ+RJ justification, which will transform the solution so that the activities are started as late as possible at the earliest possible completion of contractual project stages.

The effect of triple RJ+LJ+RJ justification is shown in fig. 2d.

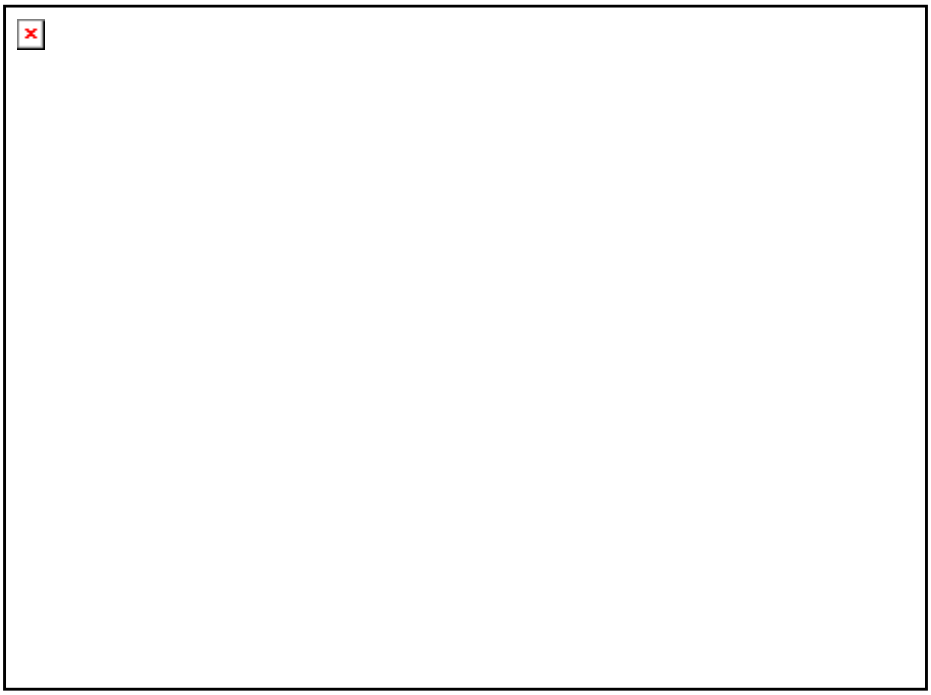

Fig. 2. a) The forward schedule generated using the serial SGS for the activity list {1, 3, 5, 2, 6, 4, 7, 8}; b) Schedule after RJ; c) Schedule after RJ+LJ; d) Schedule after RJ+LJ+RJ

In fig. 2a a schedule generated using the SGS serial procedure for the activity list {1, 3, 5, 2, 6, 4, 7, 8} (value of the objective function for this solution $F = 63.94$) is presented. This schedule is subjected to right justification, for which successive activities with a maximum time of completion are chosen – activities 7, 8, 4, 6, 5, 3, 2, 1 (when they have the same completion time, the activity with a higher number is analysed earlier). The modified technique of justification to the right of a given activity consists in setting the starting time as late as possible, so as not to exceed the current completion time of the project stage ($MT_1 = 2$, $MT_2 = 9$, $MT_3 = 13$), to which this activity belongs, taking into account the precedence and resource constraints. As a result of right justification, thanks to the postponed start of activities 3, 5, 6 and 8, a schedule with a higher value of the objective function $F = 65.29$ is created.

Then left justification is performed for the schedule from fig. 2b which is followed by successive activities with a minimum starting time of respectively 1, 2, 5, 3, 4, 6, 7, 8 (where the starting time is equal, the activity with a lower number is analysed first). As a result of LJ, the schedule shown in fig. 2c with a higher value of the objective function $F = 78.88$ is created due to the earlier execution of stages 1, 2 and 3 ($MT_1 = 2$, $MT_2 = 7$, $MT_3 = 10$) and meeting contractual deadlines for their completion.

The schedule from fig. 2c is subjected to a modified RJ technique with the assumption of new completion times of contractual project stages (MT_1 = 2, MT_2 = 7, MT_3 = 10). Activities 7, 6, 8, 5, 4, 3, 2, 1 undergo successive justification, and the new schedule is created, shown in fig. 2d, with the objective function value F = 78.94, higher than the schedule in fig. 2c, due to the later start of the activity 8. The schedule in fig. 2d is the final solution to the analysed problem obtained by using the triple justification technique for the activity list {1, 3, 5, 2, 6, 4, 7, 8}.

The backward scheduling procedure for optimising (shifting) the completion times of contractual work stages is yet another technique for generating solutions used in this paper. This technique performs unitary time shifts of the planned completion time MT_m. Individual shifts of all the stages are analysed starting from the first one and ending with the last one. They continue to be conducted as long as this operation increases the value of the function F. The process of optimising completion times of contractual work stages is illustrated in fig. 3.

The backward schedule arranged for the analysed activity list {1, 3, 5, 2, 6, 4, 7, 8}, the serial SGS, with such completion times for stage completion as contractual deadlines, are shown in fig. 3a (value of the objective function for this solution F = 77.52). The procedure of the left shifts for the stages of the project is as follows:

- the left shift of the first stage, assuming the shift of the MT_1 = 3 for stage completion by one unit, the objective function value F increases from 77.52 to 77.92, assuming the shift of the MT_1 = 2 stage completion time by a successive unit, the objective function value F increases from 77.92 to 78.22 due to the increased discounted first stage payment, it is not possible to complete the first stage within the MT_1 = 1 due to the duration of activities executed at this stage (d_1 = 2, d_2 = 2), the procedure proceeds to the second stage of works;
- the left shift of the second stage, assuming a shift of the MT_2 = 7 by one unit increases the value of the objective function F from 78.22 to 78.28 due to the increased discounted second stage payment, it is not possible to complete the second stage within the MT_2 = 6 because with such setup the starting time of activity 1 or activity 2 is determined as "negative", the procedure proceeds to the third stage of works;
- the left shift of the third stage, assuming a shift of the MT_3 = 11 stage completion time by one unit, the objective function value F increases from 78.28 to 78.71, assuming a shift of the MT_3 = 10 stage completion time by a successive unit, the objective function value F increases from 78.71 to 78.94 due to the increased discounted payment for the third stage, it is not possible to complete stage within the MT_3 = 9 because at this time the starting time of activity 1 or activity 2 determined by the backward procedure is "negative", the algorithm terminates.

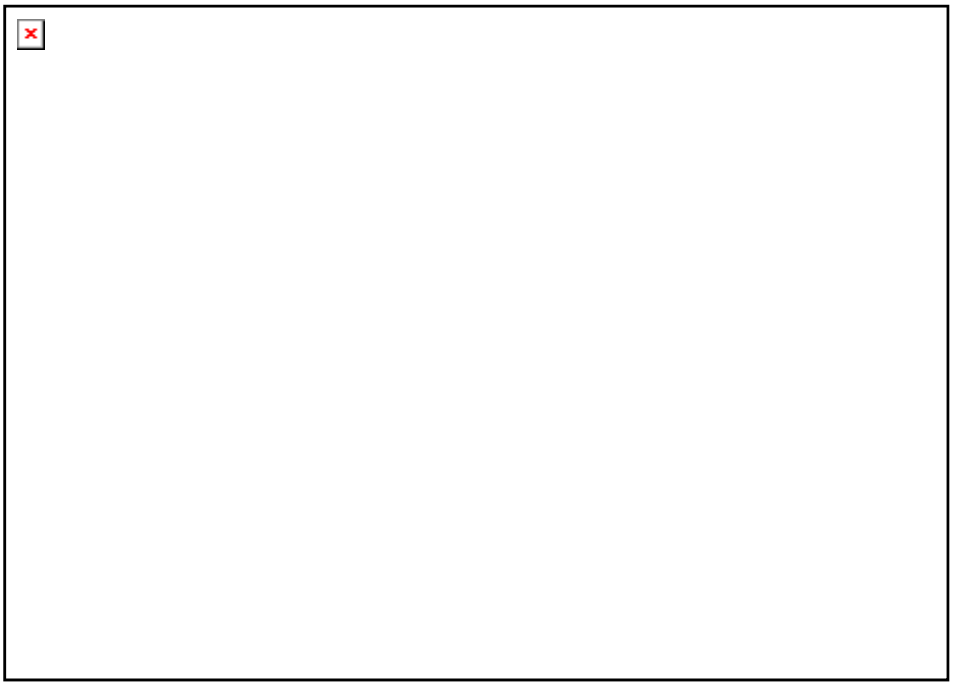

Fig. 3. a) The backward schedule generated using the serial SGS for the activity list {1, 3, 5, 2, 6, 4, 7, 8} and at the completion times for stages $MT_1 = MD_1 = 4$, $MT_2 = MD_2 = 8$, $MT_3 = MD_3 = 12$; b) The backward schedule determined as a result of the optimisation of the completion time for the first stage of the project $MT_1 = 2$, $MT_2 = 8$, $MT_3 = 12$; c) The backward schedule determined as a result of the optimisation of completion times for the first and the second stage of the project for $MT_1 = 2$, $MT_2 = 7$, $MT_3 = 12$; d) The backward schedule determined as a result of the optimisation of completion times for all the stages of the project for $MT_1 = 2$, $MT_2 = 7$, $MT_3 = 10$.

The schedule presented in fig. 3d was created after subjecting the project stages to left shifts in time.

4. PRIORITY ALGORITHMS

The problem of scheduling a project with limited resources as a generalisation of the job shop problem is a considerably NP-Hard problem (Błażewicz, Lenstra & Kan, 1983), for which it is more practical to use effective approximate heuristic algorithms finding solutions within an acceptable time period, especially for larger problems. A review of the heuristics used for RCPSP and a comparison of their effectiveness can be found in literature (Hartmann & Kolisch, 2000; Kolisch & Hartmann, 2006).

Amongst the heuristic algorithms one may distinguish constructive heuristics (priority, insertion) which create inaugural solutions for local search algorithms (simulated annealing, genetic algorithms). The aim of this work is to establish the effective priority heuristics that use SGS procedures and presented scheduling techniques that construct a schedule based on an activity list built in an ascending order of priorities of particular activities calculated for the adopted priority rules. The following procedures are analysed:

- single-pass ones - creating one solution based on an activity list arranged in an ascending order of activity priorities, they are quick and very easy to implement but they are characterised by low efficiency, even for the most effective priority rules: LFT (Latest Finish Time), EFT (Earliest Finish Time), MTS (Most Total Successors) and MTSPT (Most Total Successors Processing Time),
- multi-pass, X-pass ones - creating more potential schedules, algorithms that apply multiple priority rule methods at the same time, or sampling methods in which priority activities are randomly assigned with considerations for the applied priority rule.

One pass of the proposed multi-pass heuristics, in which one activity list *L* is generated, may be described as follows (Klimek, 2010):

Step 1:
Setting an empty activity list *L*. Placement of all of the successors with the initial operation number 0 on the list *LA* in the order determined by the priorities of the activities determined for the applied priority rule.

Step 2:
Selecting randomly one activity *i* from the list *LA* with considerations for "chances" determined on the basis of the ranking of the activities on the list *LA*: the first activity has the highest number of chances for selection, equal to the number of activities on the list *LA*, ..., the last activity has one chance for selection.

Step 3:
Deletion of the randomly selected activity *i* from the list *LA* and putting it on the list *L*. Adding all the successors of the activity *i*, of which all the predecessors are already on the list *L*, to the *LA* retaining the order established on the basis of the priorities of the activities assigned to the applied priority rule.

Step 4:
Repetitions of steps 2-3 until the list *L* is complete with all the activities carried out in the project.

In each pass, the resultant activity list L is decoded using SGS procedures and modified using solution generating techniques dedicated to the analysed problem (forward scheduling and justification technique, backward scheduling with optimisation of stage completion times). The result of a multi-pass algorithm is the schedule of the highest value of the objective function F (see formula 1), determined for all the passes from the analysed activity lists L.

The effectiveness of the developed heuristics can be influenced by the applied priority rules (Kolisch, 1996b). Table 1 presents the priority rules (rules R_0–R_6), developed for the investigated problem of the financial optimisation of a multi-stage project, which are used in computational experiments.

Tab. 1. Priority rules

Rule	Rule description
R_0	random priorities of activities
R_1	the minimum latest starting time of the activity with considerations for the contractual deadlines for the completion of project stages
R_2	minimum latest deadline for the completion of the activity with considerations for the contractual deadlines for the completion of project stages
R_3	maximum number of all the successors of the activities
R_4	the maximum sum of the duration periods of a given activity and all of its successors
R_5	the minimum number of the project stage in which the activity is performed, the minimum cost of the activity CFA_i at the same stages
R_6	minimum cost of the performance of the activity

If, when using a given priority rule, the activities have the same priorities, the activities marked with lower numbers are listed in the earlier position in the activity list.

5. COMPUTATIONAL EXPERIMENTS

The experiments were conducted with a computer Intel Core I7, 3.0 GHz, 8 GB RAM and using an application implemented in the C# programming language of the Visual Studio.NET environment for test instances from the PSPLIB within the set J30 (480 30-activity instances) and J90 (480 90-activity instances). The manner of defining contractual project stages for each project from PSPLIB is the following:

- baseline schedule S is created using the serial SGS procedure for an activity list sorted in the ascending order of activity numbers {1, 2, ..., 30} for the set J30 or {1, 2, ..., 90} for the set J90,
- three stages of project are set for the accepted deadlines: $MD_1 = T/3$, $MD_2 = 2T/3$ and $MD_3 = T$, where T is the duration of the project in the baseline schedule S, successive sets of activities MA_m performed at individual

stages are determined on the basis of the baseline schedule S. The set MA_1 includes all the activities whose completion time is lower than or equal to MD_1. The set MA_2 includes all the activities whose completion time is lower than or equal to MD_2 and greater than MD_1, while the set MA_3 contains the remaining activities.

In the financial settlements for each test instance: $MP_1 = 60$, $MP_2 = 60$, $MP_3 = 120$, $MC_1 = 1.5$, $MC_2 = 1.5$, $MC_3 = 3$, while the costs related to the execution of activitiess CFA_i are determined as proportional to the total demand for resources and time spent on a given activity assuming their sum for all the activities is 100:

$$CFA_i = \frac{d_i \cdot \sum_{k=1}^{K} d_{ik}}{\sum_{j=1}^{N_A} (d_j \cdot \sum_{k=1}^{K} r_{jk})} \cdot 100, \qquad \text{for} \quad i = 1..N_A. \tag{6}$$

The discount rate assumed in the experiments is: $\alpha = 0.01$.

The purpose of the experiments is to verify the effectiveness of the proposed priority heuristics (single-pass and multi-pass), to find the best priority rules (from amongst the rules R_0–R_6) and techniques of generating solutions dedicated to the investigated problem. In randomised multi-pass heuristics for each instance of the problem, the number of verified solutions (passes) is equal 500. In table 3 and 5 are presented average values of the objective function F for 960 experiments (two schedules are generated for each 480 test instances). The results of the computational experiments are presented in tables 2–5.

Tab. 2. The results of the computational experiments for single-pass priority algorithm for the projects in the set J30

	Forward, serial SGS		Forward, parallel SGS		Backward, serial SGS	
	RJ	RJ+LJ+RJ	RJ	RJ+LJ+RJ	–	LJ+RJ
Rule R_0	54.73	66.75	63.26	69.47	62.24	71.63
Rule R_1	67.02	71.41	69.31	72.26	62.81	73.51
Rule R_2	69.57	73.05	69.72	72.51	64.41	74.22
Rule R_3	65.67	71.49	68.79	71.71	63.31	73.29
Rule R_4	63.44	70.27	67.88	71.59	63.64	73.15
Rule R_5	64.11	69.83	67.63	71.19	61.34	72.85
Rule R_6	56.34	66.73	64.20	69.72	62.86	72.08

Tab. 3. The results of the computational experiments for multi-pass priority algorithm for the set J30

	Forward, serial SGS		Forward, parallel SGS		Backward, serial SGS	
	RJ	RJ+LJ+RJ	RJ	RJ+LJ+RJ	–	LJ+RJ
Rule R_0	75.71	77.13	75.29	76.67	77.08	77.45
Rule R_1	77.13	77.47	75.97	76.96	77.17	77.52
Rule R_2	77.13	77.48	75.97	76.99	77.28	77.55
Rule R_3	76.63	77.33	75.71	76.84	77.14	77.53
Rule R_4	76.56	77.26	75.65	76.81	77.09	77.52
Rule R_5	76.57	77.40	75.78	76.94	77.30	77.51
Rule R_6	75.69	77.26	75.38	76.80	77.24	77.48

Tab. 4. The results of the computational experiments for single-pass priority algorithm for the projects in the set J90

	Forward, serial SGS		Forward, parallel SGS		Backward, serial SGS	
	RJ	RJ+LJ+RJ	RJ	RJ+LJ+RJ	-	LJ+RJ
Rule R_0	19.78	39.85	32.27	42.51	29.19	47.95
Rule R_1	36.58	46.17	40.35	46.76	28.99	49.10
Rule R_2	37.78	46.79	41.08	47.16	29.19	49.55
Rule R_3	29.41	43.18	36.65	44.22	29.55	48.73
Rule R_4	27.43	42.90	35.51	43.85	29.25	48.47
Rule R_5	31.55	44.60	38.18	45.54	28.93	48.53
Rule R_6	21.14	40.16	32.55	42.68	29.01	47.36

Tab. 5. The results of the computational experiments for multi-pass priority algorithm for the set J90

	Forward, serial SGS		Forward, parallel SGS		Backward, serial SGS	
	RJ	RJ+LJ+RJ	RJ	RJ+LJ+RJ	–	LJ+RJ
Rule R_0	42.80	50.87	46.17	50.83	50.58	52.49
Rule R_1	49.71	52.25	49.66	51.96	50.71	52.63
Rule R_2	49.37	52.25	49.53	52.00	51.15	52.64
Rule R_3	45.84	51.07	47.66	51.11	50.22	52.58
Rule R_4	45.98	50.78	47.52	50.89	50.00	52.60
Rule R_5	46.73	52.30	48.52	51.97	51.63	52.59
Rule R_6	41.80	51.45	46.30	51.00	51.40	52.53

Applying a multi-pass priority algorithm significantly improves the quality of the generated schedules. The best results are achieved for multi-pass heuristics using combined solution generation techniques: backward scheduling with optimisation of contractual activity completion times and then improvement of the solution by double justification LJ+RJ. For the priority rule R_2 (minimum latest deadline for the completion of the activity), which turned out to be the most effective for both the set J30 and J90, in two experimental studies, this algorithm found 352 or 362 (108 or 102) best solutions from amongst those generated by all analysed heuristics for 480 test instances investigated for the set J30 (J90).

Using effective priority rules improves the quality of the obtained solutions. Schedules generated for algorithms using a rule with random priority activities R_0 are characterised by poor quality – the lowest average value of the objective function F. The effective priority rules are R_1, R_2, R_5. Quality improvement of the solutions is always observed after applying triple justification of schedules.

Using the schedules found by the proposed priority algorithms as initial solutions for metaheuristics can bring good results. It will be the subject of further research studies by the author.

6. CONCLUSIONS

In this paper, the problem of discounted cash flows maximising for a multi-stage project has been discussed from the contractor's perspective. The proposed optimisation model takes into account the expenses assigned to activities and client's payments for the completed stages of the project.

Single-pass and multi-pass priority algorithms for the analysed problem have been presented and tested. These algorithms use techniques of generating schedules with considerations for the specific nature of the discussed problem: activities should be planned as late as possible but with the earliest completion times of the project stages. Appropriate justification and backward scheduling techniques, which take into consideration completion times of contractual project stages, have been developed. The efficiency of priority algorithms and procedures of generation solutions has been verified for test instances from the PSPLIB library. Numerical experiments have confirmed good efficiency of the backward scheduling procedure with optimisation of contractual stages completion times and then improvement of the solution by double justification LJ+RJ.

The investigated issues are important and the results of the research work may be useful in the execution of practical projects in which stage settlements are beneficial for both the contractor and the customer. The proposed priority heuristics will be used to create inaugural solutions in metaheuristics, i.e. simulated annealing, which will be the subject of further research by the author.

REFERENCES

Błażewicz, J., Lenstra, J., & Kan, A. (1983). Scheduling subject to resource constraints classification and complexity. *Discrete Applied Mathematics*, *5*, 11–24.

Hartmann, S., & Briskorn, D. (2012). A Survey of Variants and Extensions of the Resource-Constrained Project Scheduling Problem. *European Journal of Operational Research*, *207*(1), 1–14.

Hartmann, S., & Kolisch, R. (2000). Experimental evaluation of state-of-the-art heuristics for the resource-constrained project scheduling problem. *European Journal of Operational Research*, *127*, 394–407.

He, Z., Wang, N., Jia, T., & Xu, Y. (2009). Simulated annealing and tabu search for multimode project payment scheduling. *European Journal of Operational Research, 198*(3), 688–696.
Józefowska, J., & Węglarz, J. (Eds.). (2006). Perspectives in modern project scheduling. Springer.
Klimek, M. (2010). Predyktywno-reaktywne harmonogramowanie produkcji z ograniczoną dostępnością zasobów (doctoral dissertation). AGH, Kraków.
Klimek, M., & Łebkowski, P. (2015a). Harmonogramowanie projektu rozliczanego etapowo. Kraków: AGH.
Klimek, M., & Łebkowski, P. (2015b). Heuristics for project scheduling with discounted cash flows optimisation. *Bulletin of the Polish Academy of Sciences Technical Sciences*, *63*(3), 613–622.
Kolisch, R. (1996a). Serial and parallel resource-constrained project scheduling methods revisited: Theory and computation. *European Journal of Operational Research*, *90*, 320–333.
Kolisch, R. (1996b). Efficient priority rules for the resource-constrained project scheduling problem. *Journal of Operations Management*, *14*, 179–192.
Kolisch, R., & Hartmann, S. (2006). Experimental Investigation of Heuristics for Resource-Constrained Project Scheduling: An Update. *European Journal of Operational Research, 74*(1), 23–37.
Kolisch, R., & Sprecher, A. (1997). PSPLIB – a project scheduling library. *European Journal of Operational Research*, *96*, 205–216.
Mika, M., Waligóra, G., & Węglarz, J. (2005). Simulated annealing and tabu search for multi-mode resource-constrained project scheduling with positive discounted cash flows and different payment models. *European Journal of Operational Research*, *164*(3), 639–668.
Ulusoy, G., Sivrikaya-Serifoglu, F., & Sahin, S. (2001). Four Payment Models for the Multi-Mode Resource Constrained Project Scheduling Problem with Discounted Cash Flows. *Annals of Operations Research*, *102*, 237–261.
Valls, V, Ballestin, F, & Quintanilla, S. (2005). Justification and RCPSP: a technique that pays. *European Journal of Operational Research*, *165*(2), 375–386.
Vanhoucke, M. (2006). A scatter search procedure for maximizing the net present value of a resource-constrained project with fixed activity cash flows. *Working Paper 2006/417*, Gent, 1–23.

Applied Computer Science, vol. 13, no. 4, pp. 35–44
doi: 10.23743/acs-2017-27

Submitted: 2017-10-25
Revised: 2017-11-13
Accepted: 2017-12-06

mass customization, computer aided planning, TOC

Janusz MLECZKO[*]*, Paweł BOBIŃSKI*[**]

PRODUCTION PLANNING IN CONDITIONS OF MASS CUSTOMIZATION BASED ONTHEORY OF CONSTRAINTS

Abstract

In accordance with the requirements of the modern market, small and medium-sized enterprises (SMEs) need to offer a wide range of products tailored to the specific and individual requirements. The success of many enterprises, which work in mass production system and use economic effect of scale production slowly is a thing of the past. There are many enterprises, generally small and medium manufacturing in unit and small batch production, for which it is necessary to develop optimal methods of production planning, taking into account the flexible production requirements, matched to the time-varying customer's demand. The article presents the production planning based on TOC in conditions of mass customization. Presented solutions are used in modern practice.

1. INTRODUCTION

Companies operating on today's market have been forced to offer a wide range of products for a long time. What is more, realization time does not increase because of this. Clients became more demanding and they want products which meet their individual needs. Instead of mass production, SME's must comply with mass customization (Tien, 2011). For many companies, it means the necessity to use the unit production in many variations. Mass customization forces a change in the approach to product design and implementation of flexible tools for manufacturing

[*]University of Bielsko-Biała, Department of Industrial EngineeringWillowa 2, 43-309 Bielsko-Biała, Poland,phone: +48 33827253, e-mail: jmleczko@ath.bielsko.pl
[**]LiuGong Dressta Machinery, Stalowa Wola, Poland

process. Mass customization forces also a change in business processes in many aspects. The standard approach assumes unified mass production of semi-finished products and manufacturing of product families based on already finished semi-finished products. However, there are product families, for which this approach is not possible. They demand using unit production. The adaptation of production system to the changing needs of the customer seems to be necessary to maintain a competitive advantage in many industries. During manufacturing in such conditions, the role of production planning becomes very important. Increasing the flexibility of organizational production preparation is often a key element of the whole process. The problem that was addressed in this paper concerns the analysis of alternative methods for planning the production of products with short production cycles in conditions of mass customization. The issue of mass customization is widely presented in the literature. The summary of this issue was shown in (Da Silveira, Borenstein & Fogliatto, 2001) and then in 2012, extension (Fogliatto, Da Silveira & Borenstein, 2012) was released. It contained an overview of the literature of the subsequent years. The implementation of mass-customization without the appropriate class of software is virtually impossible (Luo, Tu, Tang & Kwong, 2008; Peng & Heim, 2011). Because of the fact, that above problem, to a large extent, applies to small and medium-sized enterprises, it is particularly important to use adequately simple and low-cost solutions. The implementation of ERP applications for this purpose is largely insufficient. This refers to both: cost area and the need to adapt the ERP application to product families management requirements. Applications to efficient management of configurable products manufacturing in small and medium-sized enterprises are rather known only in theory than in practice (Kumar, 2007).The general trend in recent years is moving away from mass production to mass customization (Kumar, 2007; Tien, 2011). The be-ginning of this meth-odology was engineered or the order strategy (Haug, Ladeby & Edwards, 2009).

2. PROBLEM FORMULATION

The problem discussed in this work concerns the manufacturing of high-variety products. To solve this problem the point is to find answers to the following questions:

- What data and what algorithms are necessary for the automatic process of gene-rating production plan for high-variety products?
- What knowledge bases to extend the ERP system for the production of high-variety products is necessary?
- Does the change of the planning method have a major impact on the or-ganization of the manufacturing process in conditions of mass custom-ization?

3. METHODS USED FOR THE CREATION OF PRODUCTION PLANS

The problem of the production flow of machine elements in conditions of unit and small batch production can be presented in a mathematical form. The solution to this task is a working schedule of individual production workstations. To define a model of the manufacturing process the following definitions, designations and assumptions were assumed (Mleczko, 2014).

An order – involves execution of the actions called operations, each of which requires the involvement of specific resources. An order can be a production process of set of elements in machine industry, an assembly process or processing batch of material for process production. The order is characterized by the following attributes:

- planned start date,
- demanded completion date,
- route of the manufacturing process (with the possibility of the multivariate route of manufacturing process).

$Zl = \{Zl_1, Zl_2, \dots, Zl_l, \dots., Zl_L\}$ means set of orders, where $L -$ means number of orders,l – means order identifier.

Each Zl_l order consists of a set of$J_k$jobs represented by $Po_{l,k}$, manufacturing processes

$$Zl_l = \{Po_{l,1}, Po_{l,2},, \dots, Po_{l,i}, \dots, Po_{l,k,}, \dots, Po_{L,K}\} \tag{1}$$

where: K– means number of jobs for the Zl_lorder,
i, k – indicates identifiers of jobs for Zl_l order.

Besides this, for each$J_k$job and corresponding to it manufacturing processes $Po_{l,i}$, $Po_{l,k}$from theZl_l order, a sequential relation is defined:

$$\forall_{i,k \in \{1,\dots,K\}} Po_{l,i} \prec Po_{l,k} \tag{2}$$

Likewise, as the product consists of the elements, such an order is made up of jobs. Jobs are semi-orders for the realization of the element of the product. The set of jobs was marked as *J*. Jobs have a hierarchical structure. To make a job, it is necessary to follow the sequence of operations of the manufacturing process. It is assumed that the realization of the jobs means the realization of the manufacturing process for the product component. The operations are carried out in a sequential system.

Each $Po_{l,k}$ manufacturing processconsists of a set of $O_k$operations. The operations in the job have to be done in the following order (technological order), i.e. every *n* operation has to be done after *n–1*, and before *n+1*. To simplify the notation set of operations of $Po_{j,k}$ process is denoted by O_k.

$$O_k = \{O_k^1, O_k^2, \dots, O_k^n, , \dots . , O_k^N\} \tag{3}$$

A resource– resources are equipment, staff, materials, machines, capital or energy raw materials needed to carry out the operations of the manufacturing process. In the case of resources their three basic categories are taken into consideration:

- reusable (employee, machine, robot),
- consumable (raw materials),
- double-limited (energy, money).

$$M = \{M^1, M^2, \dots, M^a, \dots, M^A\} \tag{4}$$

means a set of resource types (homogeneous in terms of the feasibility of the operation of the manufacturing process), where A – number of resource types (group of workstations), a – resource type identifier.

On each of the workstations operations assigned to the group of workstations can be done.

Reusable resources have limited availability, consumable resources – have limited quantity, and the double-limited – both kinds of limitation.

Among the many important features of reusable resources the most frequently mentioned are:

- availability,
- quantity,
- cost.

The above attributes can be written as

$$M^a = (Ca^a, g^a, K^a) \tag{5}$$

where: Ca^a – calendar of working time of a type of resource specifying availability,
g^a – number of a workstation types,
K^a – labour cost of a resource type.

Using iterative methods to solve scheduling problems guarantees receiving all possible trajectories of decision, leading to receiving the set of schedules, from which we must choose one – fitting the best to our optimization criteria. The process of generating all the possible solutions to this task – due to the high

computational complexity – may not be possible in conditions of unit and small batch production and even more in mass customization. The main barrier, which makes it impossible to carry out a full course of calculations, is most of all the time, which is dependent on the used computer equipment and on the algorithms. In the case of generating a list of solutions using multi-stage programming, there is a possibility to reduce the number of generated solutions, efficiently at the stages prior to the final. This greatly reduces the time of searching for optimal solutions and enables real implementation of the given model under variable manufacturing conditions.

The problem of finding the solution of optimal plan was an issue repeatedly taken into consideration by researchers. It should also be noted – that solution requires high computational power and defining parameters e.g. operations and times, which are challenging to achieve in conditions of mass customization. There are two main reasons for this situation: a very big amount of potential products and defined routes of production process.

For these reasons an alternative solution has been sought. This solution should be good enough, requiring significantly less data and realized in production practice.

4. ASSUMPTIONS OF PRODUCTION PLANNING BASED ON TOC

For the manufacturing system in conditions of high-variety, TOC was used in the production planning process. Following the 5 steps of concentration in the TOC, underlying assumptions were presented.

4.1. Identification of constraints

There are constrains of 2 types in manufacturing enterprises – internal constraints (appearing inside the organization) and external constrains (appearing in the environment of the system and at the market – this constraint is usually a customer demand).

In the case of production in conditions of mass customization, in many cases internal constraints will apply to two areas: the design area and manufacturing area.

According to the theory of constraints, the flow is determined by constrain "bottleneck". The production system was built in such a way that:

1. Given product family (or set of them) was limited by one bottleneck.
2. Due to the simplification of the management system, the bottleneck was located on the last operations in the process (usually assembly operations).
3. Bottlenecks accounted for disjoint set.
4. Bottlenecks were stable – they did not move under the operation of one product family.

Bottlenecks $C_S = \{1, \dots, S\}$ were definied from the process. Due to the variability of resource availability in time (schedule, shift system) it was defined for individual units of time (taken as a basic planning parameter). In the analysed in the further part of this paper example, because of the short manufacturing time in the bottleneck, 1 day was taken as a time unit.

The correlation between the consumption time in bottleneck onproduct family design should also be defined. In many cases product family's options have significant influence on consumption time in bottleneck. It means that dependence between options in a product family and manufacturing time in the bottleneck should also be defined. From the above assumptions results also ability to assign to the product family to one bottleneck, determining the manufacturing process.

The method of production planning assumes multi-level scheme:

1. The division of the manufacturing process into stages:
   a. Production of semi-finished products – separate planning method of the level of semi-finished products – as outlined in chapter 3.
   b. Production of the finished product – planning of assembly manufacturing of finished products and components with high variability resulting from the configuration, that storage in the processed form is pointless, e.g. components dependent on the dimensions.
2. Verification of the availability of raw material.
3. Production planning of the finished product – based on the algorithm of automatic planning and visualization – allowing correction of the plan by the planner in emergency situations.
4. Distribution planning of the finished product.

The multistage planning method assumes sequence of actions 1 to 4, herein in the forward planning method first point 3 is carried out, then point 4. In backward scheduling first point 4 is carried out, next point 3.

Visualization of the process of bottleneck occupation time will enhance the decision making process concerning the deadline for taking orders from customers.

	T1	T2	T3	...	Tn
Cs1	89	67			89
Cs2	35	5			6
Cs3	4	60			4
Cs4	65	6			6
Cs5	56	77			56
...					6
Csn	12	33			12

Fig.1. Example matrix of bottleneck availability

Fig. 1. shows an example of matrix of bottleneck's availability which is crucial for the planning process.

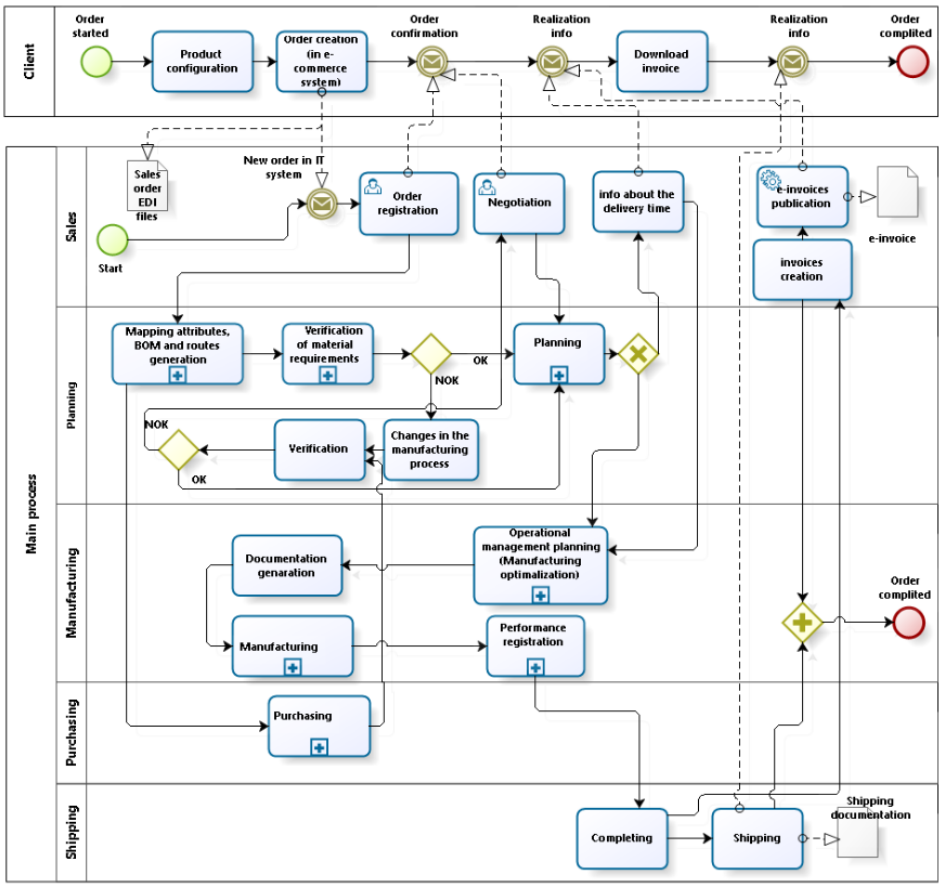

Fig. 2. The main process of production planning

The main process is shown below (Fig. 2.). Further simplification of the planning process results from the adopted assumptions. Since semi-finished products at the level of finished products were separated from manufacturing order, the order takes the form of only one job (subset of order) (Zl_{PR})

$Zl_{PR} = \{Po_{PR}\}$,in manufacturing process Po_{PR}, the operation passing through the bottleneck was separated.

$$O_{PR} = \{O_{PR}^1, O_{PR}^2, \dots, \boldsymbol{O_{PR}^{WG}}, , \dots . , O_{PR}^N\} \tag{6}$$

where O_{PR}^{WG}, means the operation of bottleneck.

The parameters of flow through the bottleneck can also be given in a simplified way:

$$Zl_{PR} = (C_S, O_S^{PR}, \gamma) \tag{7}$$

where: C_S – specified element of the set of bottlenecks in the process, s – bottleneck identifier,
O_S^{PR},– operation on S bottleneck for process of PR finished product,
γ – occupancy of bottleneck expressed by the accepted unit (eg. time) for proces of PR finished product.

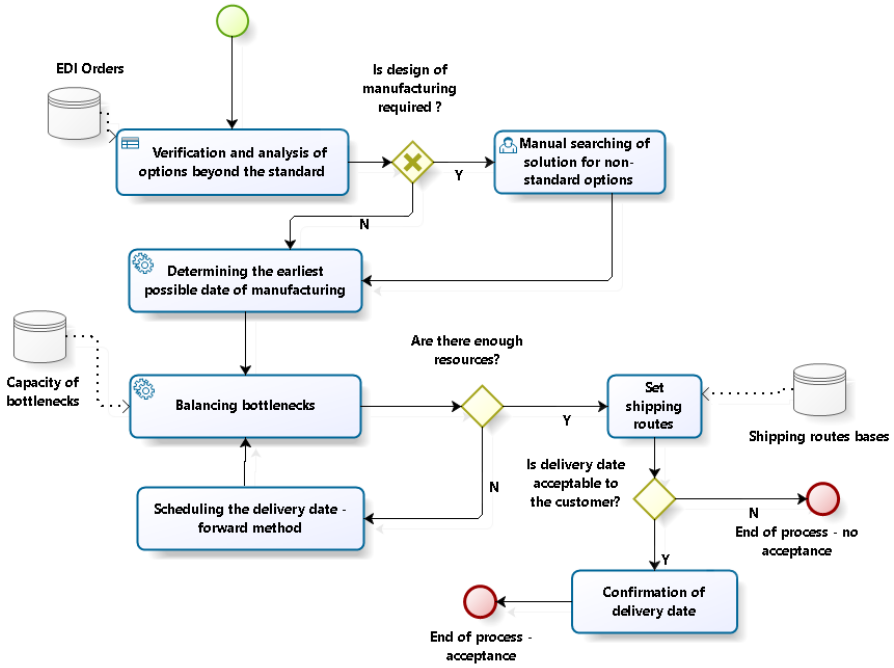

Fig. 3. Process of production planning – „forward" method

4.2. Production planning using forward method

In determining the order of realization of the tasks two strategies for scheduling are basically used – "backward" and "forward" strategies. In some practical solutions mixed method, which is a unique combination of these two strategies, is also used.

Forward scheduling (Fig. 3) answers the question: When manufacturing of the product will be completed, if you know the date of commencement of the associated manufacturing process?

"Forward" scheduling involves making the following algorithm:

- start of production of the product components, as the earliest possible,
- "forward" calculation of the deadlines for the products searching for empty places in the production plan,
- calculation of availability time and quantity of planned to buy materials.

This procedure of forward scheduling enables determination of the earliest date of products availability.

The time needed to manufacture the batch of products, parts or subassemblies is calculated with the using the available data of the operation of the manufacturing process (the time of the task working on the manufacturing resource) for every operation on a specific machine or line.

4.3. Visualization of the production plan

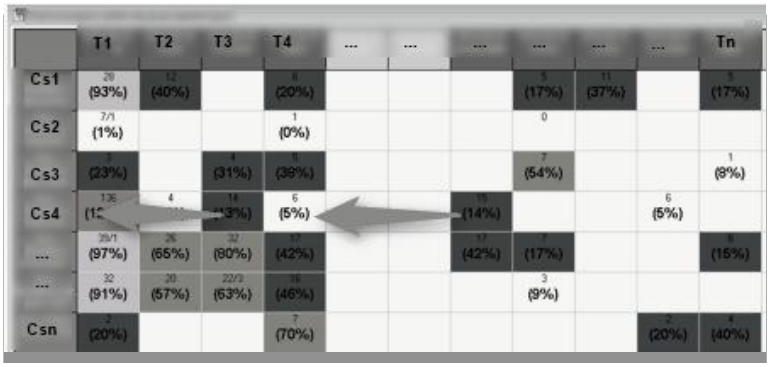

Fig. 4. Visualization of production planning – „forward" method

Fig. 4 showed the result of automatic planning procedures. It is possible to tune the plan by manually moving jobs. In practice, manual tuning is rare and it is used only in exceptional situations. Postponing of the production date results from the prioritization of the delayed or pledged orders.

5. CONCLUSIONS

The change of the planning method has a major impact on the organization of the manufacturing process. In forward planning method, the solution is always found by the system. By moving the completion dates forward, sooner or later the company will find a period of time, in which there are spare

capacities for the fulfilment of customer orders. Of course, the date may be unacceptable for the customer and then the company loses the order. However, it does not have an impact on the increase of the demand for capacities. Unfortunately, in this method we do not really know how much the company loses due to not taking orders because of too distant dates. Moreover, we do not have a major influence on this. In the forward method, a real market demand for capacity in specific bottlenecks was not entirely transparent. Nevertheless, using this method it is possible to significantly automate planning and also reliably and immediately respond to the customer's question about the delivery time. The method was verified for a production, where about 2000 different orders were produced every day. Both studies and production practice have proven utilitarianism of the proposed solutions. After applying this method, studies on the implementation of a more demanding method (backward scheduling) were also carried out.

REFERENCES

Da Silveira, G., Borenstein, D., & Fogliatto, F. S. (2001). Mass customization: Literature review and research directions. *Int. J. Production Economics, 72*, 1–13. doi: http://dx.doi.org/10.1016/ S0925-5273(00)00079-7

Fogliatto, F., Da Silveira, G. & Borenstein. D. (2012). The mass customization decade: An updated review of the literature. *International Journal of Production Economics, 138,* 14–25. doi:http://dx.doi.org/10.1016/ j.ijpe.2012.03.002

Haug, A., Ladeby, K., & Edwards, K. (2009). From engineer- to- order to mass customization. *Management Research News, 32*(7), 633–644. doi: 10.1108/01409170910965233

Kumar, A., (2007). Mass customization: manufacturing issues and taxonomic analyses. *Int. J. Flex. Manuf. Syst., 19*, 625–629. doi: 10.1007/s10696-008-9049-5

Luo, X., Tu, Y., Tang, J., & Kwong, C. K., (2008). Optimizing customer's selection for configurable product in B2C e-commerce application. *Computers in Industry*, *59*, 767–776. doi:http://dx.doi.org/10.1016/j.compind.2008.03.003

Mleczko, J., (2014). *Manufacturing processes creating with use of dynamic classification in conditions of unit and small-batch production*. Bielsko-Biała: Publishing House of University of Bielsko-Biała.

Peng, D. G., Heim, G. (2011). Impacts of information technology on mass customization capability of manufacturing plants. *International Journal of Operations& Production Management, 31*(10), 1022–1047.doi: 10.1108/01443571111182173

Tien, J. M., (2011). Manufacturing and services: From mass production to mass customization. *Journal of Systems Science and Systems Engineering*, *20*(2), 129-154.doi: 10.1007/s11518-011-5166-x

Applied Computer Science, vol. 13, no. 4, pp. 45–55
doi: 10.23743/acs-2017-28

Submitted: 2017-07-14
Revised: 2017-09-09
Accepted: 2017-10-03

physical modelling, Cockroft-Latham criterion, cross-wedge rolling

Łukasz WÓJCIK[*], *Zbigniew PATER*[**]

LIMITING VALUE OF COCKROFT-LATHAM INTEGRAL FOR COMMERCIAL PLASTICINE

Abstract

The paper presents the results of experimental and numerical research in the scope of commercial plasticine cracking. The purpose of the study was to determine the limit value of the Cockroft-Latham integral. The value of the integral was determined on the basis of the stretching test and computer simulations. Experimental studies utilized axially symmetrical samples made of commercial black and white wax based plasticine. Samples were cooled to 0, 5, 10, 15 and 20°C. After the completion of experimental studies, finite element numerical simulation was performed under the conditions of 3-dimensional state of deformation in DEFORM 3D simulation software. Based on the results of experimental and numerical studies, the Cockroft-Latham limit value was calculated.

1. INTRODUCTION

Over the last few years, entrepreneurs in the forging industry have empowered their tendency to reduce costs and production preparation time, while emphasizing the high quality of the final product. Companies following this trend are required to optimize design processes which are often difficult and time-consuming. Limitations occurring during optimization process are mainly due to complex and costly experimental tests, often impossible to perform in industrial conditions.

[*] Lublin University of Technology, Nadbystrzycka Street 36, 20-618 Lublin, Poland, +48 81 538 43 64,e-mail: l.wojcik@pollub.pl
[**] Lublin University of Technology, Nadbystrzycka Street 36, 20-618 Lublin, Poland, +48 81 538 42 42,e-mail: z.pater@pollub.pl

Therefore, new methods are being sought to streamline the design of metal forming processes that will reduce the costs of industrial research using actual materials. Such methods allow conducting research on the metal forming process in laboratory conditions.

The methods used by companies to optimize the process of constructing tools and technologies of plastic processing include computer modelling as well as physical modelling.

Computer modelling (numerical) is an approximation of a discrete model to an actual model. The discrete model is composed of finite number of elements and nodes. Each element and node is described by physical differential equations. The main advantage of computer modelling is the ability to produce results for complex shapes for which analytical calculations can not be made and simulations are easy to perform (Balasundar, Raghu, & Sudhakara, 2009; Dębski, Lonkwic & Rozylo, 2015; Gontarz &Winiarski, 2015; Rozylo & Wojcik, 2017; Lis, Pater & Wojcik, 2016b). The main limitation of the numerical method is the un-certainty of the obtained results.

Physical modelling makes it simpler to analyse and optimize the design of plastic technological processing. The physical simulation method allows the substitution of actual material with model material (lead, wax, resin, plasticine) (Dziubińska & Gontarz, 2015).This technique is based on the analysis of phy-sically similar phenomena that occur in the actual object as well as in the model. Replacing the actual material with the model material allows for the use of tools made of much cheaper and more easily machined materials (Kowalczyk, 1995; Świątkowski,1994a,b).

The physical modelling method is based on the similarity of actual and model material. The main similarity criteria include the similarity of flow curves for model and actual material, the similarity of friction conditions, the similarity of tool shapes, the similarity of process kinematics (Gontarz, Łukasik, & Pater, 2003)

2. THE ANALYSIS OF THE STATE OF THE PROBLEM

Physical modelling of solid shaping in hot forming processes allows for analysis of the process. In many metal forming processes the final product suffers from certain limitations, one of them is the cracking component occurring during the plastic processing. These cracks are often invisible to the human eye, but have a very negative effect on the finished element (Pater, 2010).

The fracture phenomenon is dependent on structural phenomena occurring in the material during shaping. Two different ways of cracking of the material are distinguished – brittle and ductile cracking. The most frequently encountered form of cracking in the hot metal forming is ductile cracking (Arikawa & Kakimotoa, 2014; Fuertesa, Leóna, Luisa, Luria, Puertasa, & Salcedoa, 2015; Gontarz & Piesiak, 2010; Pires, Song, & Wu, 2016). Plastic cracking occurs

by the formation of cracks and narrowing of the matrix material. In the case of model materials, cracks are represented by voids and gas bubbles inside the material. The formation of ductile scrap is accompanied by an increase in plastic deformation of the material.

The research object is commercial wax based plasticine, produced by "Primo" in white and black colour. Plasticine is a mixture of clays, silts, oils, waxes, and colouring pigments. It is characterized by very high plasticity at room temperature. This material is classified in the group of non-metallic model materials. The main advantage of using this model mass is the possibility of multiple use (material that has not been contaminated with oils, dust, etc.). Plasticine has been used repeatedly for experimental analysis of various plastic forming technological processes (Assempour & Razi, 2002; Komori & Mizuno, 2009).

In the scientific literature, the results of empirical studies on mechanical properties of materials used for physical modelling have been repeatedly described (Moon & Van Tyne, 2000; Rasty & Sofuoglu, 2000) Laboratory analyses omitted issues related to cracking of model materials in the forming processing.

In the paper it was considered advisable to conduct experimental and theoretical studies in the scope of determination of the Cockroft-Latham limit value for commercial plasticine. The Cockroft-Latham criterion accurately determines the moment of separation of the material in which narrowing and plastic separation occurs. This criterion is described by the equation:

$$\int_0^{\varphi^*} \frac{\sigma_1}{\sigma_i} d\varphi = C \tag{1}$$

where: σ_i – reduced stress [MPa],
σ_1 – highest main stress [MPa],
φ^* – limiting cracking deformation,
C – material constant.

The plasticine mass used was previously plastometrically examined (Lis, Pater & Wojcik, 2016a). Plastometric studies have shown that the material is highly sensitive to temperature variations and deformation rates. The drop in temperature had a significant effect on the increase of plasticizing stresses. The highest values of plasticizing stresses were observed at 0°C (with the highest stress strain rate σ_{pl} = 0.67MPa).Fig. 1 shows the flow curves for plasticine tested at a temperature range of 0 to 20 °C.

Studied materials were described by the constitutive equations, the white plasticine described by the equation (2), while the equation (3) describes the black plasticine:

$$\sigma_p = 0{,}48057 \cdot \varepsilon^{-0{,}03127} \cdot \exp(0{,}08705 \cdot \varepsilon) \cdot \dot{\varepsilon}^{(0{,}24508 - 0{,}00262T)} \cdot \exp(-0{,}03283T) \quad (2)$$

$$\sigma_p = 0{,}6817 \cdot \varepsilon^{-0{,}0711} \cdot \exp(0{,}07203 \cdot \varepsilon) \cdot \dot{\varepsilon}^{(0{,}2701 - 0{,}0037T)} \cdot \exp(-0{,}07358T) \quad (3)$$

where: σ_p – plasticizing stresses [MPa],
ε – reduced strain,
$\dot{\varepsilon}$ – strain rate [s^{-1}],
T – test sample temperature [°C].

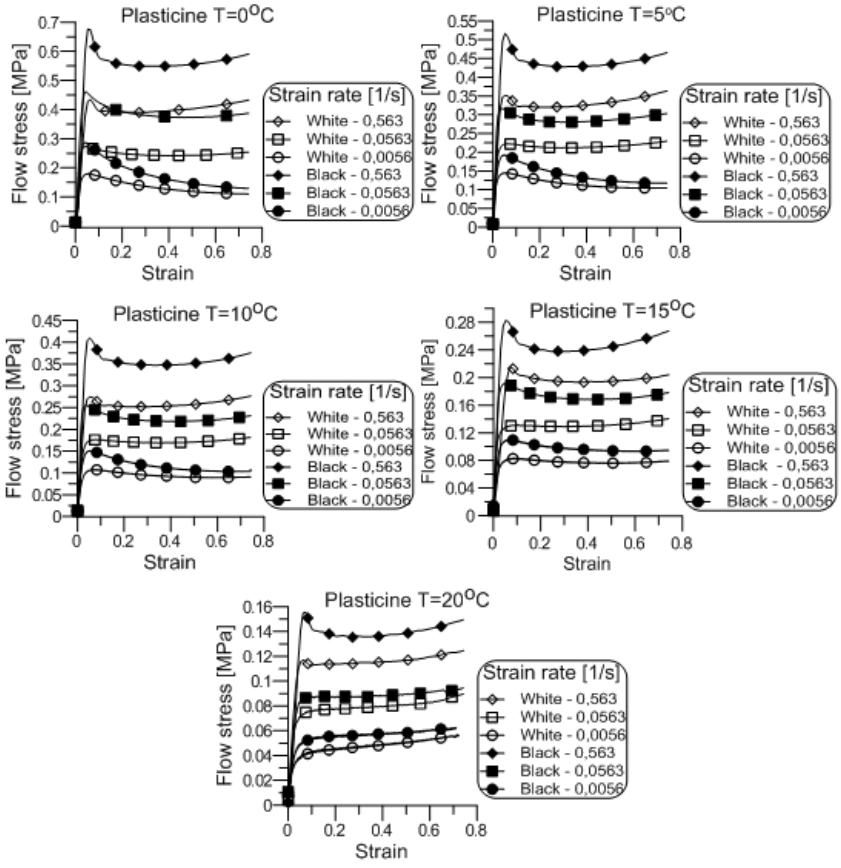

Fig. 1. Plasticine flow curves at temperatures of 0, 5, 10, 15, 20 °C

2.1. Experimental research

In order to determine the limit value of the Cockroft-Latham integral, the axially symmetrical samples were subjected to the tensile test. The geometrical dimensions of the test samples are shown in Fig. 2. Experimental studies were carried out using the Instron 3369 universal testing machine. The testing machine is characterized by a maximum load of 50 kN and a speed range of 1 to 500 mm/min. The measuring device allows for the accuracy of the measurement to be within ± 0.5% of the obtained value. The stand is equipped with software that allows registering the displacement of the slider and the force as a function of time.

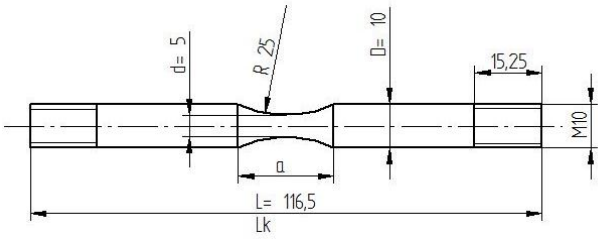

Fig. 2. Shape and dimensions of the sample used for tensile tests

In order to determine the influence of temperature on the variation of the limit value of the Cockroft-Latham integral, the studies were conducted for five different temperatures 0, 5, 10, 15, 20°C. The test was repeated three times for each test temperature. A total of 30 axially symmetric samples were used. The literature shows a number of methods for the preparation of samples made of a model material (Altan & Vazquez, 2000; Assempour & Razi, 2003). Samples used for testing were performed according to the following procedure.

The first step in the preparation of the samples was to heat the plasticine billets to a temperature of about 30–35°C, which facilitated the repeated manual processing and shaping of the test material. Use of this stage allows for removal of the air bubbles caused by the production process. The presence of air bubbles negatively affects the subsequent processing of the material and the quality of the final sample.

In the second stage, cylindrical blocks with a diameter of 32 mm and a height of about 60 mm were formed. Then the shaped body was subjected to an extrusion process which resulted in a bar of 10 mm in diameter (Fig. 3).

In the next step, the obtained bar was divided into smaller cylindrical samples of 120 mm length.

Such semi-finished products were subjected to a cross wedge rolling process.

The obtained axially symmetric samples were then trimmed to 116.5 mm. The samples were measured and their geometrical dimensions are shown in Table 1.

Fig. 3. The order of sample preparation (starting from the left: bar extrusion, narrowing of the bar, cutting of the sample to the length)

Tab. 1. Parameters of samples used for tensile test (marking according to Fig. 2)

White Plasticine							
No.	T [°C]	D [mm]	d [mm]	a [mm]	L [mm]	L_k [mm]	ΔL
1	0	9,96	4,65	21,7	100,1	105,2	5,1
2		10,19	4,54	21,3	100,5	105,3	4,8
3		10,21	4,6	21,5	100,7	105,1	4,4
1	5	10,1	4,7	20,9	100,7	106,5	5,8
2		10,2	4,65	21,1	100,8	106,4	5,6
3		10,4	4,68	21,6	100,7	105,3	4,6
1	10	10,15	4,64	21,5	100,3	106,7	6,4
2		10,06	4,58	21,7	100,5	107,9	7,4
3		10,21	4,69	21,7	100,5	107,2	6,7
1	15	10,18	4,85	20,9	100,5	109,3	8,8
2		10,3	4,73	21,8	100,3	107,7	7,4
3		10,28	4,78	21,7	100,7	108,6	7,9
1	20	10,13	4,91	21,8	100,6	108	7,4
2		10,18	4,75	21,9	100,9	109,9	9
3		10,2	4,73	21,2	101	110,2	9,2
Black Plasticine							
1	0	10,1	4,8	21,3	100,7	104,7	4
2		10,23	4,99	21,4	100,4	104,8	4,4
3		10,28	5	21,2	100,3	104,8	4,5
1	5	10,26	5,02	21,5	100,4	105,9	5,5
2		10,23	4,94	21,6	100,6	105,4	4,8
3		10,21	4,9	21,4	100,3	105,9	5,6
1	10	10,11	4,97	21,5	100,7	106,5	5,8
2		10,19	4,92	21,6	100,4	106,8	6,4
3		10,14	4,96	21,6	100,6	106,6	6
1	15	10,2	5,01	22,2	100,8	107,7	6,86
2		10,1	4,94	21,9	100,4	107,1	6,68
3		10,3	5,02	21,8	100,5	107,2	6,68
1	20	10,18	4,94	21,4	100,2	108	7,84
2		10,2	4,9	21,9	100,6	108,3	7,72
3		10,2	4,93	21,3	100,9	108,7	7,82

In order to properly secure the samples in testing machine, special inserts were designed and manufactured for correct grip (Fig. 4).The inserts used for the study were made by 3D printing. The 3D printing technique is carried out by placing thin layers (one on top of another) of molten plastic (in this case ABS). The tools were made on the uPrint SE printer.

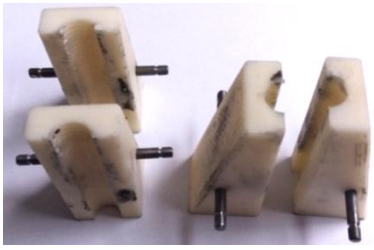

Fig. 4. Sample mounting inserts. Samples were stretched at 300 mm/min (Fig. 5)

During the test, the force, the path and the time with an acquisition rate of 100 Hz were recorded. Based on the recorded force values, the force function graphs in the stretching process were determined. The obtained experimental research results were used in numerical research.

Fig. 5. Slip of the charge due to tensile test

2.2. Numerical studies

To determine the limit value of the Cockroft-Latham integral numerical modelling method was used. To perform the numerical simulation, DEFORM 3D software was used, which uses finite element method. The DEFORM simulation implemented 13 different criteria, including the Cockroft-Latham criterion.

Computer simulations were performed for the stretching of samples made from model material. The computer models used for the simulation were designed according to the dimensions of the actual samples. In order to facilitate the simulation, the computer models of the samples have been redesigned to fit the virtual handles (Fig.6). The shape of the ends of the samples did not affect the results, due to the tensile strain occurring in the region of the constriction.

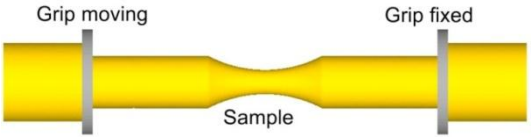

Fig. 6. Sample and mounting system in DEFORM-3D

Samples were modelled using quadratic mesh elements. The average number of elements describing the sample was 150,000.In place of the expected major deformation, these elements have been concentrated.

Computer modelling was based on the results of earlier studies (Wojcik, Lis, Pater, 2016,a), which were incorporated into the DEFORM-3D software in tabular form.

Numerical simulations were performed for the white and the black samples at five different temperatures. For simulation calculations, the tensile velocity and temperature were determined according to the experimental parameters.

Numerical studies allowed to determine the forces and map deformation, stress, strain rate and Cockroft-Latham integral (Fig. 7). In areas where narrowing occurs, the highest values of these parameters has been observed.

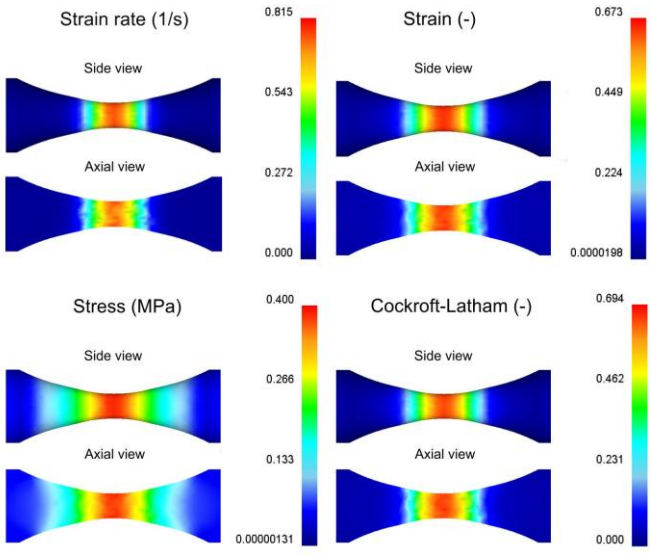

Fig. 7. Distribution of velocity, deformation, strain and damage criterion

3. TESTING RESULTS

Based on experimental studies and numerical simulations, Cockroft-Latham limit values were calculated, which corresponded to the moment of an actual sample slip. The results of the study are presented in Tab. 2.

Tab. 2. Parameters of the samples used for tensile test

	Temperature / Type	0 °C	5 °C	10 °C	15 °C	20 °C
Cockroft - Latham Integral	White	0.646	0.786	1.27	1.377	1.453
	Black	0.691	1.134	1.25	2.037	2.0

Based on the conducted studies, the limit value of the Cockroft-Latham integral (C) increases along with the increase of the temperature. The C values for the temperatures 0÷15 °C vary between 0.646÷1.453 for the white material and 0.691÷2.037 for the black material. Fig.8 shows the average values of the limiting integral dependent on temperature. The following figure shows the trend lines which are described by the equations.

The black model material:

$$C= 0.718+0.07T \tag{4}$$

The white model material:

$$C= 0.665+0.44T \tag{5}$$

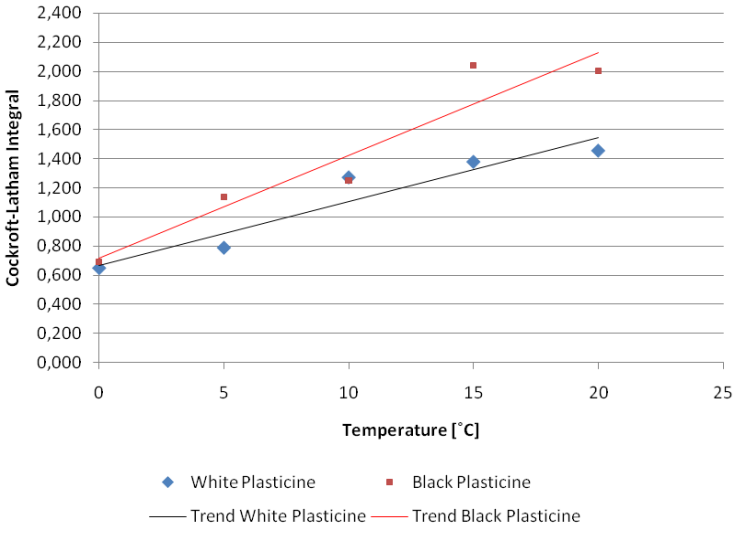

Fig. 8. Cockroft-Latham integral limit value for model materials, depending on temperature

4. CONCLUSION

The study presented the methodology and the results allowing for determination of limiting value of Cockroft-Latham integral for commercial plasticine.

The used test method was based on experimental and numerical studies of the stretching of the narrowed samples. The use of samples of such shape allowed to force the slip in a predictable place. Narrowing the sample allows to eliminate the problems associated with the location of deformation in numerical studies.

The limiting value of the C-L integral for both materials increased with the increase of temperature in which they were deformed. The values for the black model material were greater than the values of the white material.

The course of change of the C-L integral limiting value represents the change in plasticity of the material along with the increase in temperature.

REFERECES

Altan, T., & Vazquez, V. (2000). New Concepts in die design – physical and computer modeling applications. *Journalof Materials Processing Technology, 98*, 212–223.

Arikawa, T., & Kakimotoa, H. (2014). Prediction of surface crack in hot forging by numerical simulation. *Procedia Engineering, 81,* 474–479.

Assempour, A., & Razi, S. (2002). Determination of load and strain-stress distributions in hot closed die forging using the plasticine modeling technique. *Archive of SID 2, 15*, 167–172.

Assempour, A., & Razi, S. (2003). Physical modeling of extrusion process. *Journal of Mechanical Ennineering, 4*, 61–69.

Balasundar, I., Raghu, T., & Sudhakara, M. (2009). Equal channel angular pressing die to extrude a variety of materials. *Materials and design, 30,* 1050–1059. doi:10.1016/j.matdes.2008.06.057

Dębski, H., Lonkwic, P., & Rozylo, P. (2015). Numerical and experimental analysis of the progressive gear body with the use of finite-element method. *Eksploatacja i Niezawodność –Main-tenance and Reliability, 17*(4), 544–550.

Dziubińska, A., & Gontarz, A. (2015). Limiting phenomena in a new forming process for two-rib plates. *Metalurgija, 54*(3), 555–558.

Fuertesa, J. P., Leóna, J., Luisa, C. J., Luria, R., Puertasa, I., & Salcedoa, D. (2015). Comparative study of the damage attained with different specimens by FEM. *Procedia Engineering, 132*, 319–325.

Gontarz, A., Łukasik, K., & Pater, Z. (2003). *Technologia kształtowania i modelowania nowego procesu wytwarzania wkrętów szynowych*. Lublin: Wydawnictwa Uczelniane Politechniki Lubelskiej.

Gontarz, A., & Piesiak, J. (2010). Model pękania według kryterium Cockrofta-Lathama dla stopu magnezu MA2 w warunkach kształtowania na gorąco. *Obróbka Plastyczna Metali, 4*, 217–227.

Gontarz, A., & Winiarski, G. (2015). Numerical and experimental study of producing flanges on hollowparts by extrusion with a movable sleeve. *Archives of Metallurgy and Materials, 60*, 1917–1921. doi:10.1515/amm-2015-0326

Komori, K., & Mizuno, K. (2009). Study on plastic deformation in cone type rotary piercing process using model piercing mill for modeling clay. *Journal of Material Processing Technology, 209*, 4994–5001. doi:10.1016/j.jmatprotec.2009.01.022

Kowalczyk, L. (1995). *Modelowanie fizykalne procesów obróbki plastycznej*. Radom: Instytut Technologi I Eksploatacji.

Lis, K., Pater, Z., & Wojcik, L. (2016a). Plastometric tests for plasticine as physical modelling material. *Open Engineering*, *6*, 653–659. doi:10.1515/eng-2016-0093

Lis, K., Pater, Z., & Wojcik, L. (2016b). Numerical analysis of a skew rolling process for producing a crankshaft preform. *Open Engineering*, *6*, 581–584. doi: 10.1515/eng-2016-0087

Moon, Y. H., & Van Tyne, C. J. (2000). Validation via FEM and plasticine modeling of upper bound criteria of a process induced side surface defect in forgings. *Journal of Materials Processing Technology*, *99*, 185–196. doi:10.1016/S0924-0136(99)00417-3

Pater, Z. (2010). Wartość graniczna całki Cockrofta-Lathama dla stali kolejowej gatunku R200. *Hutnik, Wiadomości Hutnicze*, *77*(12), 702–705.

Pires, F. M. A., Song, N., & Wu, S. (2016). Numerical analysis of damage evolution for materials with tension-compression asymmetry. *Procedia Structural Integrity*, *1*, 273–280. Doi: 10.1016/j.prostr.2016.02.037

Rasty, J., & Sofuoglu, H. (2000). Flow behavior of plasticine used in physical modeling of metal forming process. *Tribology International*, *33*(8), 523–529. doi:10.1016/S0301-679X(00)00092-X

Rozylo, P., & Wojcik, L. (2017). FEM and Experimental Based Analysis of the StampingProcess of Aluminum Alloy. *Adv. Sci. Technol. Res. J.*, *11*(3), 94–101. doi:10.12913/22998624/70691

Świątkowski, K. (1994a). Analiza badań modelowych z użyciem materiałów modelowych z użyciem materiałów woskowych. *Obróbka Plastyczna Metali*, *5*, 5–14.

Świątkowski, K. (1994b). Własności mechaniczne woskowych materiałów modelowych. *Obróbka Plastyczna*, *5*, 15–21.

Applied Computer Science, vol. 13, no. 4, pp. 56–64
doi: 10.23743/acs-2017-29

Submitted: 2017-10-30
Revised: 2017-11-15
Accepted: 2017-12-06

Abaqus Finite Elements, Plane Stress, Orthotropic Material

Bartosz KAWECKI[*]*, Jerzy PODGÓRSKI*[*]

NUMERICAL RESULTS QUALITY IN DEPENDENCE ON ABAQUS PLANE STRESS ELEMENTS TYPE IN BIG DISPLACEMENTS COMPRESSION TEST

Abstract

The paper presents a brief description of the Abaqus Simulia plane stress quadrilateral elements (CPS4R, CPS4I, CPS4, CPS8R, CPS8). Comparison of the results quality obtained using each of them was done. There was considered two dimensional big displacements compression test for a highly orthotropic material. Simulations were performed for the compression in two perpendicular directions.

1. INTRODUCTION

Abaqus Simulia software makes many finite elements available to its users. The basic problem is the criterion of choosing an appropriate element to the specific investigation.

The paper presents the description of five plane stress quadrilateral elements available in Abaqus. Brief outline of nodes, degrees of freedom and the Lagrange polynomial shape functions was done (Zienkiewicz, 2000; Bathe, 2014; Liu & Quek, 2014). The paper provides a comparison of the results obtained for a highly orthotropic material using each of elements in a big displacements compression test. Constitutive law for the material was defined basing on (Jones, 1999; Lekhnitskii, 1981). The general aim of the numerical experiment was the need of determination element's suitability for usage in the analyses, where considerable distortion of the elements is anticipated. The problem of oversize distortion was raised in several papers (Macneal & Harder, 1985; Barlow, 1989; Lee & Bathe, 1993).

[*] Lublin University of Technology, Faculty of Civil Engineering and Architecture, Department of Structural Mechanics, Nadbystrzycka 40, 20-618 Lublin, Poland, b.kawecki@pollub.pl, j.podgorski@pollub.pl

As a report from numerical analyses there was specified σ_{11} and σ_{22} stress distribution in dependence on element type, direction of compressing and applied mesh. Modelling and mesh study was based on the scientific papers (Turcke & McNeice, 1974; Amstrong, 1994). Additionally, there were prepared diagrams of P-δ relation to notice any discontinuities or disturbances in the model. Basing on the numerical results there were made general conclusions and recommendations for using the Abaqus plane stress quadrilateral elements with highly orthotropic materials.

2. ELEMENTS DESCRIPTION

The simplest elements are 4-node bilinear plane stress quadrilateral elements, which are presented in Fig.1.

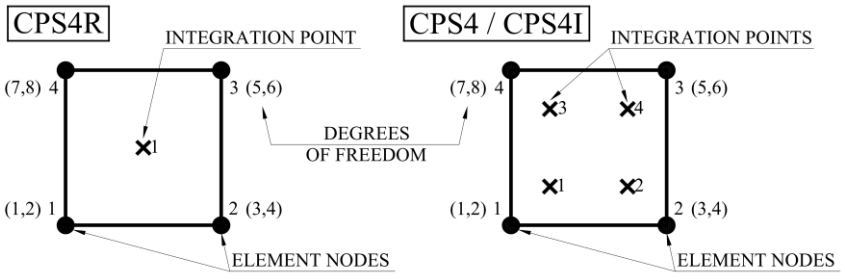

Fig. 1. Linear geometric order (first order) plane stress elements (author's study basing on Abaqus User's Manual)

The difference between CPS4 and CPS4I is an occurrance of the additional internal degrees of freedom preventing the element from overly stiff behavior in bending, called shear locking. The phenomenon is more precisely described in (Cook, Malkus, Plesha & Witt, 2002) and Abaqus User's Manual.

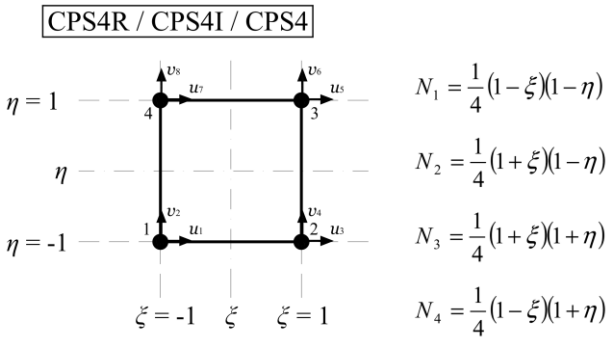

Fig. 2. 4-node element shape functions based on Lagrange polynomials

General functions describing work of the finite elements are the shape functions (Zienkiewicz & Taylor, 2000; Bathe, 2014; Liu & Quek, 2014). In most cases they are based on Lagrange polynomials. Defining coordinate system using η and ξ axes, shape functions may be written as it was shown in Fig. 2. Denotations u and v describe nodal translation degrees of freedom. More complex elements are 8-node biquadratic plane stress quadrilateral elements, which are presented in Fig.3.

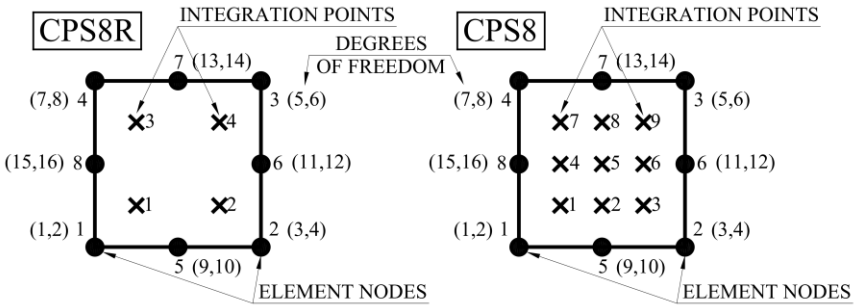

Fig. 3. Quadratic geometric order (second order) plane stress elements (author's study basing on Abaqus User's Manual)

Defining coordinate system as before, using η and ξ axes, shape functions may be written as it was shown in Fig.4. Denotations u and v describe nodal translation degrees of freedom.

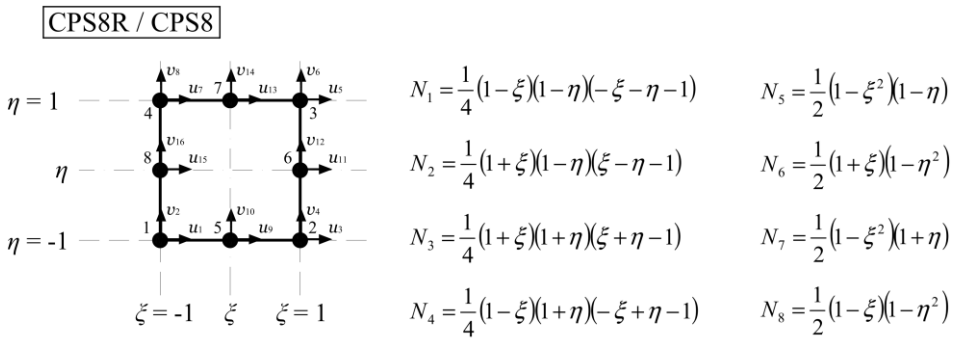

Fig. 4. 8-node element shape functions based on Lagrange polynomials

In both 4-node and 8-node elements the equation given below is met:

$$\sum_{i=1}^{n} N_i = 1 \tag{1}$$

Displacement field is described by formula:

$$u = \sum_{i=1}^{n} N_i u_i \qquad v = \sum_{i=1}^{n} N_i v_i \tag{2}$$

In both elements types there are considered reduced and full integration modes. Reduced integration provides lower computational cost in the numerical analysis, but on the other hand may lead to the lower quality of the results. These aspects will be discussed in the next paragraph.

3. COMPRESSION TEST FEM MODEL

There were prepared two numerical models with different local coordinate systems orientations. For highly orthotropic materials, orientation of the specimen is crucial for obtained stresses and strains values.

Fig. 5. a) presents set of compression in a longitudinal direction, and Fig. 5. b) set of compression in a transversal direction. Predicted results of the stresses distribution should be completely different from each other.

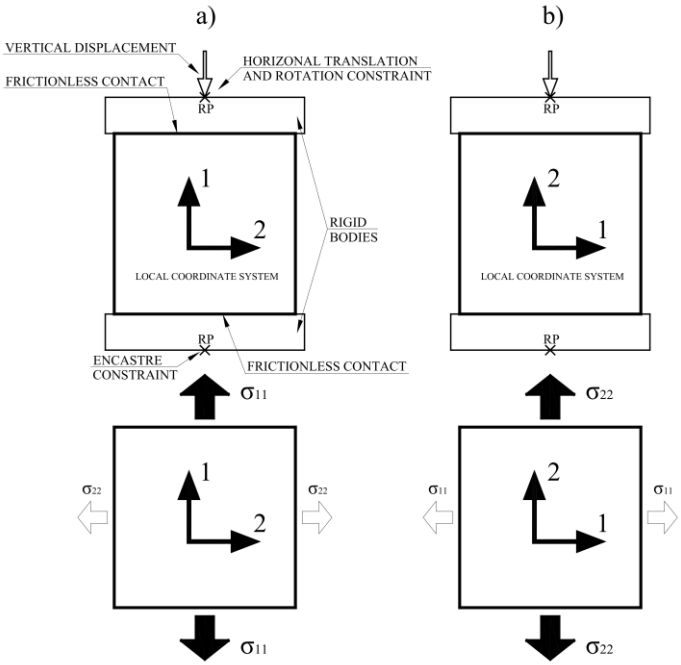

Fig. 5. Compression test with different local coordinate systems orientation: a) longitudinal compression, b) transversal compression

Compressing steel parts were modeled as rigid bodies to prevent them from deformations. Lower support was fixed in the reference point, upper steel plate was constrained in the horizontal direction and in the plane rotation. There was added constant vertical displacement of the upper steel plate and frictional contact between the specimen and steel plates.

There were two mesh sizes taken into account: 16 elements and 64 elements, which is presented in Fig. 6.

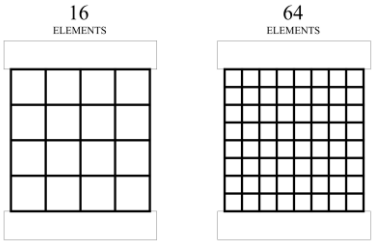

Fig. 6. Number of finite elements used in the numerical simulation

For both directions of compression there was added the same vertical displacement δ = 5 mm.

4. NUMERICAL RESULTS

Numerical results contain comparison of the elements behaviour under big displacement compression and description of σ_{11} and σ_{22} stresses distribution in the specimen. Expected values σ_{11} stresses were much higher than σ_{22} because of a great difference in the elastic modules depending on the direction. For better understanding work of the whole specimen there were made diagrams with P-δ relation. Results for mesh with 16 elements are shown in Fig. 7–11.

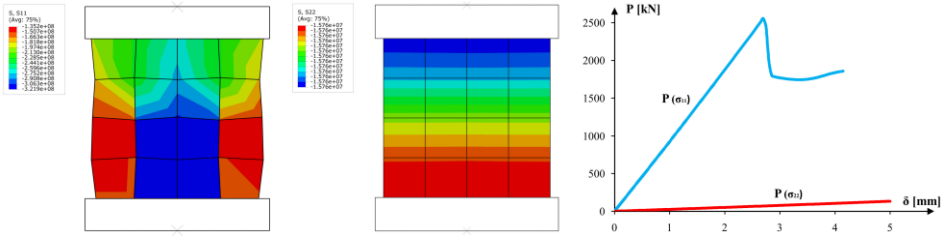

Fig. 7. CPS4R elements displacements, σ_{11}, σ_{22} stresses distribution and P-δ relation

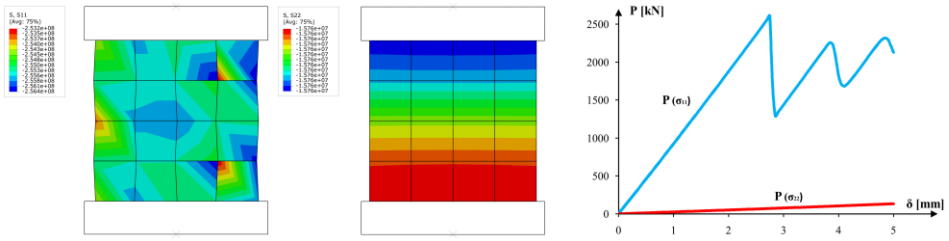

Fig. 8. CPS4I elements displacements, σ_{11}, σ_{22} stresses distribution and *P-δ* relation

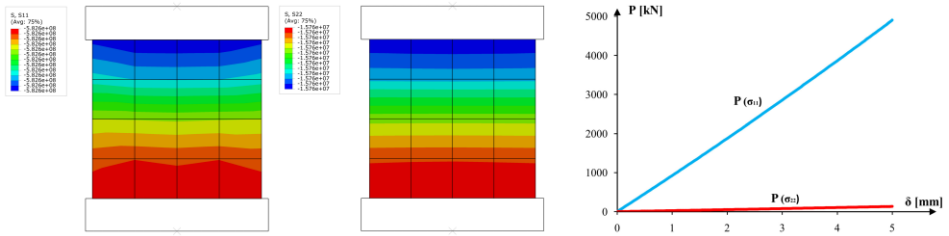

Fig. 9. CPS4 elements displacements, σ_{11}, σ_{22} stresses distribution and *P-δ* relation

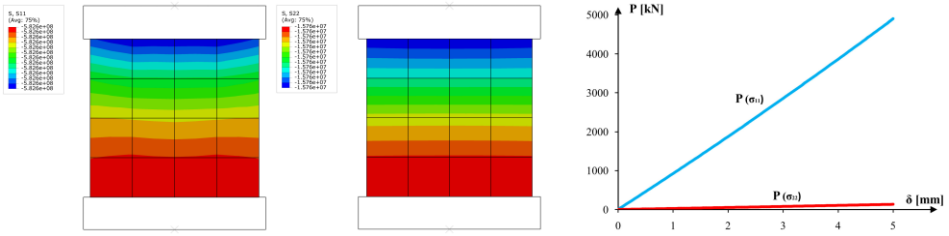

Fig. 10. CPS8R elements displacements, σ_{11}, σ_{22} stresses distribution and *P-δ* relation

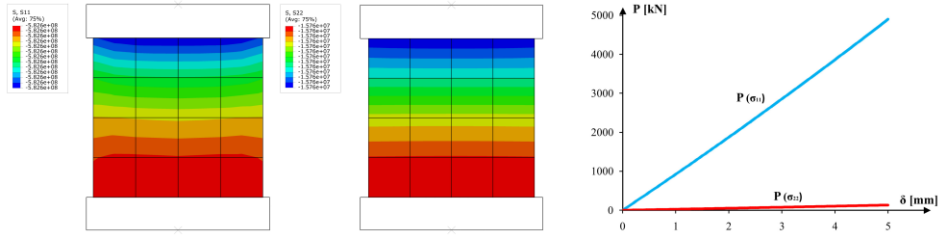

Fig. 11. CPS8 elements displacements, σ_{11}, σ_{22} stresses distribution and *P-δ* relation

CPS8 presented the most precise results. Comparing other elements to the CPS8 it was visible that CPS8R and CPS4 gave accurate results while CPS4I and CPS4R gave inaccurate results in σ_{11} direction, due to the excessive elements distortion.

Additionally, for CPS4R element, analysis convergence ends in about 80% of the analysis progress and the shape of the elements is unphysical. *P-δ* relation diagrams clearly shows the disturbances in the whole model caused by CPS4R and CPS4I elements, while for CPS4, CPS8R and CPS8 relation is smooth.

General principal to get the proper results from the numerical model was considering lower and higher mesh density. Only then an interpretation of the results might be correct. Because of that there was prepared the second mesh with 64 finite elements in the specimen. This approach allowed to find out how mesh density influence the solution. Results of the investigation are presented in Fig. 12–16.

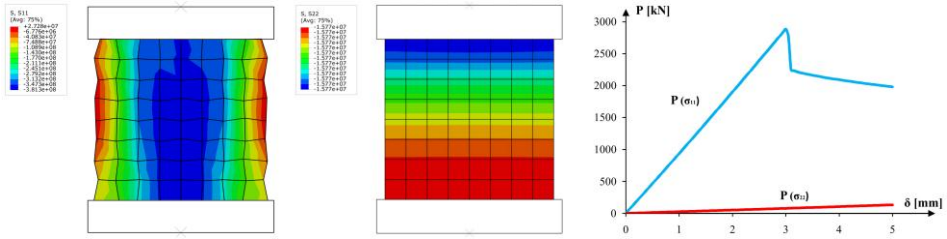

Fig. 12. CPS4R elements displacements, σ_{11}, σ_{22} stresses distribution and *P-δ* relation

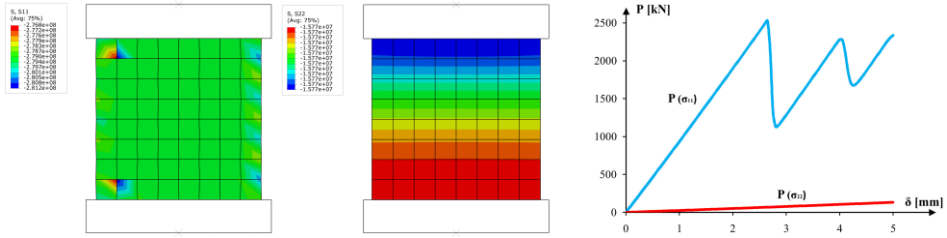

Fig. 13. CPS4I elements displacements, σ_{11}, σ_{22} stresses distribution and *P-δ* relation

The same as in case of 16 elements mesh, there were visible inaccurate stress results for CPS4R and CPS4I. It seemed that mesh density had a low influence on the elements work. There was a visible progress in proper stress distribution range in case of CPS4R elements, however after reaching some stress limit, these elements behaviour was still unphysical.

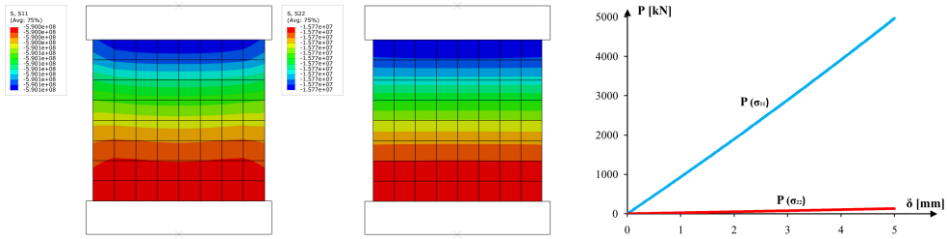

Fig. 14. CPS4 elements displacements, σ_{11}, σ_{22} stresses distribution and *P-δ* relation

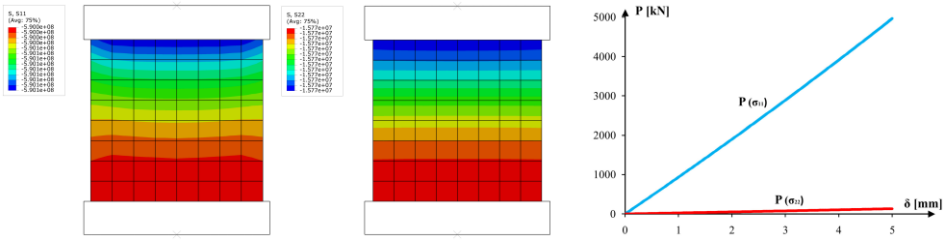

Fig. 15. CPS8R elements displacements, σ_{11}, σ_{22} stresses distribution and *P-δ* relation

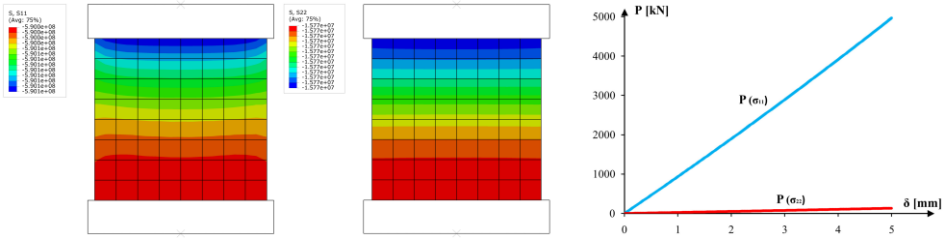

Fig. 16. CPS8 elements displacements, σ_{11}, σ_{22} stresses distribution and *P-δ* relation

5. CONCLUSIONS

Basing on the performed numerical analyses there were made several conclusions about using Abaqus plane stress quadrilateral elements.

CPS4R and CPS4I elements were recommended only to use with small displacements and linear problems. Nonlinearity would probably cause similar inadequate effects as an orthotropic material as presented in the paper. In case of these finite elements, making mesh more dense may have no influence on getting better numerical results.

CPS4 elements gave the same good results in the compression as CPS8R and CPS8 elements. However it was worth to remember that shear locking occurs in CPS4 elements.

The best solution for almost all of the plane stress problems are second order quadrilateral elements CPS8R and CPS8, which give proper results in compression, big displacements, works well with highly orthotropic materials and with bending.

The author's study provides precise information about how the Abaqus plane stress elements work under compression. It is a very important case for a further research. There are planned several numerical modelling validations in delamination and damage processes in highly orthotropic materials. It is possible only when accurate results are provided by the finite elements.

REFERENCES

Abaqus/CAE V6.14 User's Manual.

Armstrong, C. G. (1994). Modelling requirements for finite-element analysis. *Computer-Aided Design*, *26*, 573–578. https://doi.org/10.1016/0010-4485(94)90088-4

Barlow, J. (1989). More on optimal stress points – reduced integration, element distortions and error estimation. *International Journal of Numerical Methods in Engineering*, *28*, 1487–1504. doi:10.1002/nme.1620280703

Bathe, K. J. (2014). *Finite Element Procedures. Second Edition*, 341–389.

Cook, R. D., Malkus, D. S., Plesha, M. E., & Witt R. J. (2002). *Concepts and Applications of FEA, 4th ed.* (98–102). John Wiley&Sons, Inc.

Jones, R. M. (1999). *Mechanics of Composite Materials. Second Edition*, 55–73. Philadelphia: Taylor & Francis Group.

Lekhnitskii, S. G. (1981). *Theory of Elasticity of an Anisotropic Elastic Body*. Mir Publishers.

Lee, N. S., & Bathe, K. J. (1993). Effects of element distortions on the performance of iso-parametric elements. *International Journal of Numerical Methods in Engineering*, *36*, 3553–3576. doi:10.1002/nme.1620362009

Liu, G. R. & Quek, S. S. (2014). *The Finite Element Method. A Practical Course. Second Edition*, 161–211. Elsevier.

Macneal, R. H., & Harder, R. L. (1985). A proposed standard set of problems to test finite element accuracy. *Finite Elements in Analysis and Design*, *1*, 3–20. https://doi.org/10.1016/0168-874X(85)90003-4

Turcke, D. J., & McNeice, G. M. (1974). Guidelines for selecting finite element grids based on an optimization study. *Computers & Structures*, *4*, 499–519. https://doi.org/10.1016/0045-7949(74)90003-0

Zienkiewicz, O. C., & Taylor, R. L. (2000). *The Finite Element Method. Fifth Edition. Volume 1: The Basis*, 164–198. Oxford, UK: Butterworth-Heinemann.

Applied Computer Science, vol. 13, no. 4, pp. 65–75
doi: 10.23743/acs-2017-30

Submitted: 2017-11-09
Revised: 2017-12-01
Accepted: 2017-12-11

GFPR composite, wood-fiber-polyester resin composites, homogenization methods, Digimat software

Wiesław FRĄCZ[*], *Grzegorz JANOWSKI*[*], *Grażyna RYZIŃSKA*[*]

THE POSSIBILITY OF USING WOOD FIBER MATS IN PRODUCTS MANUFACTURING MADE OF POLYMER COMPOSITES BASED ON NUMERICAL SIMULATIONS

Abstract

In this work the calculations for predicting the properties of wood fiber mats – polyester resin composite using numerical homogenization method were performed. For this purpose, the microstructural strength properties were calculated using DIGIMAT FE commercial code. In addition, for comparative purposes a calculation of polyester resin – glass fiber composites was conducted. This allowed to compare the properties of two types of compositions. In addition, the obtained strength properties were used to simulate the work of product made of these composites. This study was performed using the Ansys commercial code. Usability of the polyester resin – wood fiber mat composite and knowledge of its properties will allow to find a correct application of this composite type and can provide an alternative way to other polymeric resin reinforced by mat.

1. INTRODUCTION

The polymer composites based on natural fibers are widely used in manufacturing of products from many areas of life. Increasingly, due to the care for environmental purity, the natural fibers can replace other fibers (for example: glass fibers) in production of composites, in the areas of life where it can be done because of their strength and economical or aesthetic reasons.

[*] Rzeszow University of Technology, Department of Materials Forming and Processing, al. Powstańców Warszawy 8, 35-959 Rzeszów, Poland, +48 17 865 1714, e-mail: wf@prz.edu.pl, gjan@prz.edu.pl, grar@prz.edu.pl

Natural fibers are used to produce the composites on the basis of phenolic, epoxy, polyester, vinyl ester and thermoplastics resins (Thakur & Thakur, 2014). The resins used to manufacture the natural fibers reinforced composites have a polymer structure modified to make it more polar in nature, making it more hydrophilic, and therefore it could interact or bond better to the OH groups on the surface of the natural fibers (Aziz, Ansell, Clarke & Panteny, 2005). Synthetic resins are widely used, for example, as a component of paints and adhesives joints too (Kubit, Bucior & Zielecki, 2016; Zielecki, Kubit, Kluz & Trzepieciński, 2017).

Among many natural fibers the cellulose fibers are primarily important. The composites based on natural cellulose fibers find applications in a number of fields ranging from automotive to biomedical. Natural cellulose fibers have been frequently used as the reinforcement component in polymers to add the specific properties in the final.

A large share of the market among cellulose fibers are WPC composites. A large proportion of wood waste has been used for years. On a wide scale, in the production of polymer products the wood particles or even sawdust are used. The share of wood fibers is smaller due to higher manufacturing costs (Campilho, 2015). The wood fibers have been used for many years in the production of polymer composites on the basis of polymers such as PVC, ABS, PP or PA. However, there are short fibers up to 1–2 mm from softwood and 3–7 mm from hardwood (Rowell, 2013). Such fibers are used in construction, automotive, aerospace industries, household products and furniture, mainly to manufacture interior components (Ho, Wang, Lee, Ho, Lau, Leng & Hui, 2011). Major processing technologies include extrusion and injection molding (Ho, Wang, Lee, Ho, Lau, Leng & Hui, 2011; Klyosov, 2007; Kutnar & Muthu, 2016).

The manufacturing of composites based on long wood fibers is limited. Long wood fibers are mainly used in manufacturing of reinforcing road mats so-called anti-erosion which are used in the construction of motorways and expressways, primarily to reinforce shafts, high slope slopes and road embankments. These mats provide high water permeability, can stabilize the substrate humidity, exhibit sufficient mechanical strength and biodegradability after a short period of time, are characterized by high thermal and acoustic insulation. They help (in the natural way) of settling vegetation (grasses, shrubs) in a new environment, preserving the terrain established in the road project.

The wood fiber geometry, specifically in varied shape of its cross section and the small smoothness of the fibers (the lateral surface is strongly frayed) does not allow the yarn to be made. These fibers are long enough to be used in the production of the mat. Such mats can also be used to reinforce laminates. The work suggest to perform these tests, thanks to the performed numerical analysis of laminates reinforced with wood fiber mat. In order to predict the composites properties, the homogenization methods, among others, are used.

The limitations encountered with the use of analytical homogenization methods require additional calculation methods. Therefore, in recent years numerical methods of direct calculation of effective material data have become increasingly numerous and significant (Bendsøe & Kikuchi, 1988). Most of these methods are only developed with respect to the linear strain range – the range of small deformations. Due to the growing calculating power of computers, several methods have been developed to predict the nonlinear behavior of composite material. Numerical calculations can be performed in 2D space, where discretization is most often used to divide the area into triangles. This solution allows to calculate the values that appear in the cross section of material. However, there are some constraints resulting from the specificity of the solution to the problem (e.g. flow direction only penetrating the modeled surface, etc.) (Abdulle, 2013). Due to the advancement of computer technology in most recent years, more simulation packages are equipped with the ability to solve 3D problems. Discretization usually consists in dividing the area into tetrahedrons finite elements (FE). Such modeling is devoid of the fundamental limitations of 2D technology but is much more demanding in terms of memory and computing power. One of the main types of FE used in microstructural calculations are Voxel finite elements (Doghri & Tinel, 2006). This type of finite element is a regular, incompatible set of brick elements. Each element is assigned to the phase material where its center is located. It is targeted for advanced RVE where discretization is difficult to reproduce the shape of matrix and analyzed inclusions (e-Xstream engineering, 2016).

2. CALCULATIONS

In the presented work, the standard properties of wood fiber and polyester laminate were considered. Numerical analyzes were carried out to predict the suitability of this type of fiber in production of composite products.The strength analysis was performed taking into account the properties of the composite, which were defined by homogenization methods. The strength analysis was made for the assumed geometric model of the product. The example of seat model, used in public transport vehicles, were analysed. The results of the strength calculations were compared with the results obtained for the fiberglass laminate on the base of the same resin.

2.1. Calculation of polyester resin – glass fibre variant of composite

Stage I

The first analysis was performed for polyester resin – glass fiber composite, especially for OCF M8610 glass fiber mat grade. This type of mat has been the subject of many research papers (Kim & Macosko, 2000; Dominguez & Rice, 1983; Hedley, 1994; Frącz, Janowski & Ryzińska, 2017). The first phase calculations were done for beam roving (thickness of 140 μm) from S glass fiber (Tab. 1). An RVE size of 0.075 mm x 0.075 mm x 0.075 mm was assumed in the calculations, taking into account parallel arrangement of the roving fibers (Fig. 1). Preliminary calculations were performed for the composition of glass fiber-air (wt. glass fiber content was approx. 99.98%), which allowed calculation of the yarn properties (Tab. 2), directly used to build the glass mat model.

Tab. 1. Properties of S-glass fiber used in calculations

Property	Unit	Value
Fiber diameter	μm	15
Density	kg/m^3	2490
Young's modulus	MPa	85500
Poisson's coefficient	–	0.22

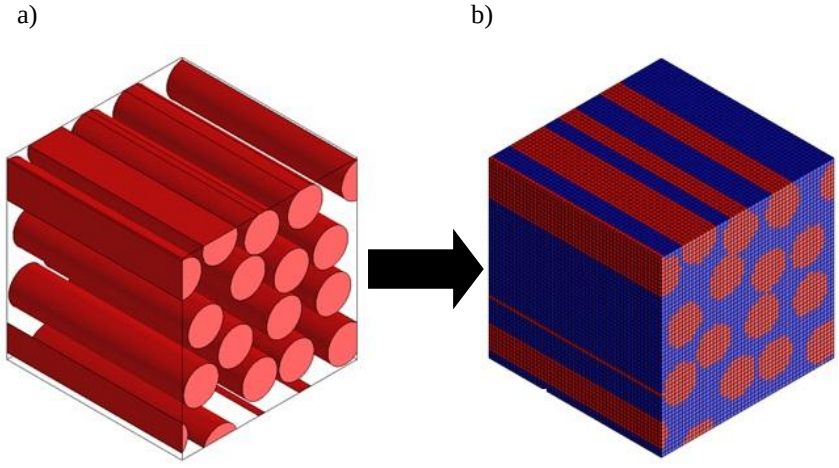

Fig. 1. Visualization for beam roving S glass fiber: a) location of fibers in RVE b) RVE after discretization of 125 000 Voxel FE (Voxel size for single cell 0.0015x0.0015x0.0015 mm)

Tab. 2. Mechanical properties of beam roving calculated by means of Digimat FE

Property	Unit	Value
Density	kg/m^3	1892.69
Young's modulus E1	MPa	130834
Young's modulus E2	MPa	123067
Poisson's coefficient v12	–	0.2699
Poisson's coefficient v21	–	0.2539
Kirchhoff's modulus	MPa	47407

Stage II

During the second stage of the calculation for the glass mat saturated with polyester resin the roving bundle data (obtained from a prior analysis) and polymer matrix data were implemented (Tab. 3). The beam diameter of yarn equal to 140 µm was assumed as the mean value (Kim & Macosko, 2000). The volume fraction of the glass mat in the composite was also determined (11.97 %), and a random fiber orientation in the plane (the orientation type in Digimat FE software: Random 2D) was defined. Based on the geometric data of glass mat, the representative RVE with dimensions of 1.8 x 1.8 x 1.8 mm was generated (Fig. 2), which was discretized by 2 125 364 voxel type FE – (size of a single voxel: 0.014x0.014x0.014 mm) and then the calculations of composite properties were made, whose results are summarized in Tab. 4. The results of the calculations are in accordance with the results contained in the publication (Trevino, 1991).

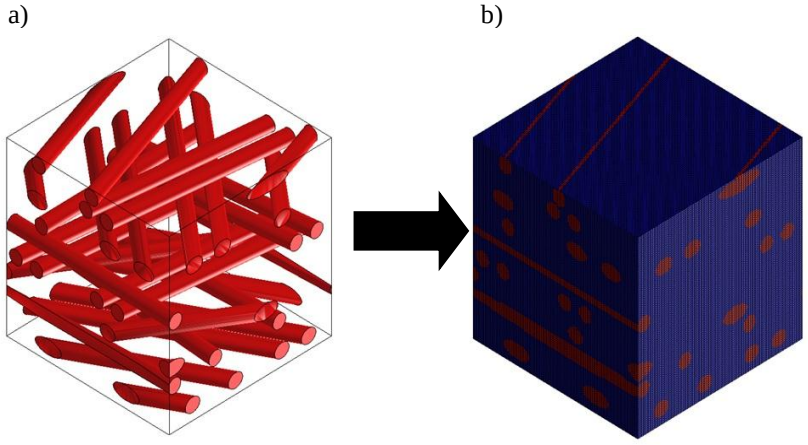

Fig. 2. Visualization of yarn: a) orientation of glass mat saturated with polyester resin, b) RVE glass mat with polymer matrix after discretization

Tab. 3. Properties of polyester resin [13]

Property	Unit	Value
Density	kg/m^3	1200
Young's modulus	MPa	4000
Poisson's coefficient	–	0.4

Tab. 4. Properties for calculated composition: glass mat – polyester resin

Property	Unit	Value
Density	kg/m^3	1282.83
Young's modulus E1	MPa	9745.89
Young's modulus E2	MPa	9568.16
Young's modulus E3	MPa	6586.12
Poisson's coefficient v12	–	0.3298
Poisson's coefficient v21	–	0.3238
Poisson's coefficient v13	–	0.4174
Poisson's coefficient v31	–	0.2821
Poisson's coefficient v23	–	0.4231
Poisson's coefficient v32	–	0.2913
Kirchhoff's modulus G12	MPa	3059.64
Kirchhoff's modulus G23	MPa	1857.91
Kirchhoff's modulus G13	MPa	1849.61

2.2. Calculation of polyester resin – wood fibre variant of composite

The basic properties of wood fiber in the analyzed composite were established on the basis of literature (Autodesk Moldflow Insight, 2013) (Tab. 5). Polymer matrix data were implemented from previous analysis (Tab. 3).

Tab. 5. Properties of wood fiber used in calculations

Property	Unit	Value
Fiber diameter	μm	100
Density	kg/m^3	2000
Young's modulus	MPa	10000
Poisson's coefficient	–	0.3

For the correct comparative analysis, the same parameters for fiber content and RVE dimensions (Tab. 6.) were chosen, relative to the previous analysis. Visualization for polyester resin – wood fiber composite is presented in Fig. 3.

Tab. 6. The input data for micromechanical analysis of polyester resin – wood fiber mat composite, using Digimat FE

Fiber volume content	11.97%
RVE dimensions	1.8 x 1.8 x 1.8 mm
The type of fiber orientation	Random
Type of FE elements	Voxel
Number of FE elements	2 125 364
Size of a single voxel	0.014x0.014x0.014 mm

a) b)

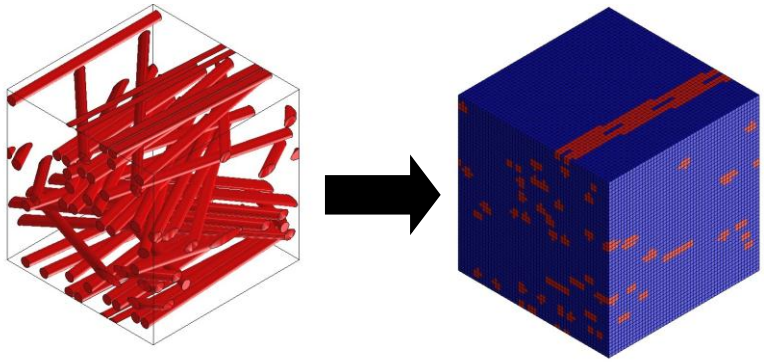

Fig. 3. Visualization for polyester resin – wood fiber composite: a) location of fibers in RVE b) RVE after discretization

The results of performed calculations are summarized in Tab. 7.

Tab. 7. The calculated properties of polyester resin – wood fiber mat composite

Property	Unit	Value
Density	kg/m^3	1295.76
Young's modulus E1	MPa	4512.58
Young's modulus E2	MPa	4610.48
Young's modulus E3	MPa	4507.64
Poisson's coefficient v12	–	0.3812
Poisson's coefficient v21	–	0.3895
Poisson's coefficient v13	–	0.3982
Poisson's coefficient v31	–	0.3977
Poisson's coefficient v23	–	0.3887
Poisson's coefficient v32	–	0.3801
Kirchhoff's modulus G12	MPa	1630.67
Kirchhoff's modulus G23	MPa	1597.50
Kirchhoff's modulus G13	MPa	1587.73

Moreover, additional calculations were performed to increase the percentage volume content of wood fibers in the polymer matrix: by about 24% and 36%. As it can be seen (Fig. 4.) by increasing the fiber contents in the polymer matrix, the Young's modulus does not increase linearly.

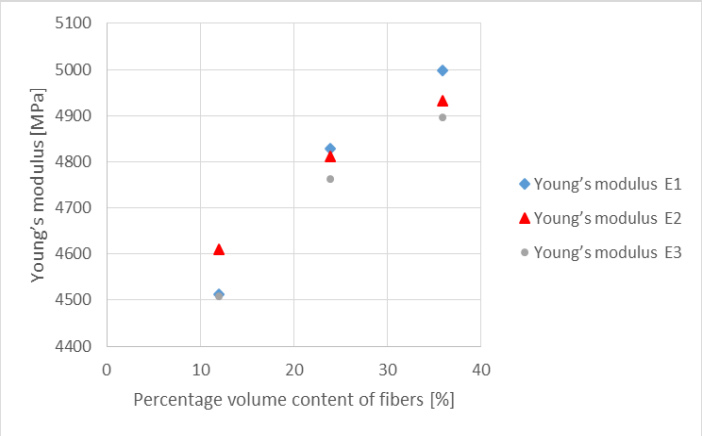

Fig. 4. The predicted Young's modulus for variable volume content: 12%, 24% and 36% of wood fiber

2.3. Strength analysis of product for reinforcement variants

The results of property calculations for heterogeneous composites make it possible to perform advanced numerical analyzes, taking into account the behavior of products made of composites under loads. For this purpose, load simulations of a car seat used as equipment in public transport vehicles were conducted. Numerical analysis was performed for three variants of reinforcement: a) polyester resin without reinforcement, b) polyester resin with glass fiber mat, and c) polyester resin with wood fiber mat. During the simulations, due to computational difficulties related to the composite model, only a single reinforcement layer was taken into account. The thickness of the real fabric layer was 0.96mm. The thickness of the real mats layer was 1.5mm. The geometric model of the seat (610 x 458 x 565 mm, thickness of 3mm) was designed by means of NX9 software. It was assumed that the seat would be equipped with a metal connector attached to the vehicle floor by means four screws. The complete seat model was imported to Ansys ver. 14.5 commercial code to carry out behavior numerical analysis under load. The analysis was performed in terms of static loads. The boundary conditions (Fig. 5), i.e. the load assumed by the seat surface (F_1 = 1000 N) and the force acting on the bearing surface (F_2 = 300 N) were introduced. Between the bottom of the car seat and the upper surface of the metal connector a displacement of 0.5 mm was allowed, which represented the clearance resulting from the assembly of components (the seat and the connector)

using screws. The lower surface of the connector was fixed. The next step was to introduce the composite properties for the three reinforcements variants to the software. Due to the anisotropic properties of the mats and fabrics, calculations by means of the Ansys code were carried out in the local coordinate systems of the seat and backrest. They were carried out in order to take into account the material properties of properly oriented reinforcement. It was assumed that the screws and connector were made of steel.

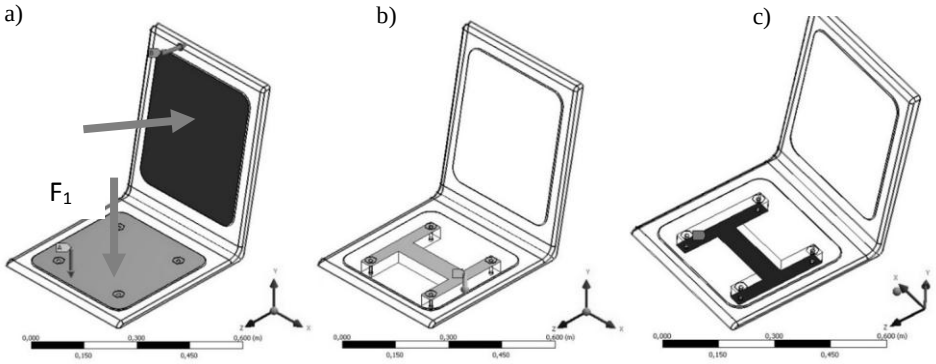

Fig. 5. Boundary conditions and loads: a) forces applied to seat surface and backrest, b) fixed displacement between lower seat surface, and connector, c) lower restraint surface

In the performed simulations of seat load, the comparison criterion was the maximum deflection of the backrest. As shown in Fig. 6 the greatest amount of deflection was found, which is evident in the case of the resin without reinforcement. For the composites reinforced by glass mat and wood mat, deflections of 80 mm and 150 mm were obtained. For the chair without reinforcement the largest deflection was 160 mm.

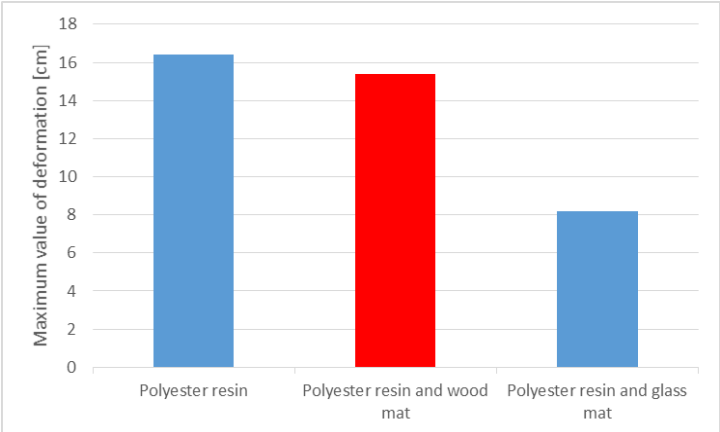

Fig. 6. The maximum deflection of seat backrest for three variants of material

3. RESULTS ANALYSIS

The results of load simulation for the model of passenger seat (for two types of composite: with wood and glass fiber reinforcement) show that the hypothetical using of wood fiber mat affects only slightly the reduction of seat backrest deflection compared to pure polyester resin. In the case of glass fiber mat the deflection can be reduced up to approx. 100% compared with a product made without reinforcement.

An increase in the percentage of wood fibers in the analyzed composite improves slightly the composite stiffness. An increase of the fiber percentage from 12% to 36% vol. content causes a growth of Young's modulus value about 5%.

4. CONCLUSIONS

The mechanical properties of wood mats – polyester resin composites (WPC) were predicted using numerical homogenization methods. For this purpose it was important to introduce the strength and geometry data of the fiber and matrix.

The use of numerical homogenization methods during strength calculations by means of Digimat commercial code allows to take into account the actual geometry data and properties of components in composite structure.

Two-step calculations for wood and glass mats saturated with polyester resin must be performed: one for beam roving, and subsequently for the representative area of mats saturated with resin.

In the case of numerical homogenization, an additional significant step was the design of RVE that reflected the heterogeneous structure of the composite. Appropriate sizing of RVE and voxel FE mesh allow to receive very high compliance between the results of the calculated grammage of glass mat composite and literature data.

In the case of taking into account the only mechanical properties, neglecting ecological and economic aspects the using of wood mat-polyester resin composites will be ineffective.

ACKNOWLEDGEMENT

The research leading to these results has received funding from the People Programme (Marie Curie International Research Staff Exchange) of the European Union's Seventh Framework Programme FP7/2007-2013/ under REA grant agreement n° PIRSES-GA-2013-610547.

REFERENCES

Abdulle, A. (2013). Numerical homogenization methods (No. EPFL-ARTICLE-184958).

Autodesk Moldflow Insight (2013) – material database.

Aziz, S. H., Ansell, M. P., Clarke, S. J., & Panteny, S. R. (2005). Modified polyester resins for natural fibre composites, *Composites Science and Technology*, 65, 525–535. doi:10.1016/j.compscitech.2004.08.005

Bendsøe, M. P., & Kikuchi, N. (1988). Generating optimal topologies in structural design using a homogenization method. *Computer methods in applied mechanics and engineering*, 71(2), 197–224. doi: 10.1016/0045-7825(88)90086-2

Campilho, R.D.S.G. (2015). *Natural Fiber Composites*. Boca Raton: CRC Press.

Doghri, I., & Tinel, L. (2006). Micromechanics of inelastic composites with misaligned inclusions: numerical treatment of orientation. *Computer methods in applied mechanics and engineering*, 195(13), 1387–1406. doi: 10.1016/j.cma.2005.05.041

Dominguez, R. J., & Rice, D. M. (1983). High strength continuous glass strand – polyurethane composites by the reaction injection molding process. *Polymer composites*, 4, 185–189. doi: 10.1002/pc.750040310

e-Xstream engineering (2016). *DIGIMAT - User's manual,* MSC Software Belgium SA, Mont-Saint-Guibert.

Frącz, W., Janowski, G., & Ryzińska, G. (2017). The strenght analysis of GFRP composite product taking into account its heterogenic structure for different reinforcements. *Composites Theory and Practice*, 2, 103–108.

Hedley, C. W. (1994). *Mold filling parameters in resin transfer molding of composites (doctoral dissertation)*. Bozeman: Montana State University.

Ho, M., Wang, H., Lee, J., Ho, C., Lau K., Leng J., & Hui, D. (2011). Critical factors on manufacturing processes of natural fibre composites. *Composites: Part B*, 43, 3549-3562. doi: 10.1016/j.compositesb.2011.10.001

Kim, D. S., & Macosko, C. W. (2000). Reaction injection molding process of glass fiber reinforced polyurethane composites. *Polymer Engineering & Science*, 40(10), 2205–2216. doi: 10.1002/pen.11352

Klyosov, A. A. (2007). *Wood-Plastic Composites*. New Jersey: John Wiley & Sons.

Kubit, A., Bucior, M., & Zielecki, W. (2016). The impact of the multiwall carbon nanotubes on the fatigue properties of adhesive joints of 2024-T3 aluminium alloy subjected to peel. *Procedia Structural Integrity*, 2, 334–341. doi: 10.1016/j.prostr.2016.06.043

Kutnar, A., & Muthu S. S. (2016). *Environmental Impacts of Traditional and Innovative Forest-based Bioproducts, Environmental Footprints and Eco-design of Products and Processes*, Singapore: Springer.

Rowell, R. M. (2013). *Handbook of Wood Chemistry and Wood Composites, Second Edition*. Boca Raton: CRC Press.

Thakur, V. K., & Thakur, M. K. (2014) Processing and characterization of natural cellulose fibers/thermoset polymer composites. *Carbohydrate Polymers*, 109, 102–117, doi: 10.1016/j.carbpol.2014.03.039

Trevino, L., Rupel, K., Young, W. B., Liou, M. J., & Lee, L. J. (1991). Analysis of resin injection molding in molds with preplaced fiber mats. I: Permeability and compressibility measurements. *Polymer composites*, 12, 20–29. doi: 10.1002/pc.750120105

Zielecki, W., Kubit, A., Kluz, R., & Trzepieciński, T. (2017). Investigating the influence of the chamfer and fillet on the high-cyclic fatigue strength of adhesive joints of steel parts. Journal of Adhesion Science and Technology, 31(6), 627–644. doi: 10.1080/01694243.2016.1229521

Applied Computer Science,vol. 13, no. 4, pp. 76–86
doi: 10.23743/acs-2017-31

Submitted: 2017-11-02
Revised: 2017-11-17
Accepted: 2017-12-05

neural network application, forecasting,sutures tensile

Robert KARPIŃSKI[*], *Jakub GAJEWSKI*[*]
Jakub SZABELSKI[**], *Dalibor BARTA*[***]

APPLICATION OF NEURAL NETWORKS IN PREDICTION OF TENSILE STRENGTH OF ABSORBABLE SUTURES

Abstract

The paper presents results of research on neural network application in forecasting the tensile strength of two types of sutures. The preliminary research was conducted in order to establish the accuracy of the proposed method and will be used for formulating further research areas. The neural network enabled evaluation of suture material degradation after 3-to-6-days' exposure to Ringer's solution. The encountered problems regarding inaccuracies show that developing a single model for sutures may be difficult or impossible. Therefore future research should be conducted for a single type of sutures only and require applying additional parameters for the neural network.

1. INTRODUCTION

Surgical sutures are widely used in numerous fields of specialist medicine, and are mainly applied to join the edges of wounds resulting from a surgical intervention or an accident. Non-absorbable sutures retain their mechanical properties over the entire period of implantation until removed from the tissue,

[*] Lublin University of Technology, Faculty of Mechanical Engineering, Department of Machine Design and Mechatronics, Nadbystrzycka 36, 20-618 Lublin, Poland, r.karpinski@pollub.pl, j.gajewski@pollub.pl
[**] Lublin University of Technology, Faculty of Mechanical Engineering, Institute of Technological Systems of Information, Nadbystrzycka 36, 20-618 Lublin, Poland, j.szabelski@pollub.pl
[***] University of Zilina, Faculty of Mechanical Engineering, Univerzitna 1, 01026 Zilina, Slovak Republic, dalibor.barta@fstroj.uniza.sk

whereas absorbable sutures lose their initial properties to the point of complete absorption. In the processes of biodegradation and absorption two major parameters are considered: absorption of suture mass and retention of initial tensile strength (Zapalski & Chęciński, 1999; Karpiński, Szabelski & Maksymiuk, 2017; Karpiński, Górniak, Szabelski & Szala, 2016a). Synthetic absorbable sutures become absorbed in the process of hydrolytic decomposition of the suture material. Premature strength loss, on account of suture material absorption occurring before the healing process completes, results in wound dehiscence. On the other hand, excessively low tensile properties may contribute to the suture acting like a surgical knife, cutting through surrounding tissues. It is therefore critical to the applicability of sutures that their selection is suitable to purpose requirements (Zapalski & Chęciński, 1999; Karpiński, Górniak, Szabelski & Szala, 2016b). As in other material testing applications, computational methods may aid testing the changes in strength profile of selected suture materials. The aim of this preliminary study is to assess the suitability of *Radial Basis Function* Networks (RBF) in prediction of suture strength (Luo, 2017; Youshia, Ali & Lamprecht, 2017; Lv & Zheng, 2017; Hasnaoui, Krea & Roizard, 2017).

1.1. Radial Basis Function Networks

Radial basis functions neural networks (RBF) consist of a single hidden layer with radial neurons and the linear output layer (including scalar product). The hidden layer consists of radial neurons which – in the predicting strength case – model the Gaussian response surface. A function of any shape can be modelled using only one hidden layer. This results from the fact that the function is of a nonlinear character. In order for the network to create an effective model of a given function, it is necessary to ensure that the network's system hasa sufficient number of radial neurons. With a suitable number of radial neurons, each important detail of the function being modelled can be assigned a relevant radial neuron, which leads to producing a solution that reflects the applied function with a satisfactory accuracy. The publications supporting the scientific achievement present the conclusions about the selection of signal features as input variables in RBF systems, comparing them to the previously used network models (Gajewski, Golewski & Sadowski, 2017).

In radial basis functions, for the input vector ϱ, the hidden neuron realises the radialchange around a given centre k function $\varphi(\varrho) = \varphi(\|\varrho\text{-}k\|)$, where non-zero values occur only in the vicinity of the centre. Based on the hidden neurons radially reflecting the space around individual points, the input neuron reflects a multidimensional space. The approximate output of an RBF, for the K basis functions can be written as:

$$y = \sum_{i=1}^{N} w_i \varphi(\|\varrho - \mathrm{k}_i\|) \quad (1)$$

where c_i is a set of determinable centres (i = 1, 2, 3, ... , N).

For the applied Gaussian radial basis function at point c_i, we can define:

$$\varphi(\varrho) = \varphi(\|\varrho - \mathrm{k}_i\|) = \exp\left(-\frac{\|\varrho - \mathrm{k}_i\|^2}{2\sigma_i^2}\right) \quad (2)$$

where σ_i is a parameter which determines width of the function.

2. ABSORBABLE SURGICAL SUTURES

What is considered an absorbable suture material is the one that is subject to loss of mechanical properties, predominantly tensile strength, over a certain period of time in the body. Degradation of suture material as a result of various enzymatic reactions commences upon application of the stitch (Zapalski & Chęciński, 1999; Zurek, Kajzer, Basiaga & Jendruś, 2016). In the literature the term "*enzymatic degradation*" tends to be used to refer to decomposition of absorbable protein sutures, such as catgut, whereas synthetic suture material degradation occurs as a result of hydrolysis. As mentioned, the process of degradation begins immediately after inserting the suture material into the tissue and is complete after the period of 15–20 weeks. It ought to be remarked that hydrolysis is also catalysed by esterase enzyme (& Chęciński, 1999; Bollom & Meister, 2013; Casey & Lewis, 1986). Absorbable surgical sutures are also divided according to their mass absorption profile into: short-term, medium-term and long-term absorption sutures (Table 1).

Tab. 1. Classification of sutures according to mass absorption profile

Mass absorption	50% of initial tensile strength	Complete mass absorption
Short-term	5–7 days	42–56 days
Medium-term	14–21 days	60–90 days
Long-term	28–35 days	180–210 days
Extremelylong-term	90 days	approx. 390 days

It is highly important to differentiate between the complete suture mass absorption time and the tensile strength retention time, as it is the latter that provides critical information regarding absorbable suture applicability (Zapalski & Chęciński, 1999).

3. RELATIVE TENSILE STRENGTH OF SURGICAL SUTURES

To determine the impact of selected environmental factors on mechanical properties of surgical sutures physical tests were carried out. The study consisted in loading the suture material in tension to measure its linear tensile strength immediately after unpacking (pre-immersion), and collating the results with the second group of suture samples that were exposed to Ringer's solution for a particular period of time (post-immersion). The sutures were tested and stored at a temperature of 22°C.

There were two different types of short-term absorbable surgical sutures selected for testing. They were divided according to absorption time in the body into non-absorbable and absorbable sutures. The intervals between subsequent tensile strength tests reflected periods of mass suture absorption declared by particular manufacturers. The tests employed Ringer's solution, *i.e.* an isotonic solution, of identical osmotic potential as plasma, 1000 ml of which contains 8.6 g of sodium chloride, 0.3 g of potassium chloride, 0.33 g of calcium chloride dihydrate which corresponds to the following electrolyte levels: sodium – 147 mmol/l, potassium – 4 mmol/l, calcium – 2.2 mmol/l, chlorides – 156 mmol/l. The sutures were cut into 20 cm long samples. The diameter was measured with a micrometer by MIB, model *IP 54* with the accuracy of 0.001 mm. Afterwards, the measured tensile strength was compared with the one provided on the packaging.

The testing was carried out on a test set-up comprising MTS Bionix – Servohydraulic Test System universal testing machine located in the Institute of Technological Systems of Information (fig. 1). MTS TestWorks software allowed us to adjust the tensile loading speed according to the structure of the suture under examination – 10 mm/min for multifilament and 25 mm/min for monofilament materials. The test was automatically stopped when the load dropped by 75% at a short interval (suture failure).

Fig. 1. a) MTS Bionix material testing machine, b) the tensile strength test gripping system

The statistical analysis to determine discrepancies in the results obtained from the strength tests and the neural network prediction was carried out by means of Statistica 12.5 software, at a standard significance level $\alpha = 0.05$ (Krysicki, Bartos, Dyczka, Królikowska & Wasilewski, 1999; Rabiej, 2012).

In order to verify whether the scatter of particular strength test results corresponds to the normal distribution, we employed three tests: Kolmogorov-Smirnov tests, Lilliefors test and Shapiro-Wilk W test.

The analysis of equality of variances was carried out with three tests: F (Fisher's exact test), Levene's test and Brown-Forsythe test. For the results exhibiting normal distribution and equal variances – for the analysis of equality of means of relative tensile strength of surgical sutures at the specified significance level Student's T test was employed. In the case of results characterised by normal distribution but showing no equality of variances, the equality of mean relative tensile strength values was conducted by means of Student's T-test with separate variances adjustment (Cochran-Cox test) (Krysicki et al., 1999, Rabiej, 2012).

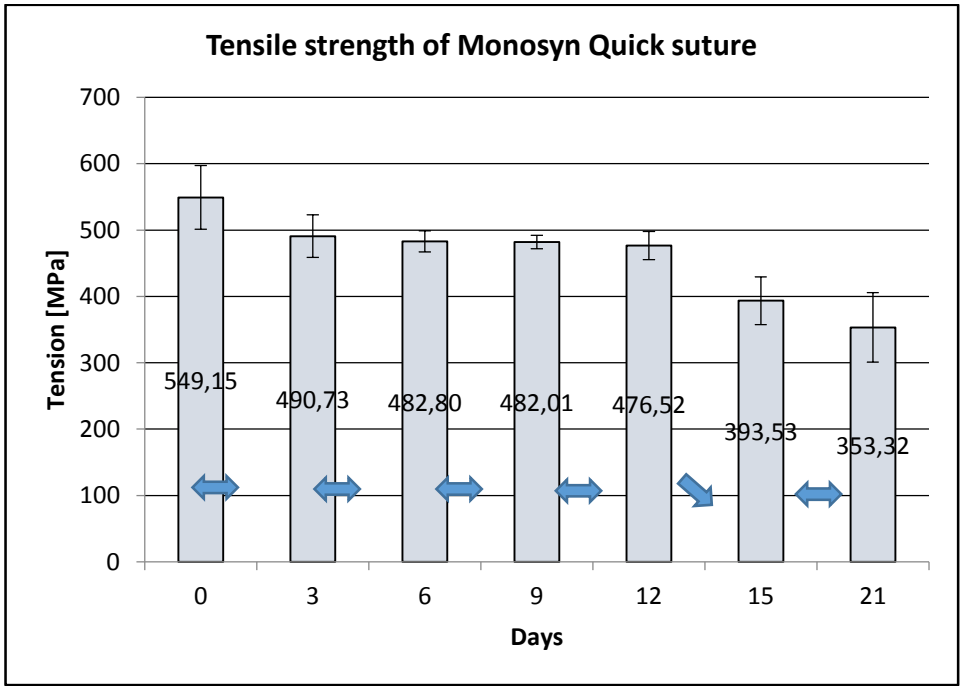

Fig. 2. Experimental results of tensile strength of Monosyn Quick sutures

The statistical analysis conducted for the Monosyn Quick sutures (fig. 2) showed no substantial differences between the pre-immersion (D0) and post-immersion sample series, including samples exposed to solution for three (D3),

six (D6), nine (D9) and 12 days (D12). Major discrepancies, however, occurred between the series tested during the 12th (D12) and 15th (D15) day of immersion. There were no significant differences between the series under examination during the 15th (D15) and 21st (D21) day in the solution either.

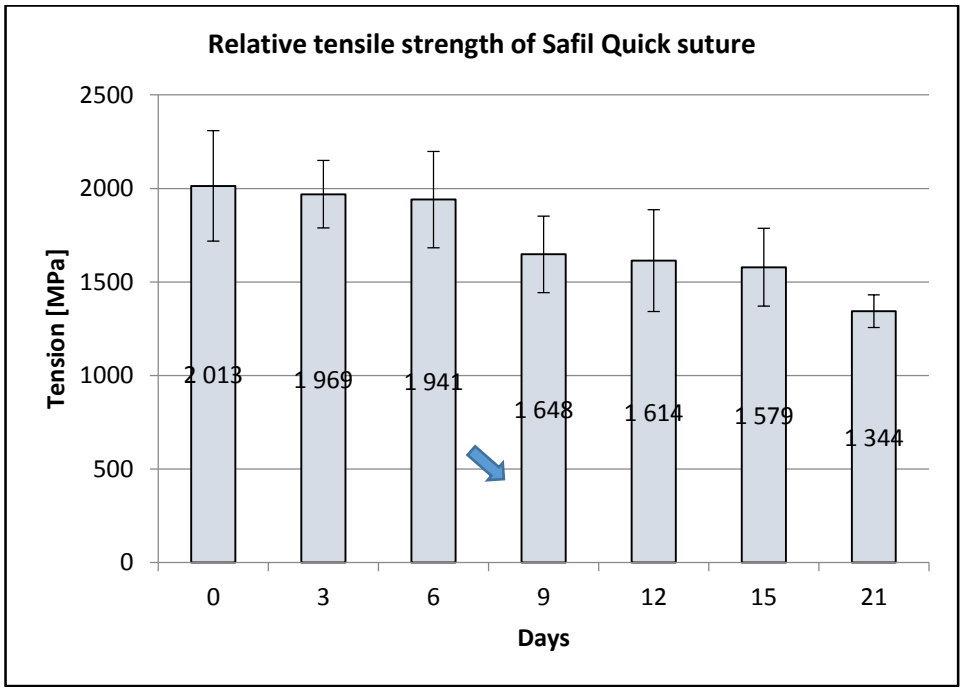

Fig. 3. Experimental results of tensile strength of Safil Quick sutures

The statistical analysis of Safil Quick sutures (fig. 3) showed no substantial differences between the pre-immersion samples (D0), including samples exposed to the solution for three days (D3) and six days (D6). Major discrepancies, however, occurred between the series tested during the 6th (D6) and 9th (D9) day of immersion. There were no significant differences between the series under examination during the 9th (D9), 12th (D12), 15th (D15) and 21st (D21) day in the solution.

4. RESULTS FROM NUMERICAL TESTS

The numerical part of this study consisted in applying artificial neural networks in prognosis of braking load of suture samples at later stages of material degradation, which were not subjected to experimental testing (Fig. 4). The numerical study was conducted by means of Statistica 13 software, which offers artificial neural network designing solutions.

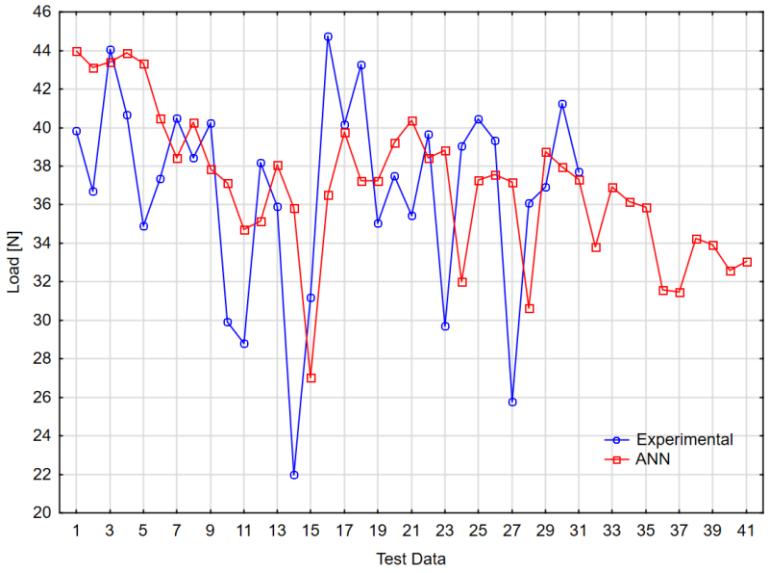

Fig. 4. Results of prognosis for Monosyn Quick suture

The figure above shows the lookahead of Monosyn Quick suture strength, evaluated by neural network. Six inputs resulted from the number of lag samples, which provided the base for further prognosis. The hidden layer consisted of 5 neurons. The data presented in the diagram show slight decrease in suture strength at subsequent stages of suture material deterioration. Although burdened with uncertainty, look ahead in neural networks indicates deterioration of tensile strength of samples in subsequent steps of the numerical experiment. The presented method may prove particularly useful in samples showing slight changes in parameters.

Tab. 2. Summary of Safil Quick network

Summary of active networks (Safil Quick / Days)			
Quality (training)	**Quality (testing)**		**Quality (validation)**
0.624576	0.682461		0.785921
Error (training)	**Error (testing)**		**Error (validation)**
13.19405	10.42415		3.045410
Training algorithm	**Error function**	**Activation (hidden)**	**Activation (output)**
RBFT	SOS	Gaussian	Linear

Table 2 shows network training quality for the training, validation and testing sets, as well as training algorithms, error function and neuron activation. The division into testing and validation sub-sets was conducted at random. The presence of both these sets is necessary to conduct further network training with immediate validation of outputs. The reliability of the network is determined by the final set of data. High discrepancy in the results of training is likely to be the consequence of the small amount of experimental data, which is shown also in Fig. 5. The graphs of breaking loads, obtained from the experimental data and from the RBF network prognosis, show certain discrepancies of the data sets. Further studies with a larger sample set and higher sampling frequency are required to determine the efficacy of the method. The graph shows certain data generalisation, which must be applied given the character of the experiment, however, the correct prognosis trend is retained.

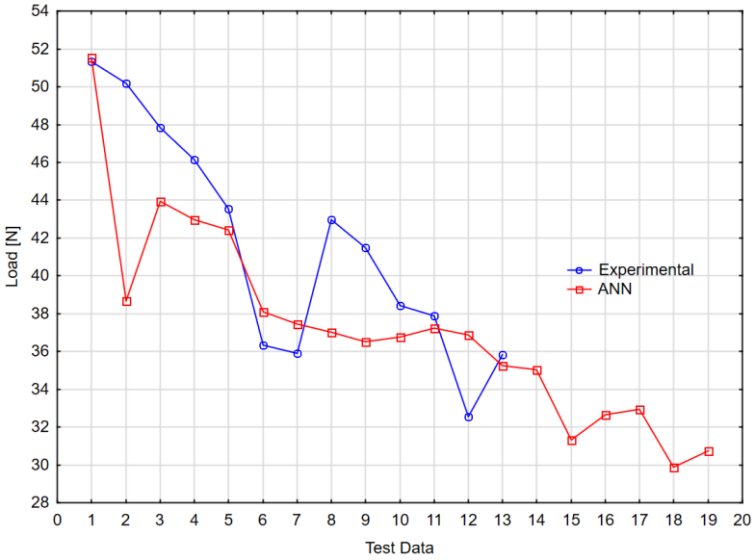

Fig. 5. Results of prognosis for Safil Quick suture

Tab. 3. Network weights for network, modelling the Safil Quick suture

Weight ID	Network weights	
	Connections	Weighted sums
1	monosyn-1 --> hidden neuron 1	-0.041493
2	monosyn-1 --> hidden neuron 2	-0.061277
3	monosyn-1 --> hidden neuron 3	-0.062243
4	monosyn-1 --> hidden neuron 4	0.635251
5	monosyn-2 --> hidden neuron 1	0.665310
6	monosyn-2 --> hidden neuron 2	0.596699
7	monosyn-2 --> hidden neuron 3	-0.276709
8	monosyn-2 --> hidden neuron 4	0.109763
9	monosyn-3 --> hidden neuron 1	-0.047365
10	monosyn-3 --> hidden neuron 2	0.648808
11	monosyn-3 --> hidden neuron 3	0.735964
12	monosyn-3 --> hidden neuron 4	0.635251
13	radial deviation hidden neuron 1	0.291209
14	radial deviation hidden neuron 2	0.081621
15	radial deviation hidden neuron 3	0.291209
16	radial deviation hidden neuron 4	0.081621
17	hidden neuron 1 --> monosyn	-0.021130
18	hidden neuron 2 --> monosyn	0.001865
19	hidden neuron 3 --> monosyn	-0.151329
20	hidden neuron 4 --> monosyn	0.005065
21	hidden shift --> monosyn	0.204858

RBF network results for Monosyn Quick suture are show in Table 4.

Tab. 4. Summary of Monosyn network

Summary of active networks (Monosyn2017 sutures)			
Quality (training)	**Quality (testing)**		**Quality (validation)**
0.841304	0.765371		0.829250
Error (training)	**Error (testing)**		**Error (validation)**
5.074944	7.207897		13.54326
Training algorithm	**Error function**	**Activation (hidden)**	**Activation (output)**
RBFT	SOS	Gaussian	Linear

The generated network error was 80%.

5. SUMMARY

This paper presents the results from the preliminary study evaluating the application of neural networks in prediction of surgical suture strength. The main objective of the study was to verify the applicability of the method for the given purpose and to pave the way for future studies. In both tested sutures, Monosyn Quick and Safil Quick, the Radial Basis Function Network exhibited good results in prediction of immediate relative tensile strength of the suture material, i.e. within the period of 3-6 days' immersion in Ringer's solution. The diagrams show that despite slight discrepancies the neural network is capable of predicting suture material degradation at a good level of certainty. The two suture materials analysed in the study exhibit slight differences in their absorption profile, which proves quite problematic in terms of developing a universal model of neural network for the strength prediction of all suture material types. It becomes evident that different suture material will require a separate neural network. In order for the future stages of this study to compensate for the limited application of neural networks, an extensive database of surgical suture materials should be created to provide a wide array of both suture material types and number. In terms of directions for future research, further work should establish the criteria for designing surgical sutures for particular purpose requirements. This will necessitate determining factors that affect mechanical properties of sutures to the greatest extent.

REFERENCES

Bollom, T., & Meister, K. (2013). Surgical principles: biodegradable materials in sports Medicine. In J. C. DeLee, D. J. Drez, & M. D. Miller (Eds.), *DeLee & Drez's Orthopaedic Sports Medicine: Principles and Practice. 2nd edition*. Philadelphia, PA: Saunders.

Casey, D. J., & Lewis, O.G. (1986). Absorbable and nonabsorbable sutures. In A.F. von Recum (Ed.), *Handbook of biomaterials. Scientific and clinical testing of implant materials*. New York: Macmillan.

Gajewski, J., Golewski, P., & Sadowski, T. (2017). Geometry optimization of a thin-walled element for an air structure using hybrid system integrating artificial neural network and finite element method. *Composite Structures*, 159, pp. 589–599. doi:10.1016/j.compstruct.2016.10.007

Hasnaoui, H., Krea, M., & Roizard, D. (2017). Neural networks for the prediction of polymer permeability to gases. *Journal of Membrane Science*, *541*, 541–549. doi:10.1016/j.memsci.2017.07.031

Karpiński, R., Górniak, B., Szabelski, J., & Szala, M. (2016b). Charakterystyka i podział materiałów szewnych, In B. Zdunek, & M. Szklarczyk (Eds.), *Wybrane zagadnienia z biologii molekularnej oraz inżynierii materiałowej* (pp. 127–139). Lublin: Wydawnictwo Naukowe TYGIEL Sp. z. o. o.

Karpiński, R., Górniak, B., Szabelski, J., & Szala, M. (2016a). Historia chirurgii i materiałów szewnych, In B. Zdunek, & M. Szklarczyk (Eds.), *Wybrane zagadnienia z biologii molekularnej oraz inżynierii materiałowej* (pp. 140–150). Lublin: Wydawnictwo Naukowe TYGIEL Sp. z. o. o.

Karpiński, R., Szabelski, J., & Maksymiuk, J. (2017). Effect of Ringer's Solution on Tensile Strength of Non-Absorbable, Medium- and Long-Term Absorbable Sutures. *Advances in Science and Technology Research Journal*, *11*(4), 11-20. doi:10.12913/22998624/76084

Krysicki, W., Bartos, J., Dyczka, W., Królikowska, K., & Wasilewski, M. (1999). *Rachunek prawdopodobieństwa i statystyka matematyczna w zadaniach. część II. Statystyka matematyczna. Wydanie Szóste*. Warszawa: Wydawnictwo Naukowe PWN.

Lv, H., & Zheng, Y. (2017). A newly developed tridimensional neural network for prediction of the phase equilibria of six aqueous two-phase systems. *Journal of Industrial and Engineering Chemistry*, *57*, 377–386. doi:10.1016/j.jiec.2017.08.046

Rabiej, M. (2012). *Statystyka z programem Statistica*. Gliwice: Helion.

Youshia, J., Ali, M. E., & Lamprecht, A. (2017). Artificial neural network based particle size prediction of polymeric nanoparticles. *European Journal of Pharmaceutics and Biopharmaceutics*, *119*, 333–342. doi: 10.1016/j.ejpb.2017.06.030

Luo, Y. (2017). Recurrent neural networks for classifying relations in clinical notes. *Journal of Biomedical Informatics*, *72*, 85–95.

Zapalski, S., & Chęciński, P. (1999). *Szwy chirurgiczne: wybrane problemy*. Bielsko-Biała: Alfa-Medica Press.

Zurek, M., Kajzer, A., Basiaga, M., & Jendruś, R. (2016). Właściwości wytrzymałościowe wybranych polimerowych nici chirurgicznych. *Polimery*, *61* (5), 334–338. doi:10.14314/polimery.2016.334

Applied Computer Science, vol. 13, no. 4, pp. 87–97
doi: 10.23743/acs-2017-32

Submitted: 2017-11-15
Revised: 2017-12-04
Accepted: 2017-12-20

modelling, computer simulation, manufacturing, production flow, job shop, Enterprise Dynamics, 4D script

Arkadiusz GOLA[*]*, Łukasz WIECHETEK*[**]

MODELLING AND SIMULATION OF PRODUCTION FLOW IN JOB-SHOP PRODUCTION SYSTEM WITH ENTERPRISE DYNAMICS SOFTWARE

Abstract

The paper presents capabilities of Enterprise Dynamics software in modelling and simulation of production process in job-shop conditions. The modelled production process was conducted on the total of 8 machine tools representing 5 different types. The conducted simulation represented production of three types of parts in an alternating sequence of jobs according to the technological machine sequence. The production process of the developed model was controlled by means of 4D Script programming language.

1. INTRODUCTON

The challenges of the modern market, such as global competition, demand from an enterprise constant effort towards increasing the effectiveness of production processes. There is an ongoing pressure on both established and newly designed production systems to reconcile highly flexible production of a wide range of goods and simultaneously ensure optimised engagement of the stock of machine tools (Esmaeilian, Behdad & Wang, 2016).

[*] Lublin University of Technology, Faculty of Mechanical Engineering, Institute of Technological Systems of Information, Nadbystrzycka 36, 20-618 Lublin, tel.: +48 81 538 45 35, e-mail: a.gola@pollub.pl
[**] Maria Curie-Skłodowska University, Faculty of Economics, Department of Management Information Systems, M. Curie-Skłodowskiej 5, 20-036 Lublin, tel.: +48 81 537 28 80, e-mail: lukasz.wiechetek@umcs.pl

Because of the great variety of existing manufacturing system structures as well as different assumptions and limitations concerned with manufacturing orders, it is very difficult to find the optimal solution using mathematical models. Most of the combinatorial optimization problems are NP-hard. Therefore, implementation of computer simulation methods to analyze the behaviour of individual systems enables obtaining interesting results over a relatively short period of time (Kłos & Trebuna, 2017).

Modelling and simulation is one of the most proper ways to deal with solutions based on the experience from the real-world complex systems (Longo, 2010). Many scientific papers include the application of computer simulation in the general design of manufacturing systems in the analysis of operational, production planning and scheduling systems (Negahban & Smith, 2014). Jahangirian *et al.* report the results of a review of the applications of simulations, published in peer-reviewed literature between 1997 and 2006 and the analysis of the role of simulation techniques within manufacturing and business (Jahangirian, Eldabi, Nasser, Stergioulas & Young, 2010). Jagstam and Klingstam use discrete event simulation as an aid to conceptual design and the pre-study of manufacturing systems through developing a virtual factory and identify the problems associated with integration of discrete event simulation into the design and manufacturing systems (Jagstam & Klingstam, 2002). Jithavech and Krishnan present a simulation-based method in order to develop and efficient layout design facility with uncertainty as to the demand of the product (Jithavech & Krishnan, 2010). Yang *et al.* propose the use of simulation and a digital factory to construct a virtual plant environment in order to implement integration between process planning and manufacturing (Yang, Zhang, Chen & Li, 2008). Joseph and Sridharan made an evaluation of the routing flexibility of an FMS with the dynamic arrival part types for processing (Joseph & Sridharan, 2011) while Gola *et al.* used the computer simulation method to analyze economic effectiveness of manufacturing system configurations (Danilczuk, Gola & Cechowicz, 2014; Gola & Świć, 2014).

In general, computer simulation methods are mostly used in maximisation of the throughput of production lines. The problem of maximizing the throughput of production lines by changing buffer sizes or locations using simulation methods was studied by Vidalis *et al.* (Vidalis, Papadopoulos & Heavy, 2005). Stanley and Kim presented the results of simulation experiments carried out for buffer allocations in closed, series-production lines (Stanley & Kim, 2012). The overview of the critical literature in the area of buffer allocation and production and production line performance was done by Demir, Tunali and Eliiyi (Demir, Tunali & Eliiyi, 2014). Finally a lot of research in the field of throughput analysis and optimization of serial and automatic production lines were done by Kłos *et al*. (Kłos & Patalas-Maliszewska, 2015; Kłos, Patalas-Maliszewska & Trebuna, 2016; Kłos & Trebuna, 2015).

In this article, computer simulation methods are used to analyze production flow in a job-shop manufacturing system. The research was performed on a production system including 8 CNC machine tools representing 5 different types. The conducted simulation represented production of three types of parts in an alternating sequence of jobs. The material flow was directed to individual machines following established technological machine sequence. The production process of the developed model was controlled by means of 4DScript programming language.

2. A SIMULATION MODEL OF A JOB-SHOP PRODUCTION SYSTEM

The model of the production system was prepared on the basis of an existing example of a manufacturing system, dedicated to the production of casing parts for the machine building sector. The model and simulation experiments were implemented using Enterprise Dynamics Software (version 7.0.0). The following constraints of the model were introduced:

- The analysed production system consists of 5 types of CNC machine tools, the total number of which is shown in Table 1 below.

Tab. 1. The number of machine tools

Machine tool name	The number of machine tools in the system
MACHINE TOOL_1	1
MACHINE TOOL_2	2
MACHINE TOOL_3	1
MACHINE TOOL_4	1
MACHINE TOOL_5	3

- The system produces three different casing parts, the average annual demand for which is show in Table 2.

Tab. 2. Average annual demand for body parts products in the system

Part	Average annual demand
PRODUCT_1	2030 pcs
PRODUCT_2	2420 pcs
PRODUCT_3	1750 pcs

- The machining is realised according to the technological machine sequence, at the time specified by the ratefixer technologist and shown in Fig. 1.

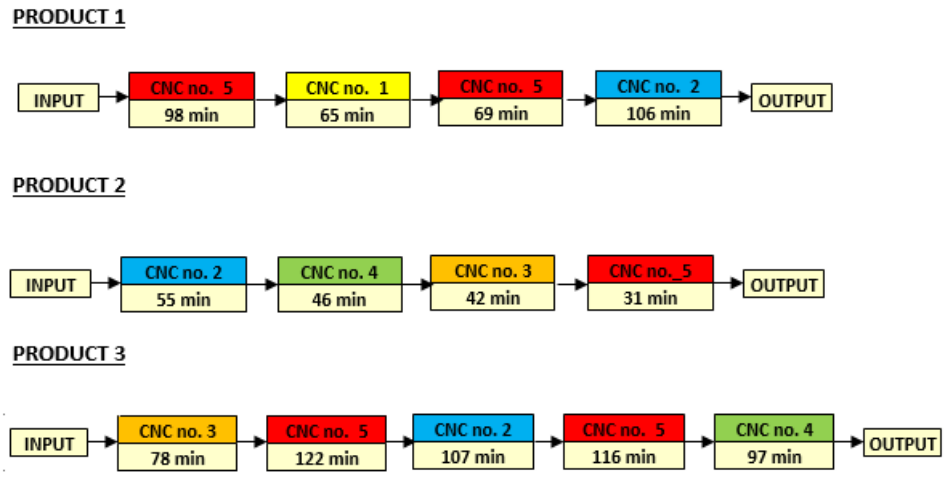

Fig. 1. Technological processes of parts processed in the system

- Input of products corresponds to the time-varying demand and is random both at the input time and the output of the system.
- Machining is carried out according to FIFO principle. In the case of identical machine tools, the product is randomly assigned to a free machine tool.
- The simulation time was specified at 8094 h, which corresponds to effective annual time of system operation.
- To enable simulation of job queue the work-in-progress stores were defined for each machine tool individually, and the storage space was constricted to 20 pcs.
- According to the study assumptions, the layout of machine tools is random, and the works transport is set to zero, as both these issues fall out of the scope of the study.

The developed production system models are shown in Fig. 2 (a basic model), and Fig. 3 (a model with channels connecting objects indicated). Products – workpieces were marked with dots of three different colours. Also implemented into the model were *Lock atoms*, which allow only a pre-defined number of products through (according to the demand) to be processed.

To represent the random character of processing products arrival times the *Uniform* function was employed. The function specifies the random *Inter-arrival time* for particular products as: Product_1: *Uniform(Mins(0), Mins(470))*, Product_2: *Uniform(Mins(0), Mins(390))*, Product_3: *Uniform(Mins(0), Mins(540))*. The average product arrival time was dictated by the effectiveness of the system operation time and the production programme, at the constraint that the last product must not arrive after the 5 days until the end of the year.

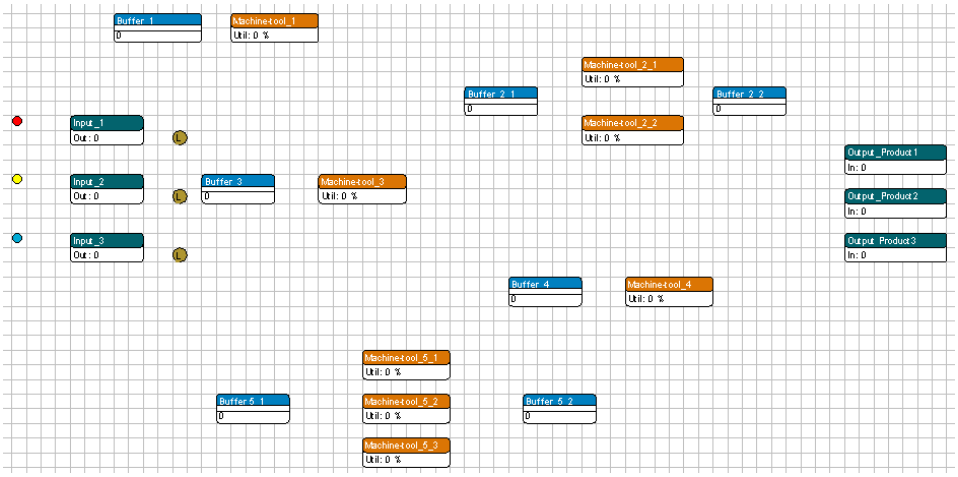

Fig. 2. Basic job-shop system modelled with Entreprise Dynamics system

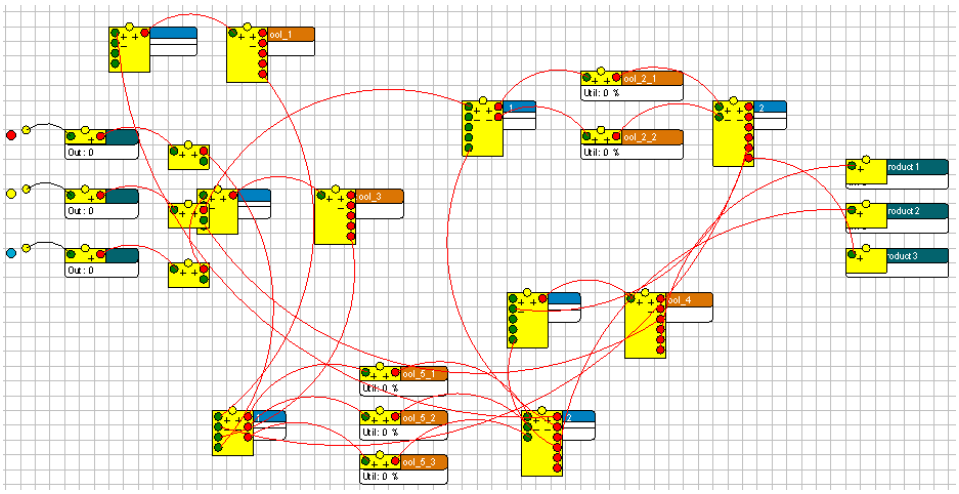

Fig. 3. The job-shop system modelled Enterprise Dynamics software including channels between objects

Since each product is characterised by different processing times on different machine tools and machine routes (governed by the technological process), 4DScript syntax was employed to define times and machine routes. The code created to control the process was developed, whose structure is shown in Tab. 3.

Tab. 3. The structure of scripts controlling the production process in the model

Type of object	Script
PRODUCT (an example of Product_1)	Trigger on exit: `Do (SetLabel([Time1],Mins(98),i), SetLabel([Time2],Mins(65),i), SetLabel([Time3],Mins(69),i), SetLabel([Time4],Mins(106),i), SetLabel([Machine2],1,i), SetLabel([Machine3],5,i), SetLabel([Machine4],2,i),SetLabel([Machine5],6,i), SetLabel([Canal],5,i), SetLabel([Step],1,i))`
BUFFER (an example of Buffer 3)	Trigger on exit: `Do (SetLabel([Canal], Case(Label([Step],i), Label([Machine2],i), Label([Machine3],i), Label([Machine4],i), Label([Machine5],i), Label([Machine6],i)),i))`

MACHINE TOOL (an example of Machine_3)	Cycletime:
	`Case(Label([Step],i),Label([Time1],i), Label([Time2],i), Label([Time3],i), Label([Time4],i), Label([Time5],i))`
	Trigger on exit:
	`Do (SetLabel([Step],Label([Step],i)+1,i))`

3. RESULTS OF SIMULATION AND DISCUSSION

The production model analysed in this paper is nondeterministic, therefore having specified the parameters and constraints, 20 simulations of the model were carried out. The results from the simulations are presented in tables 4–6.

Tab. 4. Numbers of input and output products in the system

Simulation No.	Input products			Output products			Production finished?
	PR_1	PR_2	PR_3	PR_1	PR_2	PR_3	
1.	2030	2420	1750	2030	2420	1750	YES
2.	2027	2420	1750	2026	2420	1750	NO
3.	2030	2420	1750	2030	2420	1750	YES
4.	2030	2420	1750	2030	2420	1750	YES
5.	2030	2420	1750	2030	2420	1750	YES
6.	2030	2420	1750	2030	2420	1750	YES
7.	2030	2420	1750	2030	2420	1750	YES
8.	2030	2420	1750	2030	2420	1750	YES
9.	2030	2420	1750	2030	2420	1750	YES
10.	2025	2420	1750	2023	2420	1750	NO
11.	2030	2420	1750	2030	2420	1750	YES
12.	2030	2420	1750	2030	2420	1750	YES
13.	2030	2420	1750	2030	2420	1750	YES
14.	2002	2420	1750	2000	2420	1750	NO
15.	2030	2420	1750	2030	2420	1750	YES
16.	2030	2420	1747	2030	2420	1745	NO
17.	2030	2420	1750	2030	2420	1750	YES
18.	2030	2420	1750	2030	2420	1750	YES
19.	2030	2420	1750	2030	2420	1750	YES
20.	2030	2420	1750	2030	2420	1750	YES

Tab. 5. Average machining times in the simulated process

Simulation No.	Average machining times							
	MT_1	MT_2_1	MT_2_2	MT_3	MT_4	MT_5_1	MT_5_2	MT_5_3
1.	27.2	55.1	55.1	49.0	57.9	57.5	56.8	56.8
2.	27.1	55.0	55.2	49.0	57.9	57.0	56.8	57.2
3.	27.2	55.2	55.1	49.0	57.9	56.5	57.1	57.4
4.	27.2	55.2	55.0	49.0	57.9	57.1	56.8	57.1
5.	27.2	55.1	55.2	49.0	57.9	56.9	57.0	57.1
6.	27.2	55.0	55.3	49.0	57.9	57.5	56.2	57.4
7.	27.2	55.2	55.1	49.0	57.9	56.9	56.8	57.3
8.	27.2	55.5	54.8	49.0	57.9	57.1	56.9	56.9
9.	27.2	55.4	54.9	49.0	57.9	56.0	57.5	57.5
10.	27.1	55.0	55.1	49.0	57.9	56.9	56.8	56.8
11.	27.2	56.0	54.3	49.0	57.9	57.2	56.9	56.9
12.	27.2	55.3	55.0	49.0	57.9	56.5	56.9	57.6
13.	27.2	55.6	54.7	49.0	57.9	57.0	57.0	57.0
14.	26.8	55.2	54.4	49.0	57.9	56.8	56.8	56.7
15.	27.2	55.1	55.2	49.0	57.9	57.2	56.9	57.0
16.	27.2	54.5	55.7	49.0	57.8	57.4	56.5	56.9
17.	27.2	54.6	55.7	49.0	57.9	57.3	57.2	56.6
18.	27.2	55.4	54.9	49.0	57.9	57.1	57.0	57.0
19.	27.2	55.7	54.6	49.0	57.9	57.0	57.1	56.9
20.	27.2	55.3	54.9	49.0	57.9	57.0	56.9	57.1

Tab. 5. Maximum number of products and average waiting times in subsequent simulations

Simulation No.	Number of products in storage (pcs.)					Average waiting time (seconds)				
	B_1	B_2	B_3	B_4	B_5	B_1	B_2	B_3	B_4	B_5
1.	2	5	5	5	6	289.0	573.3	951.9	1381.6	310.6
2.	2	4	4	5	5	263.9	538.2	961.8	1355.0	278.5
3.	2	5	4	5	6	268.9	522.3	959.1	1428.4	281.0
4.	2	4	3	4	6	299.3	565.6	1014.6	1444.9	321.8
5.	2	5	4	4	7	281.2	562.0	955.1	1385.3	319.4
6.	2	5	5	5	6	233.2	554.8	1040.9	1520.3	306.4
7.	2	4	4	5	7	289.2	545.4	975.1	1444.2	332.2
8.	2	4	4	5	5	231.2	533.3	982.4	1374.8	267.0
9.	2	5	5	5	6	243.8	540.7	1030.5	1487.8	326.2
10.	2	6	4	5	6	247.3	583.7	984.5	1543.2	301.0
11.	2	4	4	4	5	227.4	523.8	988.3	1435.4	284.7
12.	2	5	4	5	5	285.5	562.5	955.1	1476.9	304.9
13.	3	4	4	4	7	319.5	575.9	914.3	1446.6	337.3
14.	2	6	4	5	6	246.8	526.0	977.2	1442.6	260.8
15.	2	5	4	5	7	314.9	536.8	922.5	1493.1	322.7
16.	2	4	3	4	6	267.1	567.8	885.9	1380.7	292.2
17.	2	5	6	5	6	303.3	554.7	1040.9	1491.1	325.4
18.	2	5	4	5	5	296.1	576.7	980.2	1506.6	297.2
19.	2	5	3	4	7	276.5	572.7	948.6	1402.6	327.1
20.	2	5	4	5	5	239.3	592.1	1005.6	1419.6	320.0

The report contains such data as: the number of products entering the production process, the number of products manufactured in simulation (tab. 4), average workload of machine tools in simulation (tab. 5) and the maximum number of products in buffers between operations and average waiting time for processing (tab. 6)

The simulation of the process shows that the job-shop system is suitable for the performance of the defined task. This is proved by both the behaviour of the system in operation as well as the workload on each of the machine tools and buffers between operations.

The analysis of production process models leads to several main conclusions:

- the analysed system is capable of providing a relatively smooth performance of scheduled production jobs, which are random time- and number-wise. In all models the system processed the specified number of input products. Failure to carry out the annual plan (observed in simulations 2, 10 and 16) resulted from not entering all the products into production in the specified time (simulation time), which was a consequence of the defined randomness of product input. In each of the three cases, the system managed to make up for the delay in another period (year),
- bottlenecks, connected with overloading machine tools and/or exceeding work-in-progress store space, were not observed in any of the simulations,
- short queue at work-in-progress storage (Figs. 4-8) and relatively short waiting time between processing jobs (Tab. 5) confirm good production flow in the system,

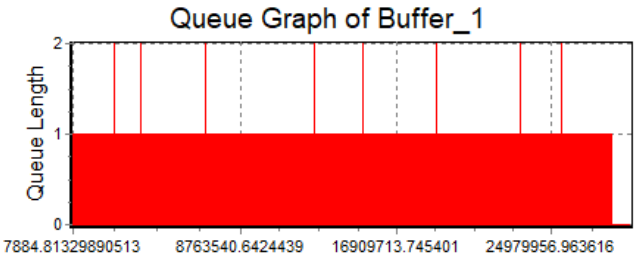

Fig. 4. Queue graph of BUFFER_1 over production process simulation

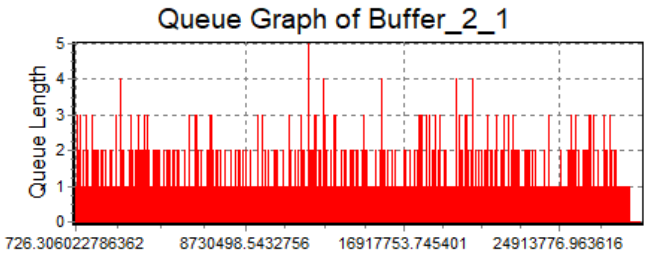

Fig. 5. Queue graph of BUFFER_2_1 over production process simulation

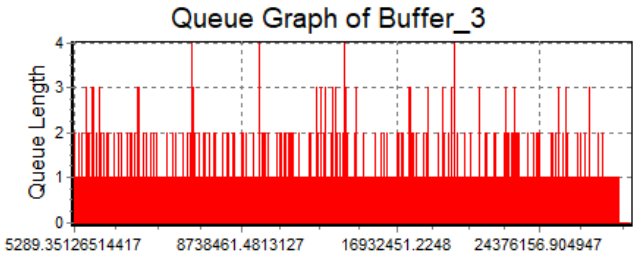

Fig. 6. Queue graph of BUFFER_3 over production process simulation

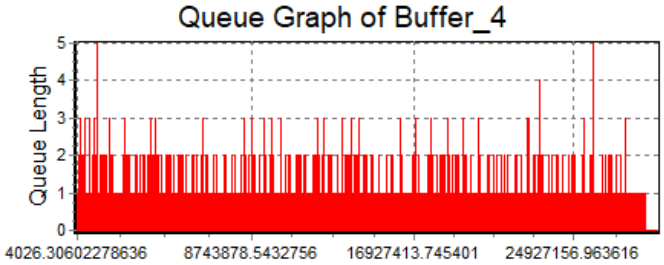

Fig. 7. Queue graph of BUFFER_4 over production process simulation

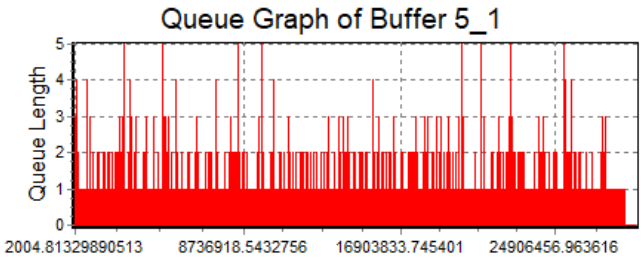

Fig. 8. Queue graph of BUFFER_1 BUFFER_5_1 over production process simulation

– despite stochastic character of the process, its high stability is confirmed by little variation of machining time results and of buffer queue indicators.

4. SUMMARY AND CONCLUSIONS

Designing a production system is a highly complicated process, partly due to the fact that there may occur certain contradictory optimisation objectives, such as flexible production of a range of products and maximisation of the set of machine tools engagement. Job-shop is a specific representative of production systems

which combines crossing routes and repeated processing of jobs on machine tools. These constraints of a job-shop model cause that the typical discrete process modelling software is unsuitable for this purpose.

This paper showed methods of modelling and workflow analysis in the job-shop environment consisting of 8 machine tools, which process 3 types of products requiring different technological processes. The system was modelled by means of Enterprise Dynamics software. Given the character of the modern market it was resolved that one-piece-flow production system should be subjected to analysis. The jobs entering the system in question do so at random order.

Despite the constraints imposed on the model the conducted analyses appear to indicate that by employing computer simulation it is possible to carry out optimisation works in job-shop environment, through identification of bottle-necks and constant analysis of machine tool engagement. The results infer that optimisation of production flow in a production system may often require developing and implementing diverse manufacturing technologies, along with dive-sifying the size of batches. These problems will be further analysed in future works.

REFERENCES

Danilczuk, W., Gola, A., & Cechowicz, R. (2014). Analiza konfiguracji linii produkcyjnych na postawie modeli symulacyjnych. In K. Bzdyra (Ed.), *Informatyczne Systemy Zarządzania* (25–42). Koszalin: Wyd. Politechniki Koszalińskiej.

Demir, L., Tunali, S., & Eliiyi, D. T. (2014). The state of the art on the buffer allocation problem: a comprehensive survey. *Journal of Intelligent Manufacturing*, *25*, 371–392. doi:10.1007/s10845-012-0687-9

Esmaeilian, B., Behdad, S., & Wang, B. (2016). The evolution and future of manufacturing: A review. *Journal of Manufacturing Systems*, *39*, 79–100. doi:10.13140/RG.2.1.2720.0402

Gola, A., & Świć, A. (2014). Economic analysis of manufacturing systems configuration in the context of their productivity. *Actual Problems of Economics*, *162*(12), 385–394.

Jagstam, M., & Klingstam, P. (2002). A handbook for integrating discrete event simulation as an aid in conceptual design of manufacturing systems. In E. Yucesan, C.-H. Chen, J. L. Snowdon, &J. M. Charnes (Eds.), *Proceedings of the 2002 Winter Simulation Conference* (*2*, 1940–1944). doi:10.1109/WSC.2002.1166493

Jahangirian, M., Eldabi, T., Nasser, A., Stergioulas, L. K., & Young, T. (2010). Simulation in manufacturing and business: a review. *European Journal of Operational Research*, *203*(1), 1–13. doi:10.1016/j.ejor.2009.06.004

Jithavech, I., & Krishnan, K. (2010). A simulation-based approach to the risk assessment of facility layout designs under stochastic product demands. *The International Journal of Advanced Manufacturing Technology*, *49*, 27–40. doi:10.1007/s00170-009-2380-5

Joseph, O. A., & Sridharan, R. (2011). Simulation modelling and analysis of routing flexibility of a flexible manufacturing systems. *International Journal of Industrial and Systems Engineering*, *8*(1), 61–82.

Kłos, S., & Patalas-Maliszewska, J. (2015). Throughput Analysis of Automatic Production Lines Based on Simulation Methods. *Lecture Notes in Computer Science*, *9375*, 181–190. doi:10.1007/978-3-319-24834-9_22

Kłos, S., Patalas-Maliszewska, J., & Trebuna, P. (2016). Improving manufacturing processes using simulation methods. *Applied Computer Science*, *12*(4), 7–17.

Kłos, S., & Trebuna, P. (2015). Using computer simulation method to improve throughput of production systems by buffers and workers allocation. *Management and Production Engineering Review*, *6*(4), 60–69. doi:10.1515/mper-2015-0037

Kłos, S., & Trebuna, P. (2017). The impact of the availability of resources, the allocation of buffers and number of workers on the effectiveness of an assembly manufacturing system. *Management and Production Engineering Review*, *8*(3), 40–49. doi:10.1515/mper-2017-0027

Longo, F. (2010). Emergency simulation: state of the art and future research guidelines. *SCS M&S Magazine*, *1*(4), 2010-04.

Negahban, A., & Smith, J. S. (2014). Simulation for manufacturing systems design and operation: literature review and analysis. *Journal of Manufacturing Systems*, *33*(2), 241–261. doi:10.1016/j.jmsy.2013.12.007

Stanley, D. R., & Kim, D. S. (2012). Experimental results for the allocation of buffers in closed serial production lines. *International Journal of Production Economics*, *137*(2), 284–291. doi:10.1016/j.ijpe.2012.02.011

Vidalis, M. I., Papadopoulos, C. T., & Heavy, C. (2005). On the workload and „phase load" allocation problems of short reliable production lines with fininte buffers. *Computers and Industrial Engineering*, *48*(4), 825–837. doi:10.1016/j.cie.2004.12.011

Yang, T., Zhang, D., Chen, B., & Li, S. (2008). Research on plant layout and production line running simulation in digital factory environment. *Pacific-Asia Workshop on Computational Intelligence and Industrial Application*, *2*, 588–593.